

1 2 9 0



UNIVERSIDADE  
**COIMBRA**

Maria Carolina de Azevedo dos Santos

**STRUCTURE OF BACTERIAL COMMUNITIES IN THE  
PRESENCE OF CHEMICAL CONTAMINANTS  
APPLICATION OF QUATERNARY AMMONIUM COMPOUNDS IN  
SOIL**

Dissertação no âmbito do Mestrado em Microbiologia e Biotecnologia Microbiana  
orientada pelo Professor Doutor José Paulo Sousa e pelo Doutor Luís Cunha e  
apresentada ao Departamento de Ciências da Vida da Faculdade de Ciências e  
Tecnologia.

Julho de 2025



1 2



9 0

UNIVERSIDADE  
**COIMBRA**

Maria Carolina de Azevedo dos Santos

**STRUCTURE OF BACTERIAL COMMUNITIES IN THE  
PRESENCE OF CHEMICAL CONTAMINANTS  
APPLICATION OF QUATERNARY AMMONIUM COMPOUNDS IN  
SOIL**

Dissertação no âmbito do Mestrado em Microbiologia e Biotecnologia Microbiana  
orientada pelo Professor Doutor José Paulo Sousa e pelo Doutor Luís Cunha e  
apresentada ao Departamento de Ciências da Vida da Faculdade de Ciências e  
Tecnologia.

Julho de 2025



I declare that this thesis was written and organized by me, and I confirm that it has not been previously submitted, in whole or in part, to obtain another academic degree. The work presented in this document is part of the EU Horizon project SYBERAC (Grant Agreement 101135213 - <https://www.syberac.eu/>) under a collaboration between the University of Coimbra and Aarhus University (AU-DK). With the exception of the site description, sampling design and microcosm experiments of QAC's exposure, that were conceived in collaboration with Prof. Dr. Kai Bester, and Dr. Sophie Lennartz (AU), and soil sampling, soil moisture measurement, and preparation of QAC's standard solutions, that were performed in AU-DK by Dr. Sophie Lennartz, I was responsible for conducting all the remaining laboratory work and data analysis.



## Acknowledgments

Firstly, I thank Prof. Dr. José Paulo Sousa for agreeing to supervise my initial steps in the research world, for allowing me to co-lead a research partnership under the SYBERAC project, and, most importantly, for giving me the opportunity to work with an incredible team.

To my co-supervisor, Dr. Luís Cunha, for his guidance, stress-management skills, motivation, support, and joyful enthusiasm for research, even amid the inevitable struggles and frustrations. He sets an example as a PI of the group I am proud to be part of, the Environmental Genomics Laboratory, also known as ENGEL.

I would also express my gratitude to Prof. Dr. Kai Bester from Aarhus University for the warm welcome in the freezing Roskilde city in Denmark, and to Dr. Sophie Lennartz for her trust in my research abilities and for enduring the long working hours with me, even on those short, sun-starved days, and being my tea-mate. I would also like to mention Pedro and Paula for showing me that you can always find a Portuguese person abroad, even in the research field. I sent my appreciation to all people whom I encounter in the Department of Environmental Science - Environmental Chemistry & Toxicology of Aarhus University.

To ENGELs for being true angels when it comes to team effort (see the dry joke worth it of a dad's dry joke contest, that I did here?). It has been both fun and enriching to do science with you.

To Ricardo Leitão, for his grit and captivating passion about soil science; for his mentorship and incredible faith in my abilities, friendship, and for giving me a tremendous amount of valuable knowledge on microbiome analysis.

To Filipa Reis and Sandra Simões for always being helpful even when stressed; for the car rides; lunch time in front of Sé Nova; for the deep-talk coffee breaks, and for all the fun memories.

To the friends I made in the group — Luísa, Diogo, Lisl, and António — thanks for the fun times and for being there through the ups and downs of starting in research.

Again, to Luísa for her undeniable support, late-night working hours, car rides, for being the glue of the group, a fearless and inspiring woman, and researcher. Thank you for the close friendship and memories that made this thesis journey a lot easier.

To my colleagues and friends whom I made during this master's. To Rebeca, Rafael, Anna, Maria, Salomé, Andreia, Catarina, and Luísa. You were really the best part of it.

To all the lifetime friends, Rita, Alexandra, André, Tatiana, Laura... but especially to my best friend Joana for being there, even if just a call away. Thank you for celebrating my wins and supporting my lows. Never thought that sitting next to you at a school desk would lead to years of friendship — one of the best decisions I have ever made.

In the end, to my parents for the education and values, for putting up with their curious, outspoken, multi-hobby daughter, and for giving me a happy childhood. Thank you to my family and to the headstrong women that I'm lucky to be related to. What an honor to be one of the most educated women in the family.



Whatever the stress, the system will redress  
*Henri Louis Le Châtelier* (Paraphrasing of Le Châtelier's Principle)



## Resumo

A rega com águas residuais, a aplicação de lamas e a pulverização de pesticidas são algumas das vias pelas quais os compostos de amónio quaternário (QACs) podem entrar e acumular-se no solo. Uma análise mais detalhada foi realizada sobre a aplicação de lamas de tratamento contaminadas em campos agrícolas, avaliando-se os efeitos individuais de três subgrupos: cloreto de hexadecil-trimetil amónio (ATMAC-C16), cloreto de dodecil-benzildimetil amónio (BAC-C12) e cloreto de didecil-dimetilamónio (DDAC-C10). Deste modo, verificou-se que o ATMAC-C16, o BAC-C12 e o DDAC-C10 alteraram a riqueza bacteriana, a uniformidade e a  $\beta$ -diversidade. Embora o ATMAC-C16 não tenha demonstrado qualquer efeito em função do tempo de exposição, as comunidades expostas ao BAC-C12 e ao DDAC-C10 revelaram ser dependentes do tempo de exposição. Ainda mais, demonstrou-se que, em resposta à dose, o ATMAC-C16 seguiu um padrão de diminuição monótona (com um *rebound* inesperado a 100 mg kg<sup>-1</sup>), enquanto o BAC-C12 apresentou um padrão sigmoidal com “ponto de viragem” em ~0,1 mg kg<sup>-1</sup> e o DDAC-C10 apenas reduziu a riqueza na dose mais elevada (100 mg kg<sup>-1</sup>). Adicionalmente, alguns taxa mostraram correlação com funções preditas sobre-expressas pelo FAPROTAX, como vias de respiração de enxofre e fermentação, assim como patógenos putativos (e.g., *Escherichia-Shigella*, *Bacteroides*) em doses elevadas. Neste sentido, esta investigação permitiu colmatar a lacuna de conhecimento sobre o impacto dos QACs no microbioma do solo, alertar para a ameaça silenciosa que os QACs representam para a saúde no conceito One Health e defender a inclusão destes compostos no quadro de monitorização e avaliação do risco dos solos da UE.

**Palavras-chave:** Compostos quaternários de amónio; Contaminantes ambientais; Microbioma do solo; Gene 16S rRNA metabarcoding; Avaliação-do-risco

## Abstract

Wastewater irrigation, sludge application, and pesticide spraying are some of the pathways by which quaternary ammonium compounds (QACs) can enter and accumulate in the soil. A closer look was taken at the application of contaminated sewage sludge in agricultural fields by analyzing the individual effects of three subgroups: hexadecyltrimethyl ammonium chloride (ATMAC-C16), dodecyl-benzylidimethyl ammonium chloride (BAC-C12), and didecyl-dimethylammonium chloride (DDAC-C10). Here, it was shown that ATMAC-C16, BAC-C12, and DDAC-C10 altered bacterial richness, evenness, and  $\beta$ -diversity. Although ATMAC-C16 didn't show any effect due to exposure time, BAC-C12 and DDAC-C10 communities appeared to be time-dependent. It was further demonstrated that, as a dose-response from soil bacteria, ATMAC-C16 followed a monotonic decrease (with an unexpected rebound at  $100 \text{ mg kg}^{-1}$ ) pattern, while BAC-C12 had a sigmoidal “tipping-point” at  $\sim 0.1 \text{ mg kg}^{-1}$  and DDAC-C10 only depressed richness at the highest dose ( $100 \text{ mg kg}^{-1}$ ). Additionally, some taxa were correlated with FAPROTAX upregulated predicted functions such as sulfur-respiration and fermentation pathways, alongside putative pathogens (e.g., *Escherichia-Shigella*, *Bacteroides*) at high doses. On this matter, this research allowed to fill the knowledge gap on QACs' impact on soil microbiome, raise awareness of the silent threat that QACs pose to One Health, and advocate for the inclusion of these compounds in the EU soil monitoring risk-assessment framework.

**Keywords:** Quaternary ammonium compounds; Environmental contaminants; Soil microbiome; 16S rRNA gene metabarcoding; Risk-assessment



## Table of Contents

<b>ACKNOWLEDGMENTS</b>	<b>VII</b>
<b>RESUMO</b>	<b>XII</b>
<b>ABSTRACT</b>	<b>XIII</b>
<b>INTRODUCTION</b>	<b>1</b>
THE IMPORTANCE OF THE SOIL MICROBIOME	1
QUATERNARY AMMONIUM COMPOUNDS AND THEIR IMPACT ON THE SOIL MICROBIOME	3
<b>MATERIALS AND METHODS</b>	<b>10</b>
SITE DESCRIPTION AND SAMPLING DESIGN	10
SETUP OF QAC'S EXPOSURE	12
BACTERIAL 16S rRNA ILLUMINA SEQUENCING	16
STATISTICAL ANALYSIS	17
<b>RESULTS</b>	<b>19</b>
ALPHA-DIVERSITY	20
<i>ATMAC-C16</i>	21
<i>BAC-C12</i>	23
<i>DDAC-C10</i>	26
BETA-DIVERSITY	27
<i>ATMAC-C16</i>	28
<i>BAC-C12</i>	30
<i>DDAC-C10</i>	32
BACTERIAL COMMUNITY COMPOSITION	34
<i>ATMAC-C16</i>	35
<i>BAC-C12</i>	36
<i>DDAC-C10</i>	37
Heatmap – Genera across treatments	38
DIFFERENTIAL ABUNDANCES ANALYSIS – DESEQ2	39
<i>ATMAC-C16</i>	39
<i>BAC-C12</i>	41
<i>DDAC-C10</i>	44
FUNCTIONAL PREDICTION – FAPROTAX	46
<i>ATMAC-C16</i>	46
<i>BAC-C12</i>	47
<i>DDAC-C10</i>	48
<b>DISCUSSION</b>	<b>49</b>
<b>FINAL REMARKS AND FUTURE STEPS</b>	<b>54</b>
<b>REFERENCES</b>	<b>56</b>
<b>ATTACHMENTS</b>	<b>69</b>



## List of abbreviations

<b>ARG</b>	Antibiotic Resistance Genes
<b>ATMAC</b>	Alkyl Trimethyl Ammonium Chloride
<b>BAC</b>	Benzyl Ammonium Chloride
<b>BPR</b>	Biocidal Products Regulation
<b>DDAC</b>	Dialkyl Dimethyl Ammonium Chloride
<b>HGT</b>	Horizontal Gene Transfer
<b>LC-MS</b>	Liquid Chromatography–Mass Spectrometry
<b>MeOH</b>	Methanol
<b>MGE</b>	Mobile Genetic Elements
<b>PNEC</b>	Predicted No-Effect Concentration
<b>QAC</b>	Quaternary Ammonium Compounds
<b>REACH</b>	Regulation on the Registration, evaluation, authorization, and restriction of chemicals
<b>ROS</b>	Reactive Oxygen Species
<b>SYBERAC</b>	System-Based, holistic Environmental Risk Assessment of Chemicals
<b>WWTPs</b>	Wastewater Treatment Plants



## List of Figures

<b>FIGURE 1 - GENERAL CHEMICAL STRUCTURE OF THE QUATERNARY AMMONIUM COMPOUNDS USED IN THE STUDY: ATMACs, BACs AND DDACs.</b> .....	4
<b>FIGURE 2 - AERIAL PHOTOGRAPH OF THE FIELD SITE.</b> .....	10
<b>FIGURE 3 - SAMPLING FIELD.</b> .....	11
<b>FIGURE 4 - EXPERIMENTAL WORKFLOW FOR ASSESSING THE IMPACT OF QACs ON SOIL MICROBIAL COMMUNITIES.....</b>	13
<b>FIGURE 5 - DNA EXTRACTION FRAMEWORK FROM NORGENTBIOTEK SOIL DNA ISOLATION KIT.</b> .....	15
<b>FIGURE 7 - SEQUENCING DEPTH CURVE. LABELS REPRESENT SAMPLE NAMES.</b> .....	19
<b>FIGURE 8 - ALPHA DIVERSITY INDICES (CHAO1, SHANNON, AND SIMPSON) COMPARING CONTROL-SOIL (SOIL WITHOUT SAND) AND CONTROL (SOIL WITH SAND).</b> .....	20
<b>FIGURE 9 - ALPHA DIVERSITY BOXPLOTS (CHAO1, SHANNON AND SIMPSON) OF THE CONTROL GROUP THROUGH TIMEPOINTS.....</b>	21
<b>FIGURE 10 - ALPHA DIVERSITY INDICES (CHAO1, SHANNON, AND SIMPSON) COMPARING CONTROL AND ATMAC-C16.</b> .....	22
<b>FIGURE 11 - ALPHA DIVERSITY INDICES (CHAO1, SHANNON, AND SIMPSON) COMPARING CONTROL AND ATMAC-C16 THROUGH TIMEPOINTS.</b> .....	22
<b>FIGURE 12 - ALPHA DIVERSITY INDICES (CHAO1, SHANNON, AND SIMPSON) COMPARING CONTROL AND ATMAC-C16 THROUGH CONCENTRATION RANGE (0.001, 0.01, 0.1, 1, 100 MG/KG).</b> .....	23
<b>FIGURE 13 - ALPHA DIVERSITY INDICES (CHAO1, SHANNON, AND SIMPSON) COMPARING CONTROL AND BAC-C12.</b> .....	24
<b>FIGURE 14 - ALPHA DIVERSITY INDICES (CHAO1, SHANNON, AND SIMPSON) COMPARING CONTROL AND BAC-C12 THROUGH TIMEPOINTS.</b> .....	24
<b>FIGURE 15 - ALPHA DIVERSITY INDICES (CHAO1, SHANNON, AND SIMPSON) COMPARING CONTROL AND BAC-C12 THROUGH CONCENTRATION RANGE (0.001, 0.01, 0.1, 1, 100 MG/KG).</b> .....	25
<b>FIGURE 16 - ALPHA DIVERSITY INDICES (CHAO1, SHANNON, AND SIMPSON) COMPARING CONTROL AND DDAC-C10.</b> .....	26
<b>FIGURE 17 - ALPHA DIVERSITY INDICES (CHAO1, SHANNON, AND SIMPSON) COMPARING CONTROL AND DDAC-C10 THROUGH TIMEPOINTS.</b> .....	26
<b>FIGURE 18 - ALPHA DIVERSITY INDICES (CHAO1, SHANNON, AND SIMPSON) COMPARING CONTROL AND DDAC-C10 THROUGH CONCENTRATION RANGE (0.001, 0.01, 0.1, 1, 100 MG/KG).</b> .....	27
<b>FIGURE 19 - PCOA WITH BRAY-CURTIS DISTANCES COMPARING CONTROL-SOIL (SOIL WITHOUT SAND) AND CONTROL (WITH SAND).</b> .....	28
<b>FIGURE 20 - PCOA OF BRAY-CURTIS DISTANCES FOR ATMAC-C16 SAMPLES, SHOWING CLUSTERING BY TREATMENT. TIMEPOINTS ARE REPRESENTED BY DISTINCT SYMBOLS....</b>	28
<b>FIGURE 21 - PCOA BASED ON BRAY-CURTIS DISTANCES ILLUSTRATING CLUSTERING OF ATMAC-C16 SAMPLES BY TIMEPOINT (T7 - RED, T14 - GREEN, T28 - BLUE).</b> .....	29
<b>FIGURE 22 - PCOA BASED ON BRAY-CURTIS DISTANCES ILLUSTRATING CLUSTERING OF ATMAC-C16 SAMPLES BY CONCENTRATION, 0 (RED), 0.001(OLIVE-GREEN), 0.01(GREEN), 0.1(LIGHT-BLUE), 1(DARK-BLUE), 100(PINK) MG/KG.</b> .....	29
<b>FIGURE 23 - PCOA OF BRAY-CURTIS DISTANCES FOR BAC-C12 SAMPLES, SHOWING CLUSTERING BY TREATMENT. TIMEPOINTS ARE REPRESENTED BY DISTINCT SYMBOLS....</b>	30
<b>FIGURE 24 - PCOA BASED ON BRAY-CURTIS DISTANCES ILLUSTRATING CLUSTERING OF BAC-C12 SAMPLES BY TIMEPOINT (T7 - RED, T14 - GREEN, T28 - BLUE).</b> .....	30
<b>FIGURE 25 - PCOA BASED ON BRAY-CURTIS DISTANCES ILLUSTRATING CLUSTERING OF BAC-C12 SAMPLES BY CONCENTRATION, 0 (RED), 0.001(OLIVE-GREEN), 0.01(GREEN), 0.1(LIGHT-BLUE), 1 (DARK-BLUE), 100(PINK) MG/KG.</b> .....	31
<b>FIGURE 26 - PCOA OF BRAY-CURTIS DISTANCES FOR DDAC-C10 SAMPLES, SHOWING CLUSTERING BY TREATMENT. TIMEPOINTS ARE REPRESENTED BY DISTINCT SYMBOLS....</b>	32

<b>FIGURE 27 - PCOA BASED ON BRAY-CURTIS DISTANCES ILLUSTRATING CLUSTERING OF DDAC-C10 SAMPLES BY TIMEPOINT (T7 - RED, T14 - GREEN, T28 - BLUE).....</b>	32
<b>FIGURE 28 - PCOA BASED ON BRAY-CURTIS DISTANCES ILLUSTRATING CLUSTERING OF DDAC-C10 SAMPLES BY CONCENTRATION, 0 (RED), 0.001(OLIVE-GREEN), 0.01(GREEN), 0.1(LIGHT-BLUE), 1 (DARK-BLUE), 100(PINK) MG/KG .....</b>	33
<b>FIGURE 29 - TOP 10 PHYLUM OF CONTROL-SOIL (LEFT) AND CONTROL (RIGHT). .....</b>	34
<b>FIGURE 30 - TOP 10 PHYLA OF ATMAC-C16 TREATED SOIL .....</b>	35
<b>FIGURE 31 - TOP 10 PHYLA IN ATMAC-C16-TREATED SOIL ACROSS TIMEPOINTS (LEFT) AND CONCENTRATIONS (RIGHT).....</b>	35
<b>FIGURE 32 - TOP 10 PHYLA OF BAC-C12 TREATED SOIL .....</b>	36
<b>FIGURE 33 - TOP 10 PHYLA IN BAC-C12-TREATED SOIL ACROSS TIMEPOINTS (LEFT) AND CONCENTRATIONS (RIGHT).....</b>	36
<b>FIGURE 34 - TOP 10 PHYLA OF DDAC-C10 TREATED SOIL .....</b>	37
<b>FIGURE 35 - TOP 10 PHYLA IN DDAC-C10-TREATED SOIL ACROSS TIMEPOINTS (LEFT) AND CONCENTRATIONS (RIGHT).....</b>	37
<b>FIGURE 36 - HEATMAP OF THE TOP 30 BACTERIAL GENERA BASED ON RELATIVE ABUNDANCE ACROSS TREATMENTS. BACTERIAL GENERA ARE SHOWN ALONG THE BOTTOM AXIS, AND TREATMENTS ARE INDICATED ON THE RIGHT.....</b>	38
<b>FIGURE 37 - VOLCANO PLOT OF ATMCA-C16 TREATED SOIL, COMPARING CONTROL AND 1 MG/KG.....</b>	39
<b>FIGURE 38 - HEATMAP OF GENUS-LEVEL LOG<sub>2</sub> FOLD CHANGES (SORTED BY VALUE). BACTERIAL GENERA ARE LISTED ON THE RIGHT, AND COMPARISONS ARE SHOWN ON THE BOTTOM AXIS. COLOR SCALE REPRESENTS LOG<sub>2</sub> FOLD CHANGE (0-1MG/KG) – ATMAC-C16.....</b>	40
<b>FIGURE 39 - HEATMAP OF GENUS-LEVEL LOG<sub>2</sub> FOLD CHANGES (SORTED BY VALUE). BACTERIAL GENERA ARE LISTED ON THE RIGHT, AND COMPARISONS ARE SHOWN ON THE BOTTOM AXIS. COLOR SCALE REPRESENTS LOG<sub>2</sub> FOLD CHANGE (0-100MG/KG) – ATMAC-C16....</b>	41
<b>FIGURE 40 - VOLCANO PLOTS OF BAC-C12 TREATED SOIL, COMPARING CONTROL AND 0.001 MG/KG (LEFT) AND 100 MG/KG (RIGHT). .....</b>	42
<b>FIGURE 41 - HEATMAP OF GENUS-LEVEL LOG<sub>2</sub> FOLD CHANGES (SORTED BY VALUE). BACTERIAL GENERA ARE LISTED ON THE RIGHT, AND COMPARISONS ARE SHOWN ON THE BOTTOM AXIS. COLOR SCALE REPRESENTS LOG<sub>2</sub> FOLD CHANGE (0-100MG/KG) – BAC-C12. ....</b>	43
<b>FIGURE 42 - VOLCANO PLOT OF DDAC-C10 TREATED SOIL, COMPARING CONTROL AND 100 MG/KG.....</b>	44
<b>FIGURE 43 - HEATMAP OF GENUS-LEVEL LOG<sub>2</sub> FOLD CHANGES (SORTED BY VALUE). BACTERIAL GENERA ARE LISTED ON THE RIGHT, AND COMPARISONS ARE SHOWN ON THE BOTTOM AXIS. COLOR SCALE REPRESENTS LOG<sub>2</sub> FOLD CHANGE (0-100MG/KG) – DDAC-C10. ....</b>	45
<b>FIGURE 44 - FUNCTIONAL CHANGES IN ATMAC-C16-TREATED SOIL RELATIVE TO CONTROL (1 MG/KG), SHOWN AS LOG<sub>2</sub> FOLD CHANGES. RED BARS REPRESENT INCREASED FUNCTIONS; BLUE BARS REPRESENT DECREASED FUNCTIONS.....</b>	46
<b>FIGURE 45 - FUNCTIONAL CHANGES IN BAC-C12-TREATED SOIL RELATIVE TO CONTROL (100 MG/KG), SHOWN AS LOG<sub>2</sub> FOLD CHANGES. RED BARS REPRESENT INCREASED FUNCTIONS; BLUE BARS REPRESENT DECREASED FUNCTIONS.....</b>	47
<b>FIGURE 46 - FUNCTIONAL CHANGES IN DDAC-C10-TREATED SOIL RELATIVE TO CONTROL (100 MG/KG), SHOWN AS LOG<sub>2</sub> FOLD CHANGES. RED BARS REPRESENT INCREASED FUNCTIONS; BLUE BARS REPRESENT DECREASED FUNCTIONS.....</b>	48



## **List of Tables**

<b>TABLE 1 - INFORMATION ABOUT THE SELECTED QACs.</b>	<b>9</b>
<b>TABLE 2 - SOIL PARAMETERS OF THE SAMPLING FIELD (INFORMATION PROVIDED BY AARHUS UNIVERSITY).</b>	<b>11</b>



# **Introduction**

## THE IMPORTANCE OF THE SOIL MICROBIOME

Soil provides several ecosystem services, with carbon retention and climate regulation, water regulation and purification, nutrient cycling, and disease and pest regulation being considered relevant ones (Creamer et al., 2022). Soil is a non-renewable resource (Halleux, 2024), with formation rates typically range from 0.01 to 1 mm per year, depending on factors such as climate and the rate of bedrock weathering (Montgomery et al., 2007). Soil can be described through its structure, texture, biological components, land use, and topography (FAO, 2006). Within this matrix resides the soil microbiome, composed mainly of bacteria, archaea, protozoa, fungi and viruses (Halleux, 2024; Roux & Emerson, 2022). It is well known that the majority of soil functions arise from interactions between soil biology and physical-chemical elements, with soil microorganisms being the key players in the vast majority of soil processes beyond those above-mentioned ecosystem services (Creamer et al., 2022). In this way, microbial communities can enhance soil development by, for example, being implicated in biogeochemical cycles (nutrient assimilation and transformation, carbon fixation, ionic element availability), promoting plant health (through growth enhancement and resistance to pests), influencing soil infiltration and percolation (soil aggregation) (Snyder & Vázquez, 2005), helping restore soil balance (climate change regulation and bioremediation) (Aislabie et al., 2013; Creamer et al., 2022; Hemkemeyer et al., 2021; Schulz et al., 2013; Song et al., 2024). Furthermore, these services interconnect soil and human microbiomes (Banerjee & van der Heijden, 2023; FAO, 2020; Silva et al., 2021).

Also, the soil microbiome originates from the microbiomes of other living organisms that interact with the soil, making the microbiome of higher trophic levels a subset of the lower ones (Zhu et al., 2023). However, this interaction is being affected by soil degradation (Zhu et al., 2023). Such degradation, shown as, e.g., soil erosion, compaction, soil contamination, and loss of diversity (Neuenkamp et al., 2024; Qiu et al., 2021) can be explained by anthropogenic stressors like excessive fertilization, chemical pollution, climate change, tillage, pH variation, and monocultures (FAO, 2020; Halleux, 2024; Lori et al., 2025). Among the consequences of these activities, particularly soil erosion (with loss of topsoil at a higher rate than soil formation) are a reduced carbon

content in soil, potentializing climate change (by increasing CO<sub>2</sub> emissions), leading to reduced crop resilience to phytopathogens and environmental stresses, heightening a potential crisis in food security and safety (Knight et al., 2024; Mattoo & Mallikarjuna, 2023; Ossowicki et al., 2021; Sáez-Sandino et al., 2023; Schlatter et al., 2017; Zhu et al., 2023). In this way, an altered soil microbiome would lead to shifts in microbial community composition, altered in the next generations after the initial impact, contributing to a change in soil functions over time (Putten et al., 2010).

Although a clear and consensual definition of soil health is still needed, especially emphasizing an optimal soil microbial community for specific land use types, according to the USDA Natural Resource Conservation Service, “*Soil health, also referred to as soil quality, is defined as the continued capacity of soil to function as a vital living ecosystem that sustains plants, animals, and humans*” (Fierer et al., 2021). The factors mentioned above contribute to 60-70% of European Union soils being considered in an “unhealthy state”, generating economic losses of around 50 billion euros per year in the EU (European Comission, 2021; Halleux, 2024). In this regard, EU policy still needs to include biological indicators and physical and chemical parameters (FAO, 2020; Halleux, 2024), since it points out a lack of knowledge on risk assessment of soil contaminants and ecotoxicological tests with different target species (European Comission, 2021; FAO, 2020; Neuenkamp et al., 2024). In this way, according to the EU Soil Strategy for 2030, a list of contaminants of major/emerging concern is currently under development to tackle before 2050 (European Comission, 2021). Additionally, biocide stability and its distribution within the system, the compound’s heat/light sensitivity, and the impact of metabolism by-products/intermediates should be taken into consideration (Ossowicki et al., 2021).

Fortunately, the European Commission Committees and a large group of stakeholders have recognized the urgent need for a robust legal framework to protect soil resources. This has led to initiatives such as the proposed “Soil Monitoring Law”, which aims to establish binding requirements for soil data collection, indicator development, and regular assessment of soil health across Member States. These efforts reflect a growing alignment with the One Health concept, a holistic framework recognizing the interconnectedness of human, animal, and environmental health (WHO, 2022). Achieving the goals of One Health requires coordinated action between scientific bodies, governments, land managers, and international organizations, as well as increased public awareness and soil literacy (Brevik et al., 2020; WHO, 2022).

Monitoring soil health is therefore not only essential for sustainable land management, but also plays a pivotal role in safeguarding broader ecosystem services and human well-being. Through a cascading effect, the protection and restoration of soil biodiversity, including microbial and fauna communities, can directly enhance plant health, support food security, reduce disease vectors, and buffer environmental stressors (Banerjee & van der Heijden, 2023; WHO, 2022).

Among the most significant threats to soil function is chemical pollution, which includes contamination by heavy metals, microplastics, pesticides, and increasingly, persistent organic pollutants (POPs) and emerging contaminants like quaternary ammonium compounds (QACs) (Li et al., 2025). These substances tend to accumulate in soils over time, disrupt microbial and faunal communities, and enter the food chain, ultimately posing risks to animal and human health. The diffuse sources of many of these pollutants, along with their long environmental residence times and strong interactions with soil organic matter, make their detection and remediation particularly complex (FAO, 2022; Brevik et al., 2020). Consequently, soil monitoring frameworks must prioritize the inclusion of chemical pollutants, especially emerging contaminants like QACs, alongside biological and physical indicators to accurately reflect the multifaceted pressures currently affecting European soils. Such monitoring is also essential for advancing the principles of the One Health concept, which, as mentioned above, recognizes the interconnectedness of soil, ecosystems, and human well-being. (Tezel & Pavlostathis, 2015).

## QUATERNARY AMMONIUM COMPOUNDS AND THEIR IMPACT ON THE SOIL MICROBIOME

One of many ways to recycle the nutrients in wastewater treatment plants (WWTPs) waste is to apply sewage sludge to the soil (Jensen et al., 2012). However, sludge can act as an entry point for chemical pollutants in the ecosystem since their presence is often dismissed (Imfeld et al., 2018; Loos et al., 2018; Wu et al., 2024). Quaternary ammonium compounds (QACs or QATs) are among these contaminants, being widespread in industrial, household, and agricultural environments where they are commonly used in disinfectants, surfactants, and antiseptic agents in commercial products (Heyde et al., 2020; Hu et al., 2024; Landecker, 2019; Mulder et al., 2018;

Nadagouda et al., 2022; Nowak-Lange et al., 2022). QACs are considered toxic and corrosive (PubChem, 2024), being already linked to skin irritation, increased inflammatory response, work-related asthma, and so forth (Arnold et al., 2023; Bobic et al., 2024; Malizia et al., 1960; Peyneau et al., 2022; Tetro et al., 2024).

Wastewater irrigation, sludge application, and pesticide spraying are some of the paths QACs enter and accumulate in the soil (R. Yang et al., 2023). Unfortunately, EU directive 86/278/EEC and Portuguese regulation (Decree-Law n.º 276/2009, Diário da República) only account for heavy metals and some organic compounds in sludge (Hudcová et al., 2019), and do not account for emerging compounds like QACs. Furthermore, agricultural soils can be subjected to high concentrations of these pollutants (Mulder et al., 2018), especially when sewage sludge or manure is applied (Heyde et al., 2021).

There is a dense variety of QACs. Its structure comprises a central ammonium group connected to different alkyl (a long chain of carbon and hydrogen atoms) and aromatic (aryl) groups (Hu et al., 2024). Here, polymeric QACs won't be considered. The most well-known monomeric QAC subgroups are benzyl ammonium chloride (BAC), alkyl trimethyl ammonium chloride (ATMAC), and dialkyl dimethyl ammonium chloride (DDAC or DADMAC) (Clara et al., 2007; Hu et al., 2024; Liu et al., 2023; W. Zhang et al., 2023) (Figure 1).

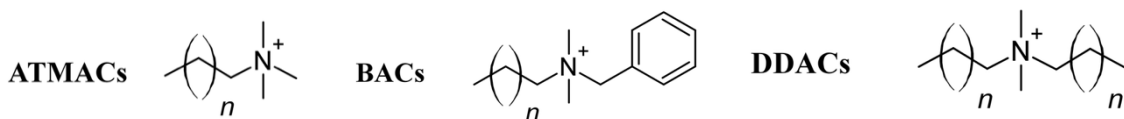


**Figure 1 - General chemical structure of the quaternary ammonium compounds used in the study: ATMACs, BACs and DDACs.**

As the chain length increases and oxygen availability decreases, these compounds become less biodegradable and more toxic (Heyde et al., 2020; Landecker, 2019; Lu et al., 2024). Also, having a hydrophobic tail next to the small positively charged heads allows QACs to adsorb to surfaces, especially sludge (Clara et al., 2007; Heyde et al., 2020; Nadagouda et al., 2022). According to a previous study, this structure determines the effectiveness of QACs and antimicrobial capacities (Seferyan et al., 2023). The most common strategy involves binding to the cell wall, which triggers reactive oxygen species

(ROS) accumulation, resulting in oxidative stress that leads to bacterial cell membrane lysis or deactivation of the lipid coating of viruses (Hu et al., 2024; Lu et al., 2024; Mohapatra et al., 2023; Nadagouda et al., 2022; K. Yang et al., 2023). The positively charged portion of these compounds binds to the membrane, replacing the stabilizing Mg<sup>2+</sup> and Ca<sup>2+</sup> cations, while the lipophilic part embeds itself into the phospholipid bilayer (Saverina et al., 2023; Seferyan et al., 2023). There seems to be a differential action according to cell type; for example, Gram-positive bacteria are more prone to QAC's action than Gram-negative bacteria and some fungi, like *Candida albicans*, but QACs do not affect bacterial spores and mycobacteria (Mulder et al., 2018; Nadagouda et al., 2022; Nowak-Lange et al., 2022; Pena et al., 2023; Peyneau et al., 2022). An exception to this may be the twin-chained DADMACs, which have higher antimicrobial activity against Gram-positive bacteria relative to BACs (Lu et al., 2024), likely due to the presence of a dual hydrophobic tail.

Being broad-spectrum, nonspecific antibacterial agents allows QACs to destabilize the surrounding ecosystem (Saverina et al., 2023; Seferyan et al., 2023). These compounds can accumulate on the surface and within the interlayers of clay minerals or organic matter in soils (Jansen et al., 2023), which may mitigate toxicological effects (Heyde et al., 2021) but, at the same time, contribute to their environmental persistence, allowing prolonged exposure of subinhibitory concentrations to soil microorganisms (Khan et al., 2017; Mulder et al., 2018; J. Zeng et al., 2022). For instance, opportunistic Gram-negative bacterial species have exhibited decreased susceptibility to BAC and may develop tolerance following repeated sublethal exposure to BAC-12 and BAC-14 (Pena et al., 2023). Also, bacterial metabolisms, such as denitrification (Lu et al., 2024; R. Yang et al., 2023; M. Zhao et al., 2023) or nitrification under a wastewater treatment plant nitrifying system (Kaj et al., 2014; Larsson et al., 2024; Xu et al., 2024), have been destabilized by QACs. For example, an up-regulation of ATP synthesis and transport carbohydrates and amino acids-related genes was observed in the presence of DDAC-C10 in one study (Hu et al., 2024).

In the end, QAC's biodegradation is done by some bacterial taxa, mainly dependent on the presence of hydrolytic enzymes like monooxygenases or amine dehydrogenases (Lu et al., 2024). In particular, bacterial communities appear to degrade BAC by  $\omega/\alpha/\beta$ -pathway or the  $\omega/\beta$ -pathway (regarding the number of carbons in the chemical structure), resulting in two persistent end-products, named TP194 (Benzyl-

(carboxymethyl)-dimethylazanium) and TP208B (Benzyl-(2-carboxyethyl)-dimethylazanium or BDMA) (Larsson et al., 2024). Although it is presumed that several microorganisms like *Xanthomonas*, *Aeromonas* (Tezel & Pavlostathis, 2015), or *Achromobacter* (Chacon et al., 2023) can metabolize QACs, the *Pseudomonas* genus is particularly notable. For example, *Pseudomonas nitroreducens* has been shown to produce amine oxidase, which is reportedly responsible for the initial dealkylation reaction of BAC (Ertekin et al., 2016).

As mentioned before, QACs are biodegradable under aerobic conditions. Despite that, studies have shown that bacterial resistance to these compounds is linked to antibiotic resistance (Mulder et al., 2018; Li et al., 2022; Ni et al., 2024; Tezel & Pavlostathis, 2015; Xu et al., 2024; Wang et al., 2025). This may be attributed to the heightened use of QACs during the COVID-19 pandemic, which led to an increase in microbial communities' resistance to both compounds (Hora et al., 2020; Li et al., 2022; Mohapatra et al., 2023; Pereira et al., 2023; K. Yang et al., 2023). Some resistance genes (*qac genes*) are thought to be carried within integrons, such as integron *intI1*, or other mobile genetic elements (MGEs), including transposases (Li et al., 2022). The great majority of these genes, *qac genes* (*qacH*, *qacE*, *qacA/B*), encode for efflux pumps through the mechanism of *qacA/qacR system* (Jennings et al., 2015), which facilitates the excretion of QACs from the intracellular space to the extracellular environment (Li et al., 2022; Lu et al., 2024). For example, a strain of *Pseudoxanthomonas mexicana* resistant to ATMAC-C16 is believed to harbor the *qacH* gene (Li et al., 2022); while pathogenic bacteria targeted in the food industry, like *Listeria monocytogenes*, exhibit resistance to BAC, which was associated with cross-adaptation to several antibiotics (Pena et al., 2023; Wu et al., 2024); a BAC-C12 (50 µg/ml) tolerant *Acinetobacter boemicus* strain was isolated from a manure sample in a German pig farm (Pulami et al., 2023), and a *Nitrospira* strain able to convert the ammonium in QAC sanitizer into nitrites was likely the main reason in conferring resistance to *Salmonella* in a mixed-species biofilm (Chen et al., 2024). It is important to mention that the co-localization of *qac* genes and antibiotic resistance genes (ARGs) facilitates the co-selection of antibiotic resistance and enhances the potential for horizontal gene transfer (HGT) (Hu et al., 2024; J. Zeng et al., 2022; J.-Y. Zeng et al., 2024). For instance, the *qacA* gene has been found on a plasmid that also contains beta-lactam resistance genes (Lu et al., 2024).

Ultimately, most of the available information is under the WWTP's scope. There has been a tentative determination of a predicted no-effect concentration (PNEC), which stands for the limit of chemical exposure for which no adverse effect has been reported. There are a few studies on sewage sludge (An et al., 2024; Kaj et al., 2014; Liu et al., 2023; Mongelli et al., 2025; Pena et al., 2023; Wang et al., 2025; Xu et al., 2024; K. Yang et al., 2023; Y. Zhang et al., 2023). However, the knowledge of QAC's impact on soil and sewage sludge application in agricultural fields is almost non-existent. In soil, a wide concentration range is found (Mulder et al., 2018): total BAC around 0.005-28.5 mg/kg (Kang & Shin, 2016; Khan et al., 2017); 3000 mg/kg (Sarkar et al., 2010); BAC-C12 with 83.6 µg/kg (Heyde et al., 2021). This highlights the necessity for research on the entry and fate pathways of QACs in soil, knowing their influence on ARGs profiles (K. Yang et al., 2023) and synergetic interactions with other compounds (Saverina et al., 2023), but most importantly, uncovering QACs' impact on the soil microbiome and multitrophic ecological interactions.

## PLACING THIS STUDY INTO CONTEXT AND OBJECTIVES

This study is included in the SYBERAC project (System-Based, holistic Environmental Risk Assessment of Chemicals), a European Union-funded project (Horizon Innovation Actions Grant Agreement No 101135213). The project aims to elucidate the impact of chemical pollution on terrestrial ecosystems. Through a Europe-wide network of case studies and stakeholder engagement, the project investigates the ecotoxicological effects of various chemical substances. In the end, the project seeks to a) trace the fate of pollutants in ecosystems; b) prevent and mitigate their harmful impacts; c) improve the conservation status of species and habitats; and, d) to strengthen and inform EU regulatory frameworks such as REACH (Registration, Evaluation, Authorization and Restriction of Chemicals) and the Biocidal Products Regulation (BPR).

This dissertation specifically focuses on assessing the ecotoxicological effects of quaternary ammonium compounds (QACs) on soil bacterial communities. QACs are emerging soil pollutants of concern due to their widespread use and persistence in the environment. The research pursues three core objectives:

- 1) To evaluate the impact of QACs exposure on the diversity and structure of soil bacterial communities.
- 2) To assess how these microbial community responses evolve over time.
- 3) To determine concentration thresholds where significant biological changes occur by exploring dose-dependent effects.

The study was done in collaboration with the Department of Environmental Science from Aarhus University under SYBERAC – case study 4A). It involves testing the response of soil microbial communities to three representative QACs (Table 1), each from a distinct chemical subgroup:

- ATMAC-C16 (Hexadecyltrimethylammonium chloride),
- BAC-C12 (Benzyl-dodecyl-dimethylammonium chloride),
- DDAC-C10 (Didecyldimethylammonium chloride)

To evaluate the impact of the three QACs on the composition and structure of soil bacterial communities, it is hypothesized that:

- Exposure to QACs will lead to a reduction in bacterial species richness.
- Increasing concentrations of QACs will progressively shift the composition and structure of microbial communities.
- The effects over time will vary according to the concentration levels of QACs.
- Certain microbial taxa will exhibit dose-dependent changes in abundance in response to each compound.
- The duration of exposure will modulate the effects on microbial taxa.
- Different QACs will selectively impact distinct microbial taxa.
- Shifts in microbial community composition will correspond to changes in predicted microbial functions, as inferred from taxonomic profiles.

Overall, by integrating bioinformatic data from microbiome analysis with chemical profiling results, the study aims to address critical knowledge gaps regarding the ecological impact of QACs on soil microbial communities, and inform risk assessment practices in support of more effective environmental regulations.

**Table 1** - Information about the selected QACs.

Common Name	IUPAC name	CAS number	Abbreviations	Formula*	PNEC**
Hexadecyltrimethyl ammonium Cl or Cetrimonium Cl	Hexadecyl(trimethyl)azanium;chloride	112-02-7	ATMAC-C16	C19H42N·Cl	1.66 mg/kg soil dw
Benzyldimethyldodecylammonium Cl	Benzyl-dodecyl-dimethylazanium;chloride	139-07-1	BAC-C12	C21H38N·Cl	1.36 mg/kg soil dw
Dimethyldidecylammonium Cl	Didecyl(dimethyl)azanium;chloride	7173-51-5	DDAC-C10	C22H48N·Cl	1.4 mg/kg soil dw

\*These compounds are usually bound to Cl, Br, I, or F anions (Mongelli et al., 2025).

\*\*In an ecotoxicological assessment, PNEC values should be considered with other indicators like LC<sub>50</sub>, NOEC, or EC<sub>50</sub> values (ECHA CHEM, n.d.)

## Materials and Methods

### SITE DESCRIPTION AND SAMPLING DESIGN

Soil was collected from a research field (named “CRUCIAL”—approximately 55.677255, 12.294958; PlotA8) in Høje Taastrup (Denmark) (Figure 2 and Figure 3) that has records of receiving only mineral fertilizers (nitrogen, phosphate, potassium, and no prior sludge application) in the past. Over the past 20 years, the crops in the field were cereals such as barley, wheat, and oats, while ryegrass was grown in 2010 and spring rape in 2005. Upper vegetation was removed (2-5 cm), and soil was collected from four different spots (Hole 1: 55.682029, 12.275204; Hole 2: 55.681868, 12.275386; Hole 3: 55.681859, 12.275300; Hole 4: 55.682042, 12.275352) and pooled (approximately 2m from the edge of each field corner), and about 20 cm soil depth (topsoil). The sampled soil was stored in decontaminated blue tons (checked for contamination in HPLC water ‘blank’ after 12 h overnight) at 7°C in a climate-controlled room.



**Figure 2** - Aerial photograph of the field site.



**Figure 3** - Sampling field (Grass strips separate plots used in the SYBERAC project).

Soil parameters are presented in Table 2.

**Table 2** - Soil parameters of the sampling field (Information provided by Aarhus University).

SOIL PROPERTIES	
C <sub>ORGANIC</sub>	1.3-1.7 %
TOTAL N	0.14-0.18 %
C <sub>ORGANIC</sub> / N	8.7-10.4
SAND	68.5 %
SILT	17.2 %
CLAY	14.3 %

After collection, and prior the spiking with the selected QACs, the soil was sieved and homogenized. Specifically, the soil was wet-sieved by manually passing it through a 2mm mesh stainless steel sieve and then homogenized in a closed mixer for 2h. Before the processing, the soil was stored in a climate-controlled room set to 15°C.

## SETUP OF QAC'S EXPOSURE

Standard solutions of each selected QAC (ATMAC-C16; BAC-C12; DDAC-C10) were prepared with the following concentrations: 200 ng/mL; 2 µg/mL, 20 µg/mL; 200 µg/mL dissolved in methanol (MeOH) to obtain 1 µg/kg-100mg/kg of soil (performed by the Danish colleagues). Compounds were selected based on their sorption behavior, solubility, persistence in soil, antimicrobial activity, and predicted environmental concentrations (PECs), as documented in sources such as the ECHA CHEM database.

About 250 mg of autoclaved sand (sea sand type) was measured into darkened vials to prepare for spiking. Then, in a fume hood, 25 µL of each compound standard solution (25 µL MeOH for the control) was added to the vials. To ensure well-mixed sand, the pipetted volume was divided into three big drops against different spots of the sand, being careful not to touch the vials' walls. This technique ensures a high retention in the sand. This was confirmed by the observation of clumps (sand aggregation). Afterward, the vials were left overnight in cleaned transparent plastic boxes to ensure methanol evaporation.

Sampled soil (with moisture equal to 60% its maximum water holding capacity) was weighed into a sterile Falcon tube. Subsequently, the spiked sand was poured into the Falcon tubes, resulting in 5g of soil with 5% sand. Both matrices were mixed manually since the overall sandy texture of the mixture could attach to the tube walls. At the same time, 197 µL of sterile distilled water was added and mixed in the same way to guarantee the soil moisture. An additional control, referred to as "control-soil," was established using only the field soil (without sand or QACs) to analyze its intrinsic microbiome. Pseudoreplicates were used for this control.

Microbial effects were assessed at four time points: T0 (day of treatment application), T7 (7 days post-application), T14 (14 days), and T28 (28 days), following guidance from the OECD 216 protocol (OECD, 2010). QACs were applied in a concentration range of 0.001, 0.01, 0.1, 1, and 100 mg/kg of dry soil. Five replicates per concentration were set up for time points T7 and T14 days, and eight replicates for time points T0 and T28. The three extra replicates were used for chemical analysis, preventing interference with samples of the microbiome analysis.

In the end, on those samples used for microbial analysis, T0 samples were grouped in a freezer box while the other time points were saved in an incubation room at 15°C to mimic soil environmental conditions. After seven days, T7 samples were stored along with T0, and the same procedure occurred for T14 after 14 days and T28 after 28 days. Soil moisture was determined gravimetrically and was constantly checked until T28 (done by the Danish colleagues). These samples are then used for:

- Metabolomic profiling, conducted using Liquid Chromatography–Mass Spectrometry (LC-MS) at Aarhus University Figure 4 (data unavailable in this thesis);
- Microbial community analysis, based on 16S rRNA gene metabarcoding using the V4 region, to assess taxonomic and predicted functional changes in the soil microbiome.

An illustration of the entire pipeline, from soil sample to chemical and metabarcoding analyses, is shown in Figure 3.

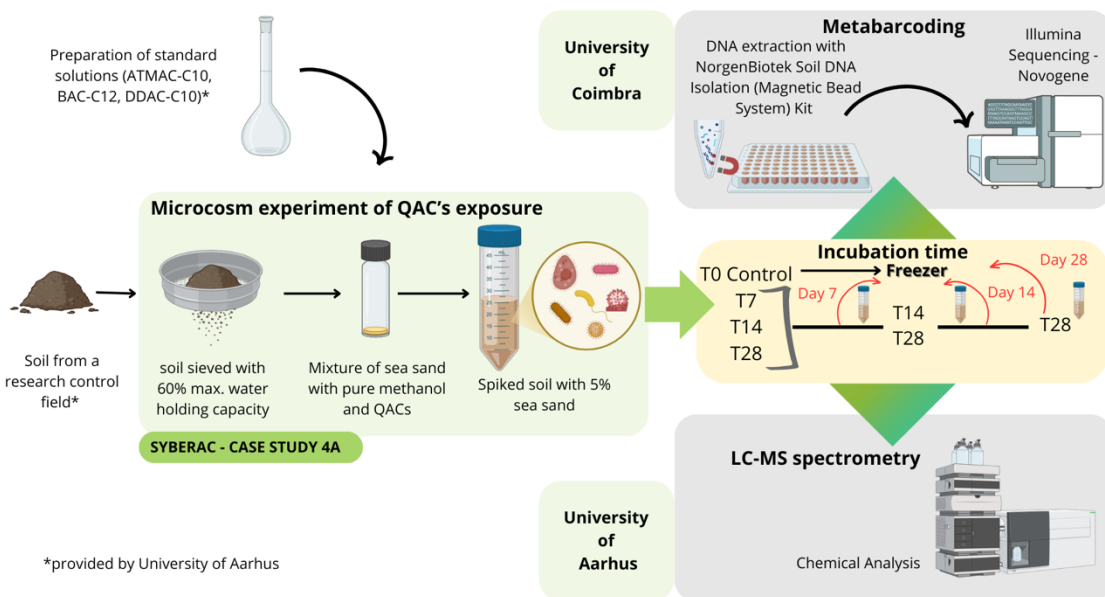


**Figure 4** - Experimental workflow for assessing the impact of QACs on soil microbial communities. Soil collected from Danish agricultural fields was homogenized, sieved, and adjusted to 60% of maximum water holding capacity (WHC). It was then spiked with 5% sea sand mixed with standard solutions of three quaternary ammonium compounds (BAC-C12, ATMAC-C16, and DDAC-C10) dissolved in methanol. Microcosms were incubated and sampled at four time points (T0, T7, T14, T28). Samples were divided for chemical analysis (LC-MS, performed at Aarhus University) and microbial community analysis via 16S rRNA gene metabarcoding (conducted at the University of Coimbra).

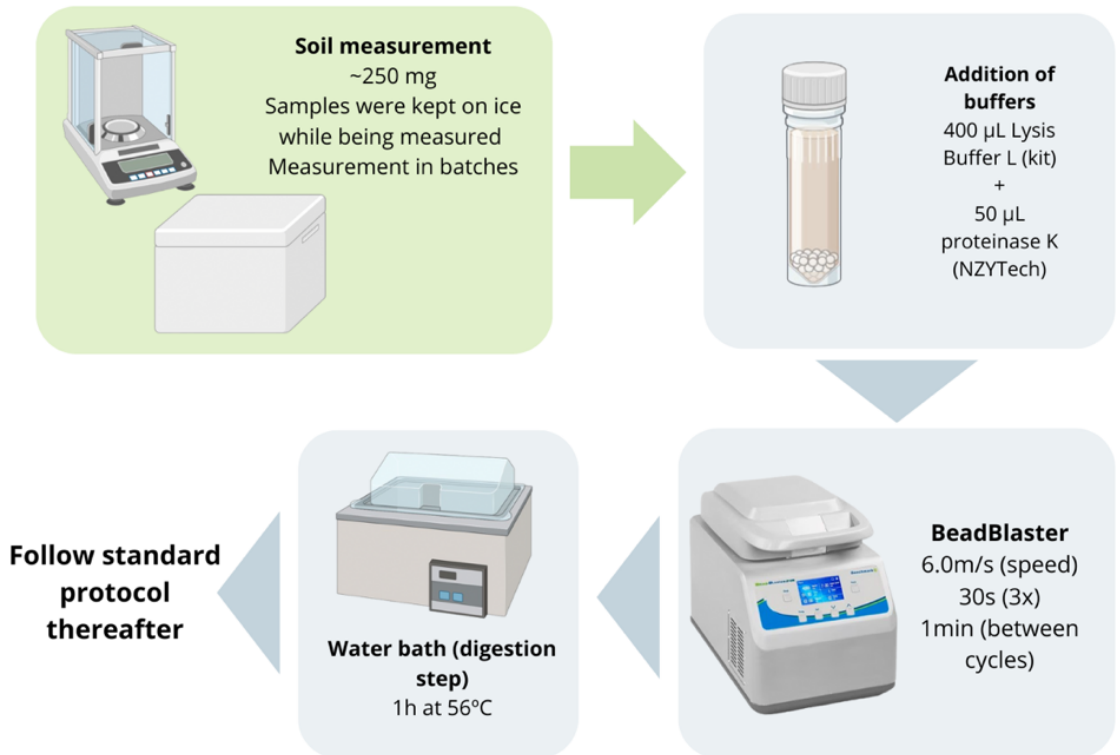
This study was conducted under SYBERAC – Case Study 4A. Schematic framework of the study. Illustration by the author.

## DNA EXTRACTION

Samples were divided into two shipments with dry ice packs from Denmark and kept in a -20°C freezer in Portugal for further microbiome analysis. The DNA extraction protocol was optimized to render maximum yield and DNA quality (see Tables 1 and 2 from Attachments) (Fierer et al., 2025). Soil DNA was extracted using the Norgen's Soil DNA Isolation (Magnetic Bead System) kit (Norgen Biotek Corp., Ontario, Canada). All samples were weighed at around 250 mg and stored at -20°C until processing. Some alterations were made: 400 µL instead of 750 µL of Lysis Buffer L; addition of 50 µl of proteinase K 20 mg/mL (NZYTech, Portugal) followed by a digestion step of 1h at 56°C in a water bath; and 50 µl instead of 100 µl of elution buffer.

For soil homogenization/disruption, Benchmark Scientific BeadBlaster™ 24R was used, with the following conditions: three cycles of 6.0m/s for 30s with a pause of a minute between cycles (Figure 5). Section 2 (2.3 DNA isolation using Manual Method) of the protocol (DNA isolation from the prepared soil lysate) was performed in Opentrons® OT-2 (Opentrons Labworks, Inc., UK) (Figure 5). Blanks were included. The protocol was designed using Opentrons Protocol Designer Version 8.4.4 and divided into three sub-protocols to prevent errors. In the effort to save time and enhance precision, mixing steps were done manually. Details about labware/OT-2 deck preparation are available in the attachments. The OT-2 made scripts can be found at the following GitHub repository: [https://github.com/MCS-micro/NorgenBiotek\\_Kit-OT2\\_Adaptation-Thesis](https://github.com/MCS-micro/NorgenBiotek_Kit-OT2_Adaptation-Thesis).

### Section 1: Soil Lysate Preparation (kit's 2mL bead tube)



### Section 2: DNA isolation of Soil Lysate - Adaptation of manual protocol in Opentrons OT-2 (96 deep well plate)

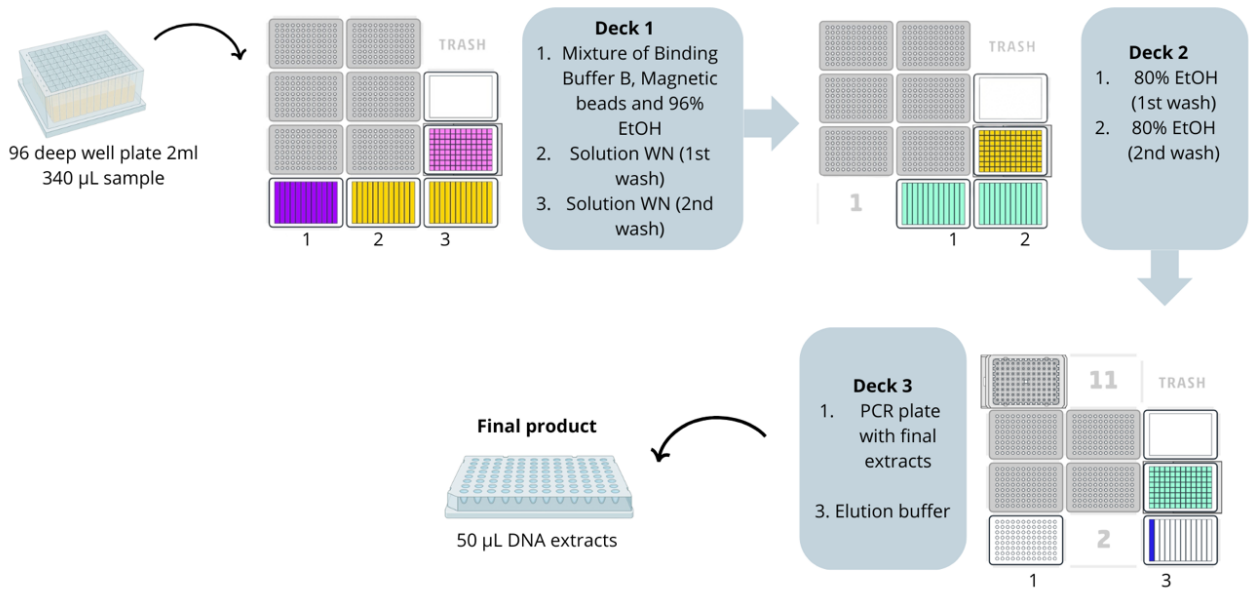


**Figure 5** - DNA extraction framework from NorgenBiotek Soil DNA Isolation kit.

Illustration by the author.

## BACTERIAL 16S rRNA ILLUMINA SEQUENCING

After extraction, DNA quality was checked in NanoDrop<sup>TM</sup> One/One C Microvolume UV/Vis Spectrophotometer (Thermo Scientific<sup>TM</sup>), and the extracted DNA (around 25 µl) was sent to Novogene Co. Ltd. (Munich, Germany) for high-throughput sequencing of the 16S amplicon V4 hypervariable region (using 515 F/806 R primers) on an Illumina platform (2x250bp).

The raw sequences obtained after sequencing were processed with QIIME2 (<https://qiime2.org>) (Caporaso et al., 2010; Estaki et al., 2020). The cutadapt tool was used on paired-end reads for primer trimming (Maki et al., 2023). Sequences were denoised, quality-controlled, trimmed, and merged using the DADA2 algorithm (Callahan et al., 2016; Hakimzadeh et al., 2024) to generate a feature table containing amplicon sequence variants (ASVs). To get some taxonomic information about the sequences, a pre-trained Naïve Bayes classifier based on the SILVA database was used (138.2, <https://www.arb-silva.de>).

For filtering and normalization of the data, a *phyloseq* object was created using the *phyloseq* package (McMurdie & Holmes, 2013) in R software version 4.4.2 (R Core Team, 2024). The number of reads and ASVs per sample was checked. Non-bacterial ASVs and ASVs with a low prevalence (ASV> 10 reads) were removed using the *Bioconductor* package (Huber et al., 2015). To normalize ASVs to account for sequencing depth across samples, DESeq2 size factor normalization was performed using the *DESeq2* R package. Size factors were estimated with the *estimateSizeFactors* function.

Differential abundance analysis at the genus level was performed using the *DESeq2* package within the R environment. The *phyloseq* object was then converted to a *DESeq2* dataset using the *phyloseq\_to\_deseq2()* function, and the differential abundance analysis was performed using the *DESeq()* function with the *fitType* set to "local". Significantly differentially abundant genera were identified based on an adjusted *p*-value threshold (Benjamini-Hochberg correction) of  $\alpha = 0.05$ . Additionally, genera with a log<sub>2</sub> fold change  $\geq 2$  were separately filtered and saved to highlight biologically relevant changes.

Functional annotation of the bacterial community was performed using FAPROTAX version 1.2.11, which maps 16S rRNA gene sequences to putative

ecological functions based on a curated literature database (Louca et al., 2016). Taxonomic assignments at the ASV level were formatted to meet FAPROTAX input requirements, and function-by-sample matrices were generated. FAPROTAX was run in a Linux command-line environment and applied to both normalized count data (used for visualization, including heatmaps) and raw (non-normalized) count data (used for differential abundance testing). The annotation was performed on the complete dataset, which included the control and all three compounds. Before statistical testing, heatmaps were generated to visually explore functional profiles across treatments. For DESeq2 analysis, performed in R with the package DESeq2 (v1.46.0) (Love et al., 2014), the dataset was subset to include only the control and one compound at a time, focusing on specific pairwise comparisons between concentrations identified in previous steps. All time points were considered together. Functions were considered significantly differentially abundant when the Benjamini-Hochberg adjusted *p*-value was below 0.05 and the absolute value of the log2 fold change exceeded 2.

## STATISTICAL ANALYSIS

Statistical analysis was done by using R software version 4.4.2 (R Core Team, 2024). To facilitate statistical analysis, the data were divided into subsets based on treatment groups: Control-Soil, Control, ATMAC-C16, BAC-C12, and DDAC-10.

To check normality and homoscedasticity, the Shapiro-Wilk test (*shapiro.test*) and Levene's test (*leveneTest*) were done, respectively. For alpha-diversity, measurements like Chao1, Simpson, and Shannon index were assessed. Significant differences were verified by the Mann-Whitney test for controls and the Kruskal-Wallis test, followed by the DUNN test as a post-hoc test. For beta-diversity, the Bray-Curtis dissimilarity was visualized using a Principal Coordinate Analysis (PCoA). Beta dispersion was checked (*p*-value<0.05); beta-dispersion was tested using the *betadisper* function, and differences between groups were tested with ANOSIM (*anosim*), both from the *vegan* package. The top 10 phyla were assessed using the *microbiome* package from the *BiocManager* package and visualized in a bar plot, and a top 30 genera were observed in a heatmap plot. Differential abundance analysis of microbial taxa was performed using the DESeq2 (*Bioconductor::deseq* package) on no-rarefied data and visualized in a

volcano and heatmap plots (Love et al., 2014). Taxa were mapped to a putative ecological function prediction tool named FAPROTAX (Functional Annotation of Prokaryotic Taxa) v.1.2.11 (Louca et al., n.d., 2025; Z. Yang et al., 2022). Results were visualized in a diverging bar plot and a heatmap (heatmap accessible in the attachments). Statistical significance was determined at a threshold of  $p$ -value<0.05.

## Results

This section presents some data to assess the impact of ATMAC-C16, BAC-C12, and DDAC-C10 on soil microbiome diversity and composition. To tackle this, alpha and beta-diversity are going to be evaluated, and significant differences are going to be characterized by differential abundance analysis with the DESeq2 tool.

From the raw sequencing data provided by Novogene Co., it was identified 11543156 reads with 38772 unique ASVs from 252 samples.

Along with this, sequencing depth was assessed to show the interaction between number of reads per sample and number of ASVs.

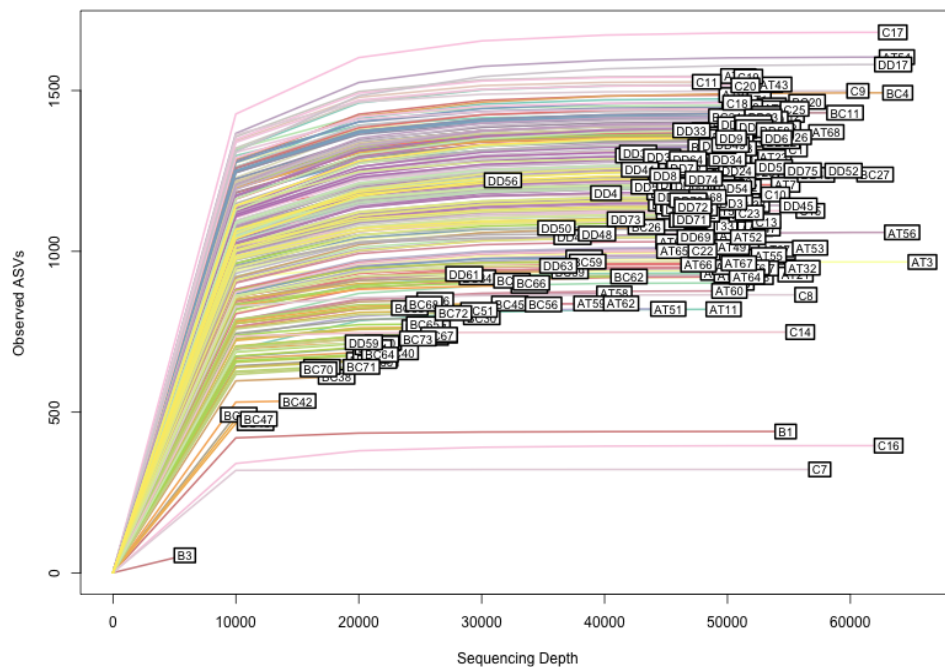


**Figure 6 - Sequencing depth curve. Labels represent sample names.**

The curve (Figure 6) suggests that most samples, except for a blank (B3), reached sufficient sequencing depth that encapsulates the majority of microbial diversity.

## ALPHA-DIVERSITY

To uncover how richness and composition were affected, alpha-diversity measurements, Chao1, Shannon Index and Simpson Index, were evaluated. First, comparisons between control groups, soil with sand (pre-treatment)(control) and soil (control-soil), didn't show any statistically significant differences by the non-parametric Wilcoxon rank sum test/Mann-Whitney U test (Chao1,  $p$ -value = 0.6905; Shannon,  $p$ -value = 0.2222; Simpson,  $p$ -value = 0.6905) (Figure 7).

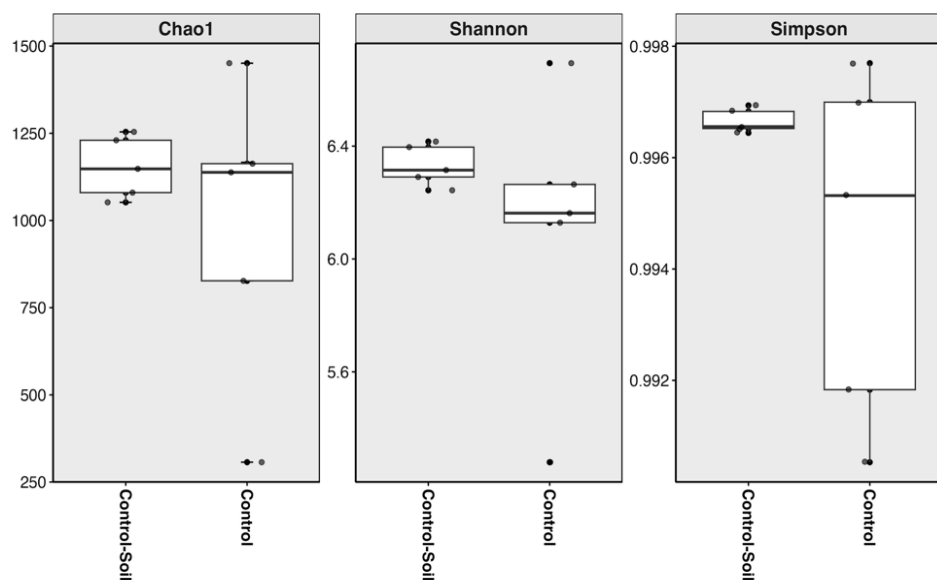


**Figure 7 - Alpha diversity indices (Chao1, Shannon, and Simpson) comparing control-soil (soil without sand) and control (soil with sand).**

Since the pre-treatment control (with sand) was evaluated through the timeline, alpha-diversity measurements were included to track potential changes over time.

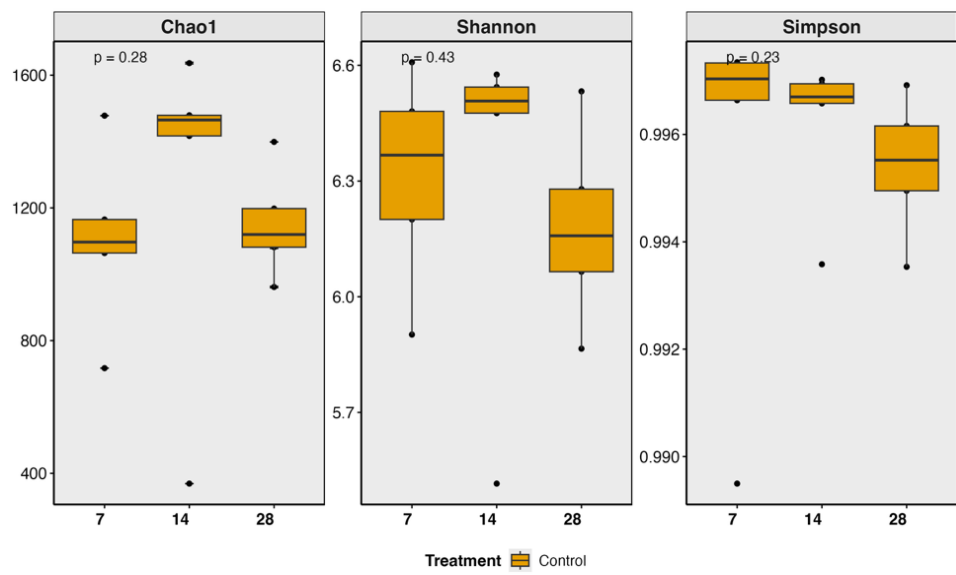


**Figure 8** - Alpha diversity boxplots (Chao1, Shannon and Simpson) of the control group through timepoints.

It's possible to observe an increase in richness on 14 days (T14) (Figure 8), although not significant (Chao1,  $p$ -value = 0.28; Shannon,  $p$ -value = 0.43; Simpson,  $p$ -value = 0.23).

### ATMAC-C16

However, a more interesting result is shown in Figure 9. Introducing ATMAC-C16 to the soil, seems to impact more the microbial evenness (Shannon,  $p$ -value <0.05) more than composition (Chao1,  $p$ -value = 0.08816; Simpson,  $p$ -value = 0.05197).

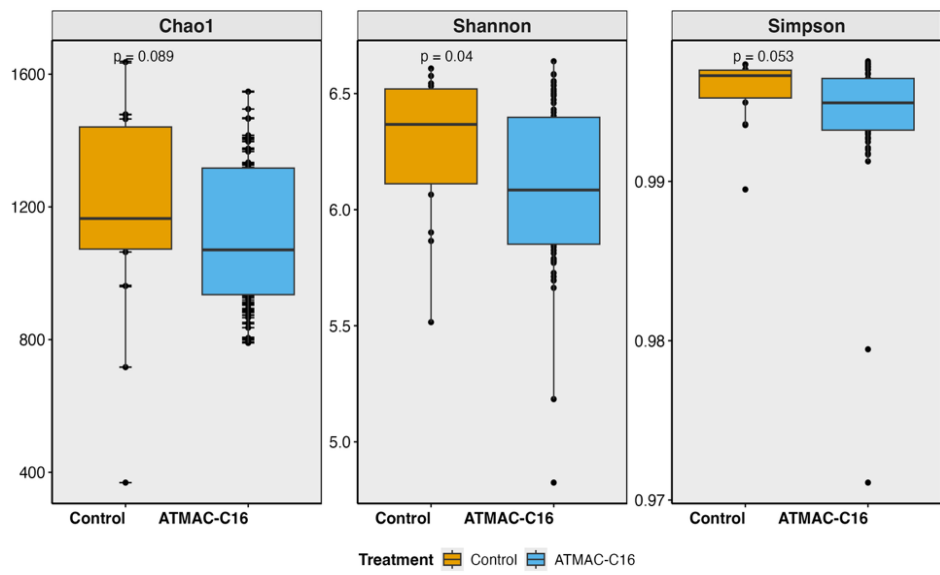


**Figure 9** - Alpha diversity indices (Chao1, Shannon, and Simpson) comparing control and ATMAC-C16.

The presence of outliers might be causing such results.

To see if our bacterial community is timepoint or dose-dependent, the same indices were applied.

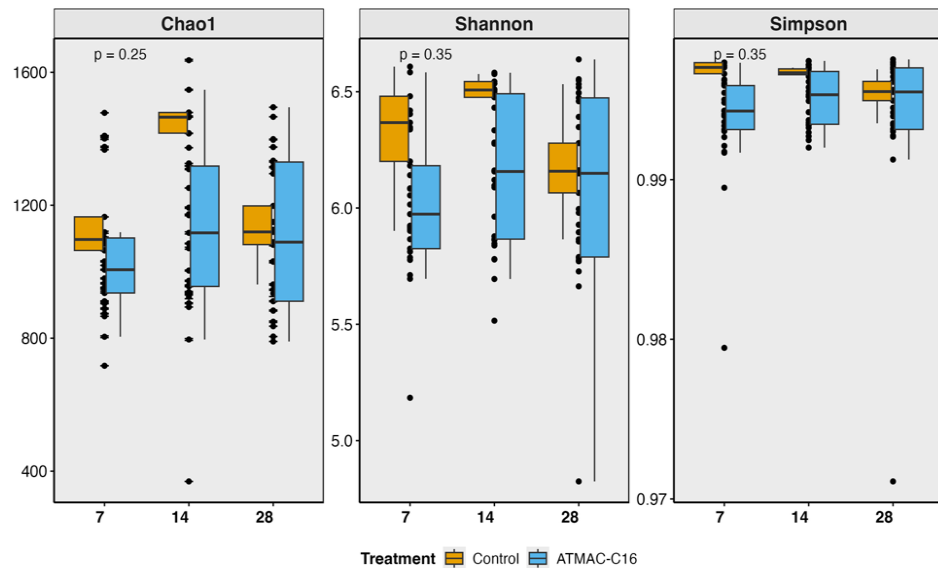


**Figure 10** - Alpha diversity indices (Chao1, Shannon, and Simpson) comparing control and ATMAC-C16 through timepoints.

Based on Figure 10, there is no tendency (Chao1,  $p$ -value = 0.2536; Shannon,  $p$ -value = 0.353; Simpson,  $p$ -value = 0.3479) throughout the time of the study for ATMAC-C16. Nonetheless, it seems to be a pattern when looking for the concentrations of this compound (Figure 11).

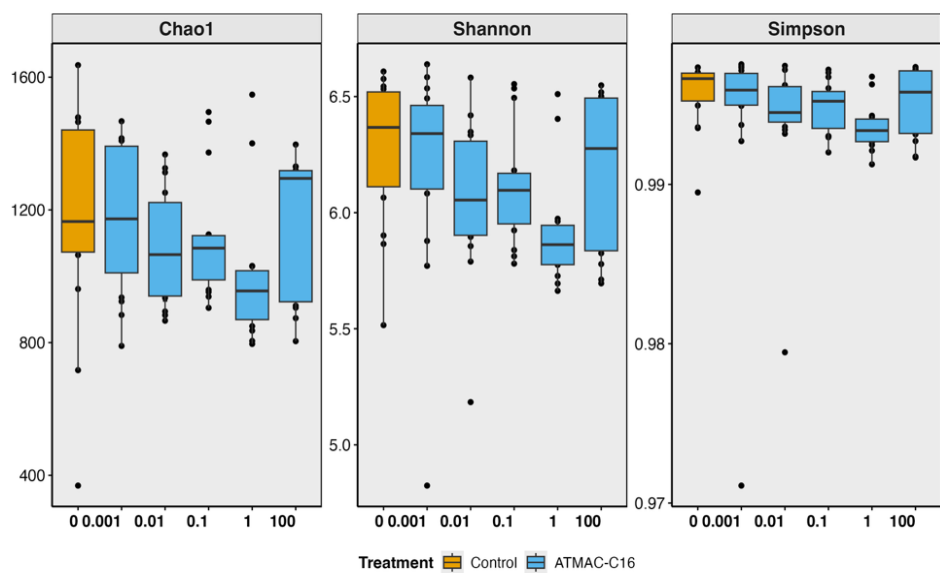


**Figure 11 - Alpha diversity indices (Chao1, Shannon, and Simpson) comparing control and ATMAC-C16 through concentration range (0.001, 0.01, 0.1, 1, 100 mg/kg).**

The figure above shows a clear downfall of bacterial richness and evenness throughout the increase of the dosage (Chao1,  $p$ -value = 0.07354; Shannon,  $p$ -value = 0.01364), even being less sensitive to dominant taxa (Simpson,  $p$ -value = 0.0117). The DUNN test confirmed this, Chao1 revealed differences on 0-1mg/kg and 0.001mg/kg-1mg/kg ( $p$ -adj Benjamini-Hochberg method < 0.05). On the other hand, an unexpected increase, especially in richness (Chao1), in the last/highest concentration, 100 mg/kg, stands out.

## BAC-Cl2

A different chemical compound might or might not mean a different response of the bacterial community in the soil. The same parameters were tested.

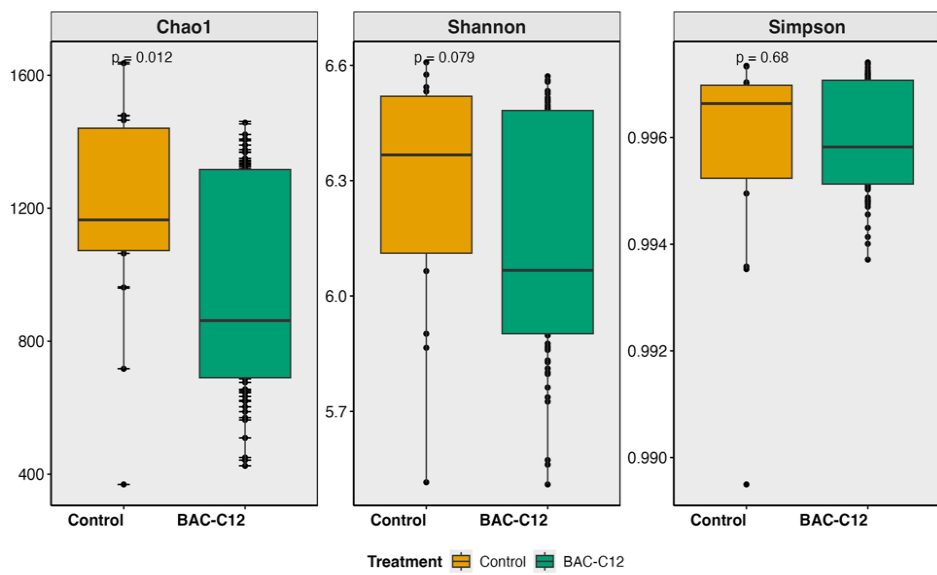


**Figure 12 - Alpha diversity indices (Chao1, Shannon, and Simpson) comparing control and BAC-C12.**

It seems that BAC-C12 reduces bacterial richness (Chao1,  $p$ -value = 0.01183) but has no statistical power to affect its distribution, being influenced by dominant taxa (Shannon,  $p$ -value = 0.07852; Simpson,  $p$ -value = 0.6768) (Figure 12).

To understand if time plays a role in the BAC-C12 effect on bacteria or if it follows the pattern started by ATMAC-C16, comparisons were made.

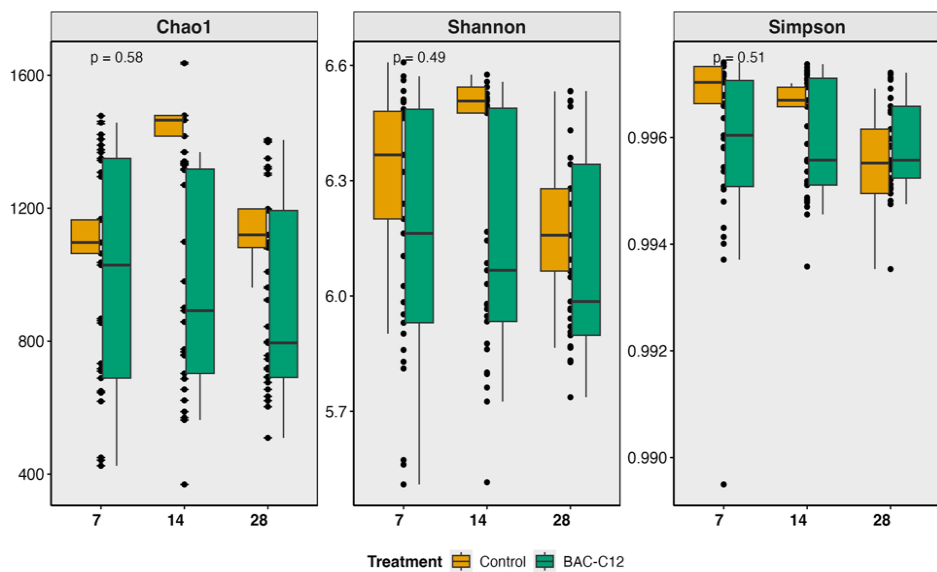


**Figure 13 - Alpha diversity indices (Chao1, Shannon, and Simpson) comparing control and BAC-C12 through timepoints.**

Again, different timepoints don't seem to be a major driver of the bacterial community behavior (Figure 13). There is no statistical difference after 7, 14, or 28 days (Chao1,  $p$ -value = 0.5817, Shannon,  $p$ -value = 0.493; Simpson,  $p$ -value = 0.5092).

To see if bacterial communities are dose-dependent on BAC-C12, pairwise comparisons were performed.

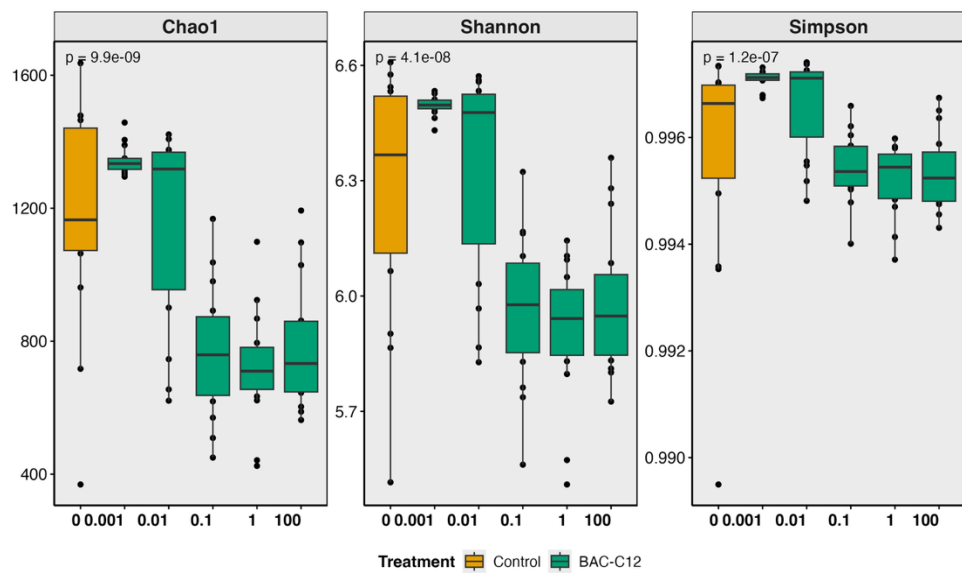


**Figure 14 - Alpha diversity indices (Chao1, Shannon, and Simpson) comparing control and BAC-C12 through concentration range (0.001, 0.01, 0.1, 1, 100 mg/kg).**

According to Figure 14, there is an initial impact until 0.1 mg/kg, with a clear reduction of richness and evenness (Chao1 and Shannon,  $p$ -value < 0.05), followed by a loss of dominant taxa (Simpson,  $p$ -value < 0.05), which stabilizes until the highest concentration, 100 mg/kg. This statement was confirmed by the DUNN test ( $p$ -adj Benjamini-Hochberg method < 0.05).

## DDAC-C10

Based on the observed trends of the previous compounds, a statistically significant impact on soil bacteria is expected.

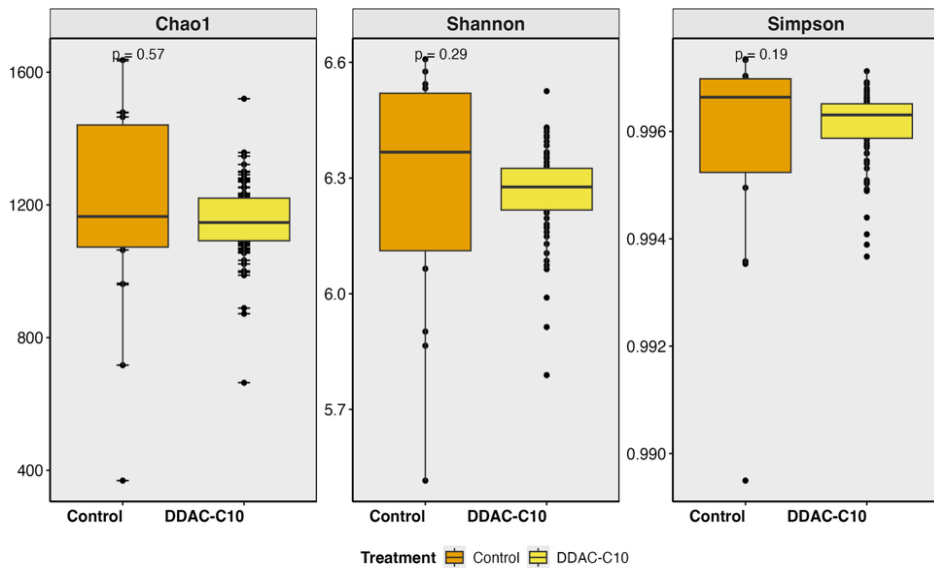


**Figure 15** - Alpha diversity indices (Chao1, Shannon, and Simpson) comparing control and DDAC-C10.

However, the figure above shows a similar response between control and the presence of DDAC-C10 (Chao1,  $p$ -value = 0.5734, Shannon,  $p$ -value = 0.2912; Simpson,  $p$ -value = 0.1884). This unanticipated result might be due to the clear presence of outliers along the yellow boxplots (Figure 15), warranting further analysis.

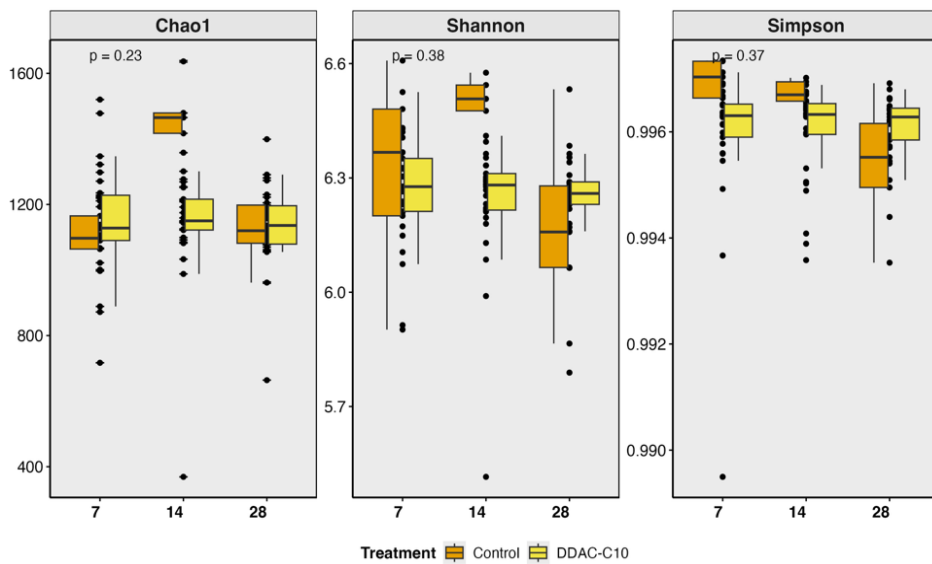


**Figure 16** - Alpha diversity indices (Chao1, Shannon, and Simpson) comparing control and DDAC-C10 through timepoints.

The timeline was also assessed (Figure 16). It follows the tendency of the other chemical compounds, ATMAC-16 and BAC-C12 (Chao1,  $p$ -value = 0.2319, Shannon,  $p$ -value = 0.3818; Simpson,  $p$ -value = 0.3676).

Finally, a dose-dependent response was evaluated for DDAC-C10.

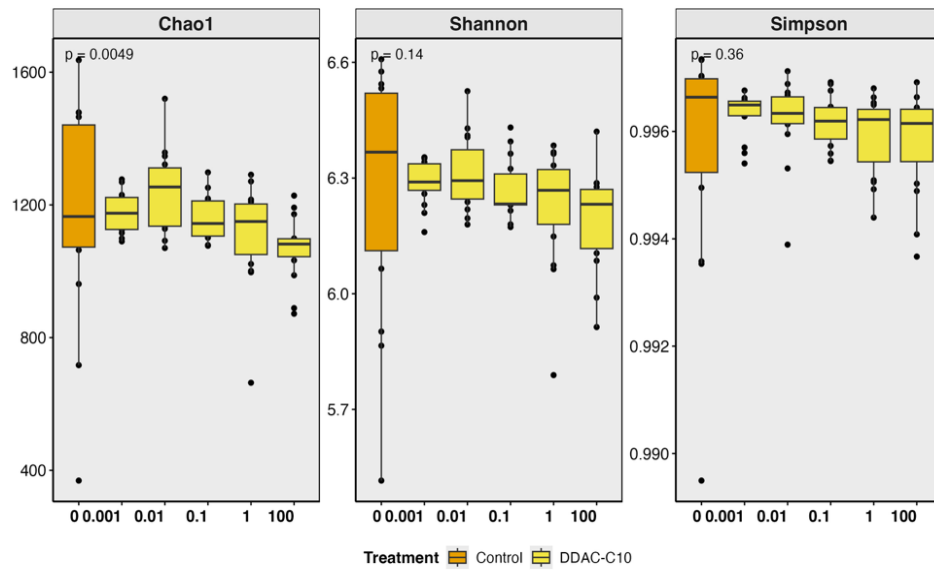


**Figure 17 - Alpha diversity indices (Chao1, Shannon, and Simpson) comparing control and DDAC-C10 through concentration range (0.001, 0.01, 0.1, 1, 100 mg/kg).**

The Figure 17 suggests that DDAC-C10 doesn't change bacterial evenness throughout the range of concentrations (Shannon,  $p$ -value = 0.144; Simpson,  $p$ -value = 0.3615), but reduces richness at the highest concentration, 100 mg/kg (Chao1,  $p$ -value = 0.004935), confirmed by pairwise comparisons between 0, 0.001 mg/kg and 0.01 mg/kg to 100 mg/kg ( $p$  adj Benjamini-Hochberg method < 0.05).

## BETA-DIVERSITY

To evaluate the structure of the bacterial communities, Bray-Curtis Distance was considered and confirmed by ANOSIM.

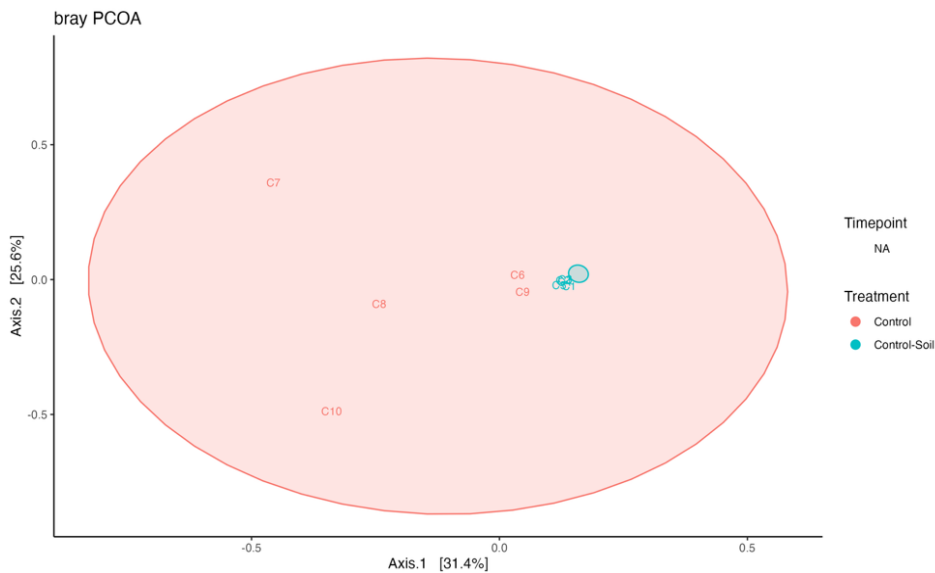


**Figure 18** - PCoA with Bray-Curtis distances comparing control-soil (soil without sand) and control (with sand).

The above PCoA plot based on Bray-Curtis distances showed significant differences between the control with sand and the control-soil in bacterial community structure ( $p$ -value  $< 0.05$ ) (Figure 18). The axis 1 explains 31.4% and axis 2, 25.6%, of the variation between samples. It was also observed that a small cluster for the control soil.

### ATMAC-C16

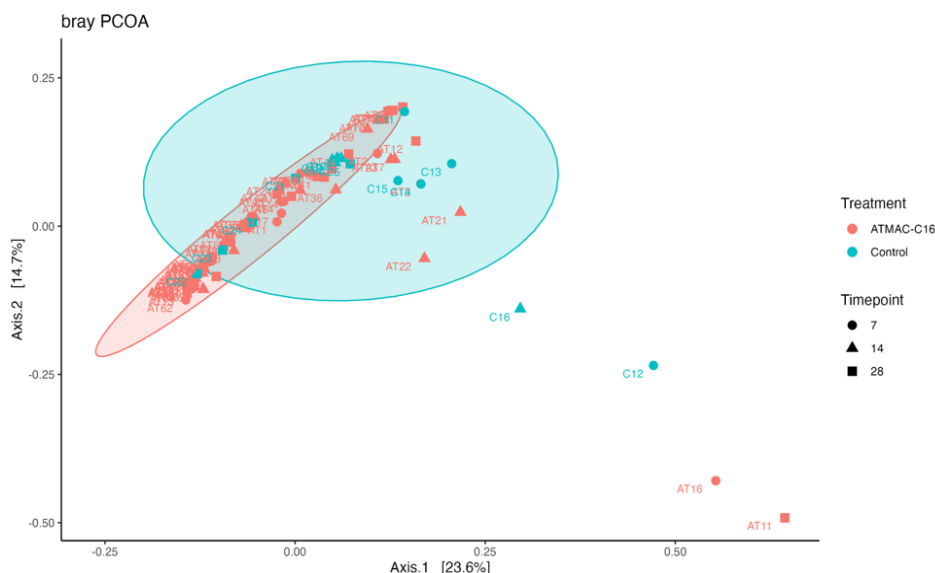


**Figure 19** - PCoA of Bray-Curtis distances for ATMAC-C16 samples, showing clustering by treatment. Timepoints are represented by distinct symbols.

Regarding ATMAC-C16 compound, the Figure 19 illustrates two distinct clusters, resulting from the shift in the community structure caused by this compound. In total, the axis represents 38.3% of the variation. Some samples, like AT11 and AT16 show dissimilarity, being potentially outliers.

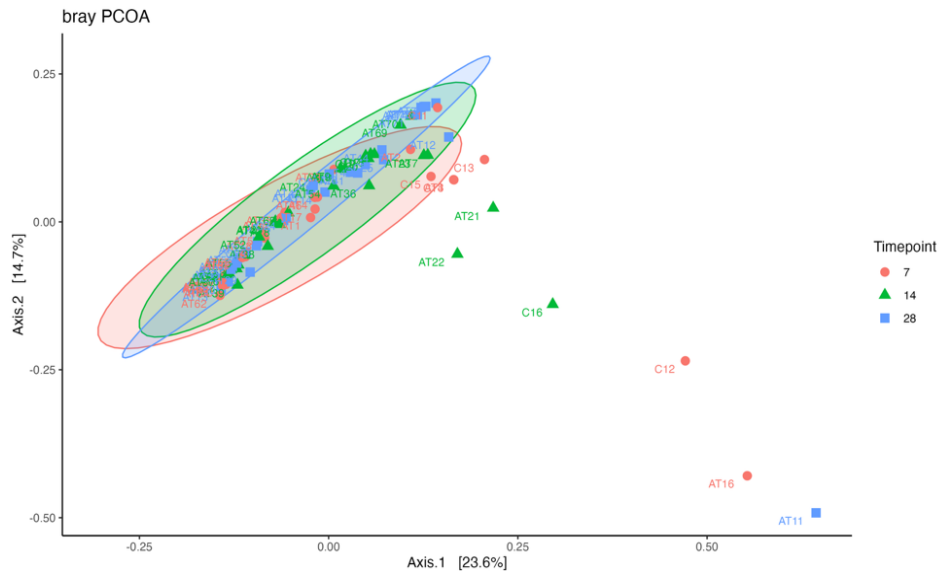


**Figure 20** - PCoA based on Bray-Curtis distances illustrating clustering of ATMAC-C16 samples by timepoint (T7 - red, T14 - green, T28 - blue).

The community doesn't change over time ( $p$ -value = 0.0676) as shown by the overlap of clusters (Figure 20). Only 23.6% axis 1 and 14.7% on axis 2 measure the variation between samples.

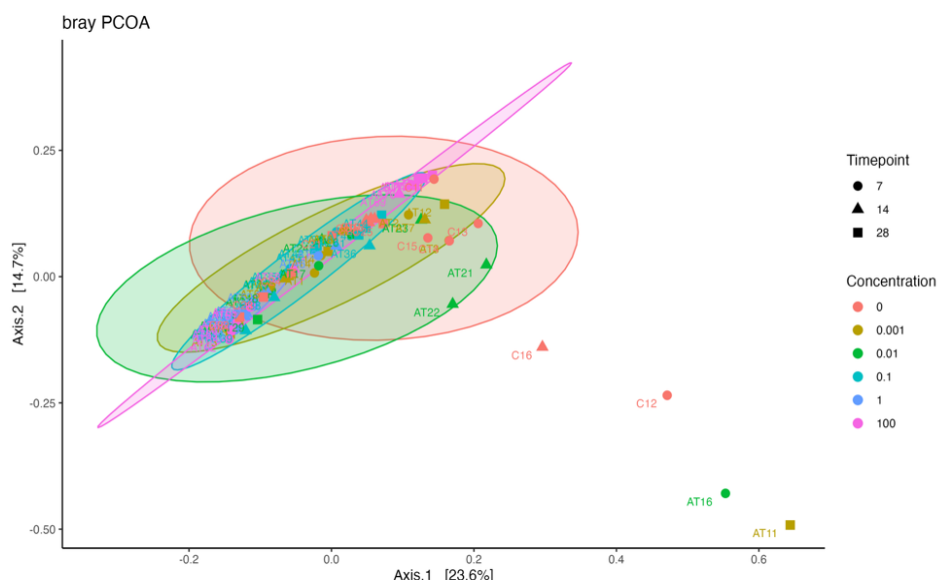


**Figure 21** - PCoA based on Bray-Curtis distances illustrating clustering of ATMAC-C16 samples by concentration, 0 (red), 0.001 (olive-green), 0.01 (green), 0.1 (light-blue), 1 (dark-blue), 100 (pink) mg/kg.

On the other hand, concentration seems to form distinct clusters, even if dissimilarity is only represented by 23.6% on Axis 1 and 14.7% on Axis 2 ( $p$ -value  $< 0.05$ ) (Figure 21).

## BAC-C12

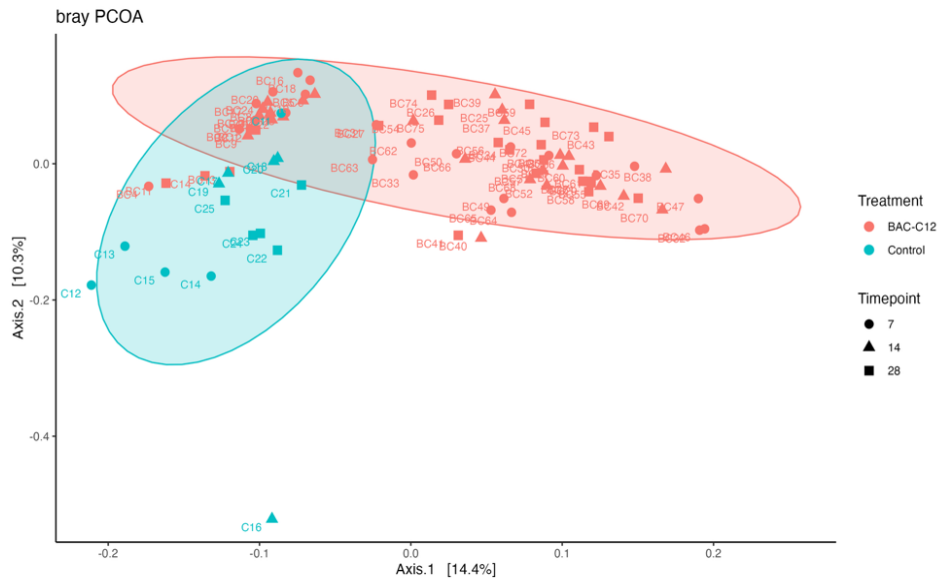


**Figure 22** - PCoA of Bray-Curtis distances for BAC-C12 samples, showing clustering by treatment. Timepoints are represented by distinct symbols.

The PCoA with Bray-Curtis distances above shows a clear clustering by treatment, despite the low variance captured by Axis 1, 14.4% and Axis 2, 10.3% ( $p$ -value  $< 0.05$ ) (Figure 22).

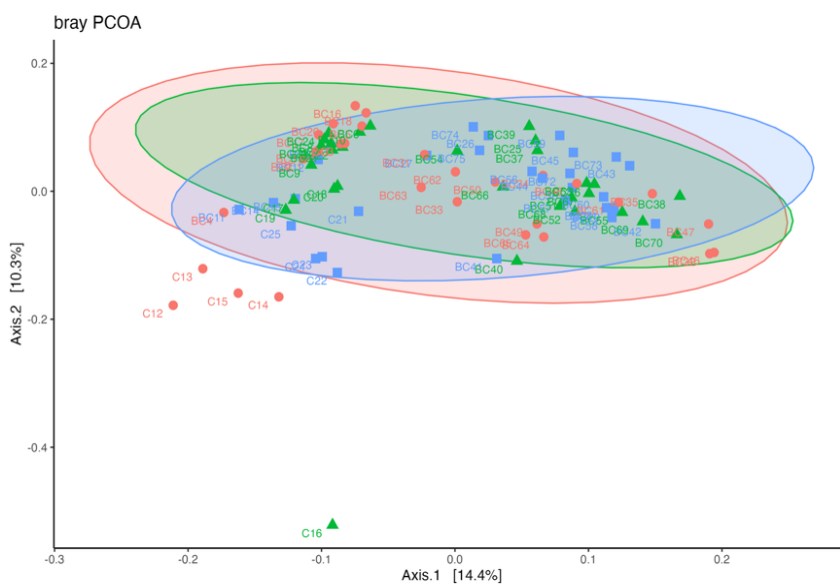


**Figure 23** - PCoA based on Bray-Curtis distances illustrating clustering of BAC-C12 samples by timepoint (T7 - red, T14 - green, T28 - blue).

As opposed to ATMAC-C16, bacterial community structure changes over time, forming a more concise clustering at time point 28 (Figure 23). The PCoA axis 1 and 2, 14.4% and 10.3% respectively, partly explained this similarity ( $p$ -value < 0.05).

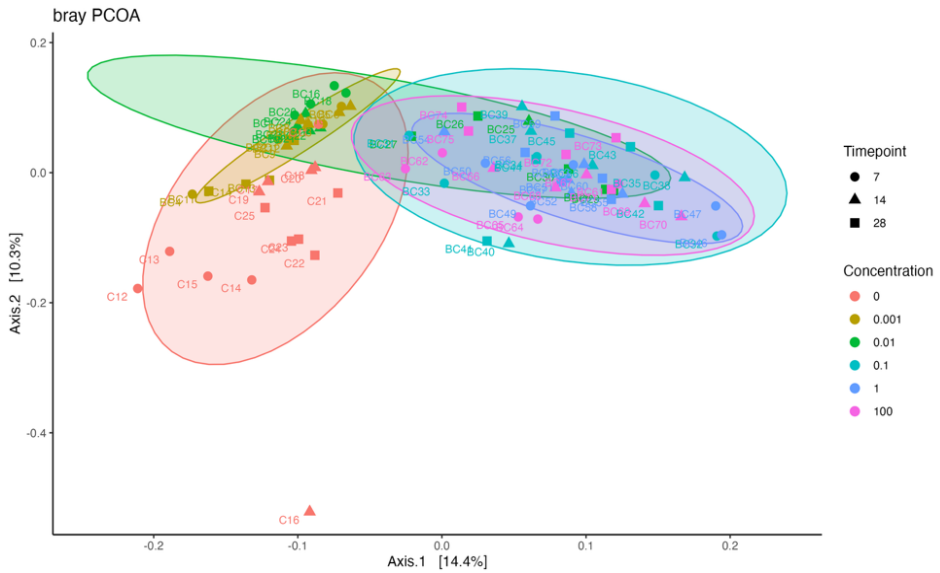


**Figure 24 -** PCoA based on Bray-Curtis distances illustrating clustering of BAC-C12 samples by concentration, 0 (red), 0.001(olive-green), 0.01(green), 0.1(light-blue), 1 (dark-blue), 100(pink) mg/kg.

It is even clearer the distinction between concentrations (Figure 24), with special emphasis between 0.001 mg/kg and 100 mg/kg, as it shows the separate clusters ( $p$ -value < 0.05). It seems to be a similarity in community structure between the last three concentrations, as it shows an overlap of clusters. This variation is only explained by 14.4% on Axis 1 and 10.3% on Axis 2.

## DDAC-C10

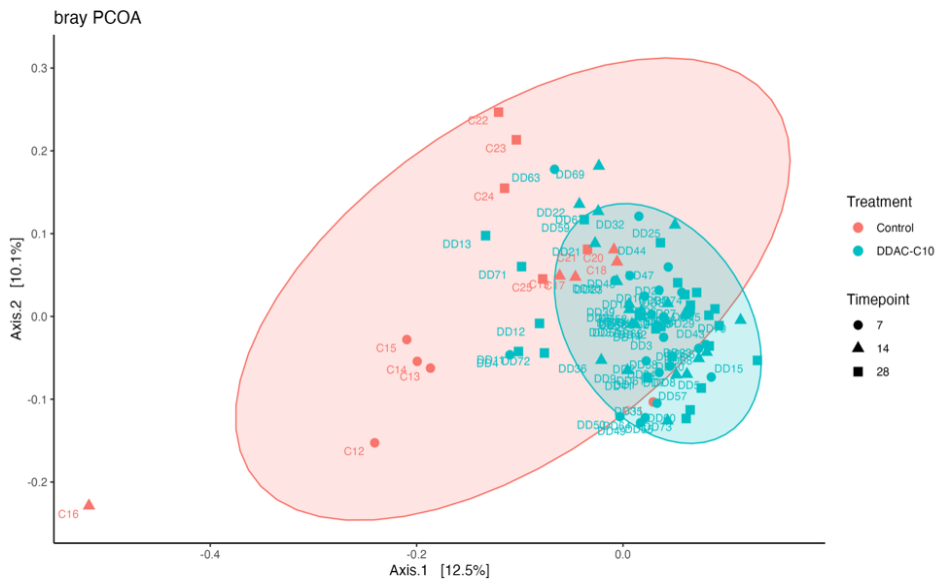


**Figure 25** - PCoA of Bray-Curtis distances for DDAC-C10 samples, showing clustering by treatment. Timepoints are represented by distinct symbols.

Regarding DDAC-C10, bacterial structure shifts in the presence of this chemical compound (Figure 25). The PCoA axis 1 and 2, 12.5% and 10.1% respectively, partly explained this variation ( $p\text{-value} < 0.05$ ).

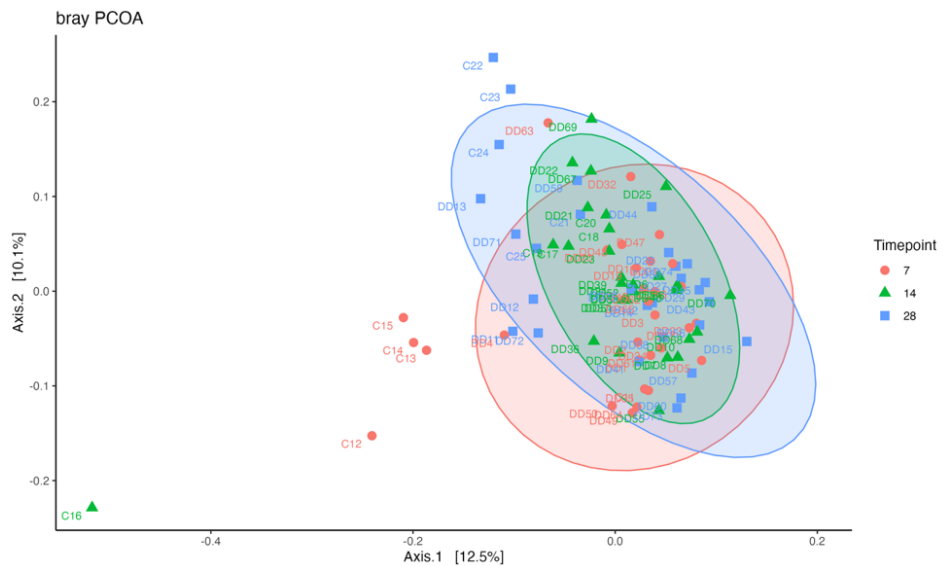


**Figure 26** - PCoA based on Bray-Curtis distances illustrating clustering of DDAC-C10 samples by timepoint (T7 - red, T14 - green, T28 - blue).

Again, time seems to drive the bacterial structure (Figure 26). The PCoA with Bray-Curtis distances shows a partial separation on timepoint 7, with few samples falling outside the

red cluster, which indicates a greater variability at this point. Axis 1 and Axis 2 explained 12.5% and 10.1% of the total variation, respectively.

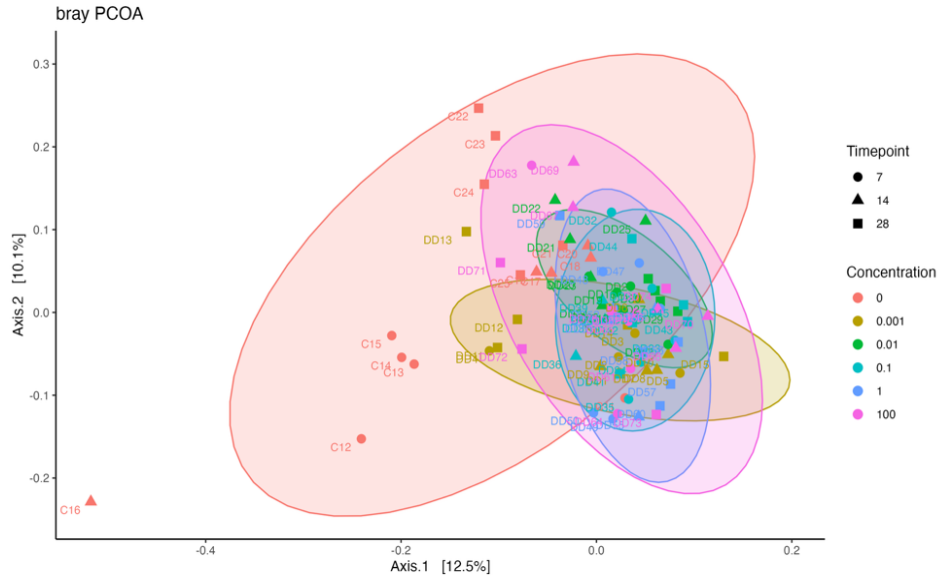


**Figure 27 - PCoA based on Bray-Curtis distances illustrating clustering of DDAC-C10 samples by concentration, 0 (red), 0.001(olive-green), 0.01(green), 0.1(light-blue), 1 (dark-blue), 100(pink) mg/kg**

The PCoA above represents the effects of different dosages of DDAC-C10 on the bacterial community (Figure 27). It was observed a more distinct separation was observed between the lowest concentration, 0.001mg/kg, and the highest, 100 mg/kg. The observed variation is partially explained by Axis 1, 12.5%, and Axis 2, 10.1%.

## BACTERIAL COMMUNITY COMPOSITION

First, to see if the sand introduced bacteria to the system or shifted the taxa composition of the soil, taxonomy plots were compared between the control-soil and the control with sand.

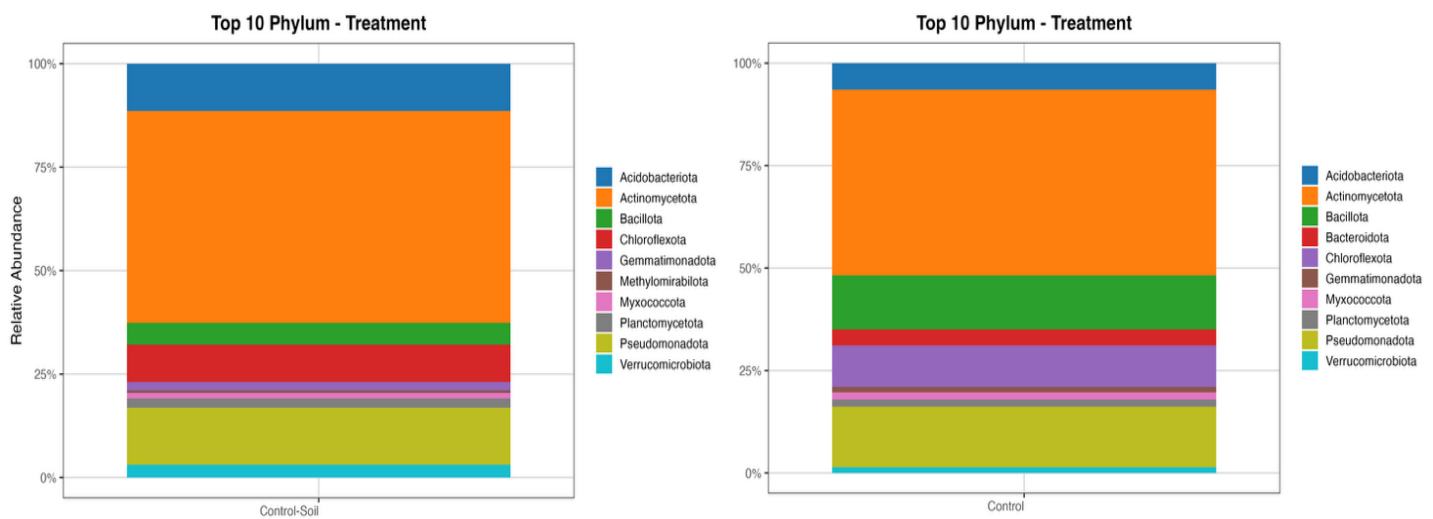


**Figure 28** - Top 10 Phylum of control-soil (left) and control (right).

The Top 10 most abundant taxa plot above display a different composition between control-soil and the control with sand (Figure 28). Both are composed of *Acidobacteriota*, *Actinomycetota*, *Bacillota*, *Chloroflexota*, *Gemmatimonadota*, *Myxococcota*, *Planctomycetota*, *Pseudomonadota*, and *Verrucomicrobiota*. The soil without sand presented a higher amount of *Actinomycetota* and *Acidobacteriota* than the soil with sand. On the other hand, *Bacillota* and *Chloroflexota* phyla were more represented in the control with sand. It was noticed the presence of *Methylophilobactera* on control soil, and *Bacteroidota* on the control with sand.

## ATMAC-C16

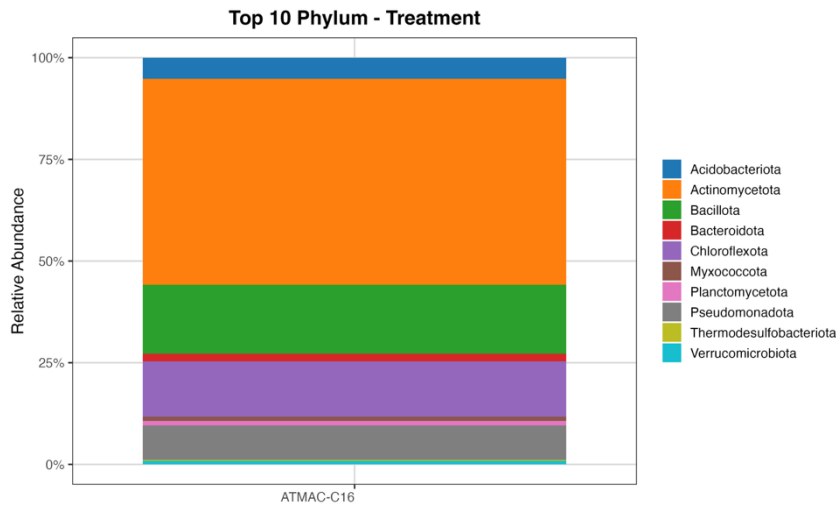


**Figure 29** - Top 10 Phyla of ATMAC-C16 treated soil.

In comparison to control groups, ATMAC-C16 has a similar composition regarding the most abundant taxa with control, with the sand, apart from the presence of the *Thermodesulfobacteriota* phylum (Figure 29). The phyla *Actinomycetota* and *Bacillota* were the most represented taxa.

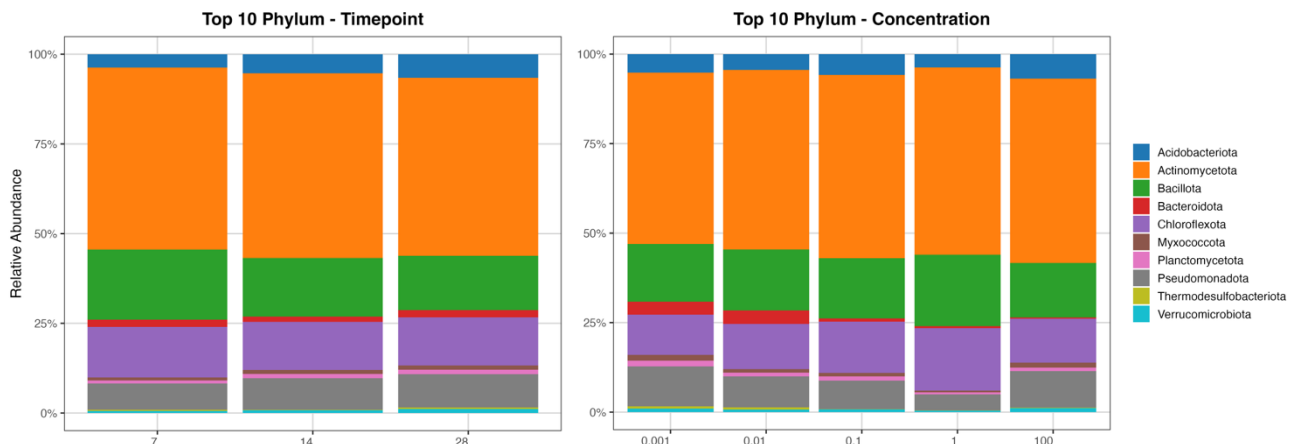


**Figure 30** - Top 10 phyla in ATMAC-C16-treated soil across timepoints (left) and concentrations (right).

There are no significant differences between the most abundant taxa over time (Figure 30 – left plot), but some variation was observed throughout the range of concentrations, being the *Bacteroidota* phylum reduced after 0.01 mg/kg.

## BAC-C12

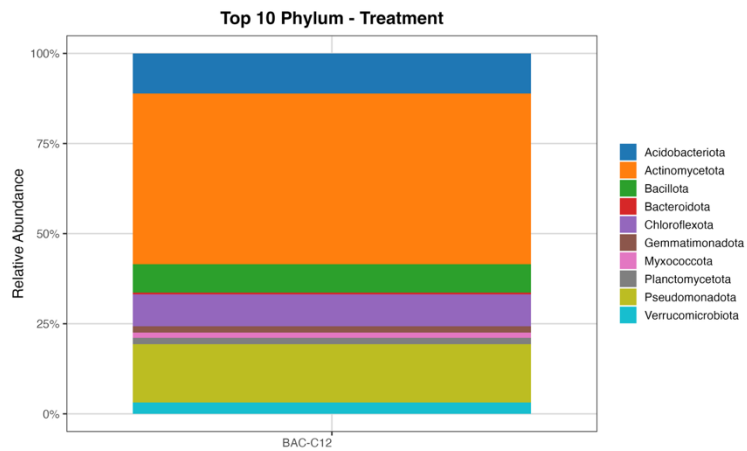


**Figure 31** - Top 10 Phyla of BAC-C12 treated soil.

The most abundant taxa in soil treated with BAC-C12 are similar to the control group (Figure 31).

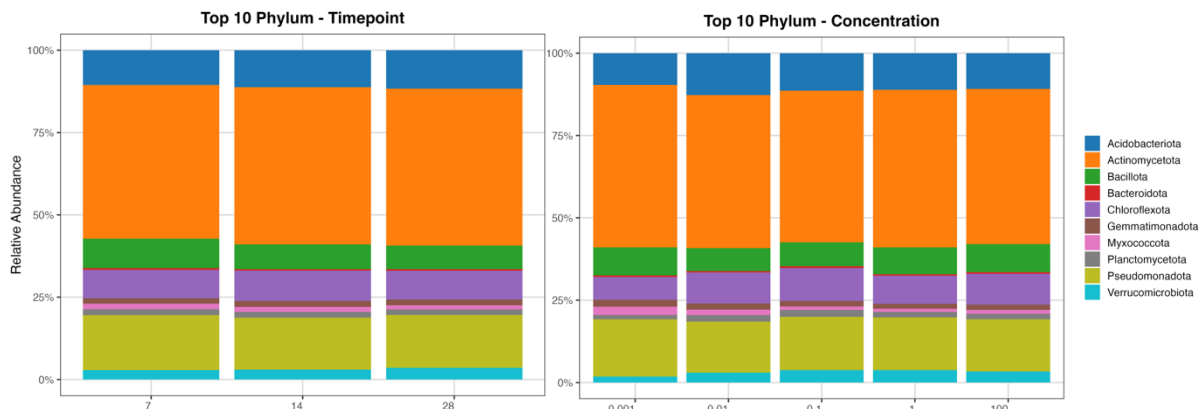


**Figure 32** - Top 10 phyla in BAC-C12-treated soil across timepoints (left) and concentrations (right).

The top 10 phyla didn't show any differences over time (Figure 32 – left) and concentration range (Figure 32 – right).

## DDAC-C10

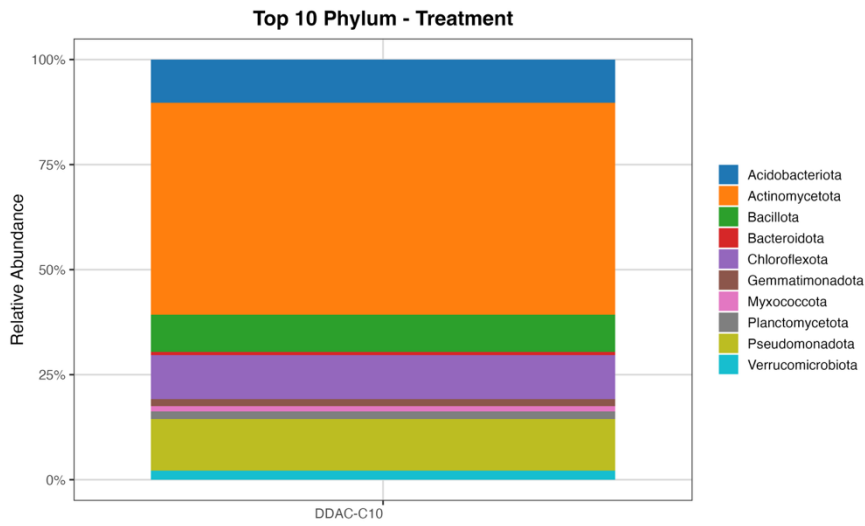


**Figure 33** - Top 10 Phyla of DDAC-C10 treated soil.

Again, the DDAC-C10 composition of the most abundant taxa is similar to the control group (Figure 33).

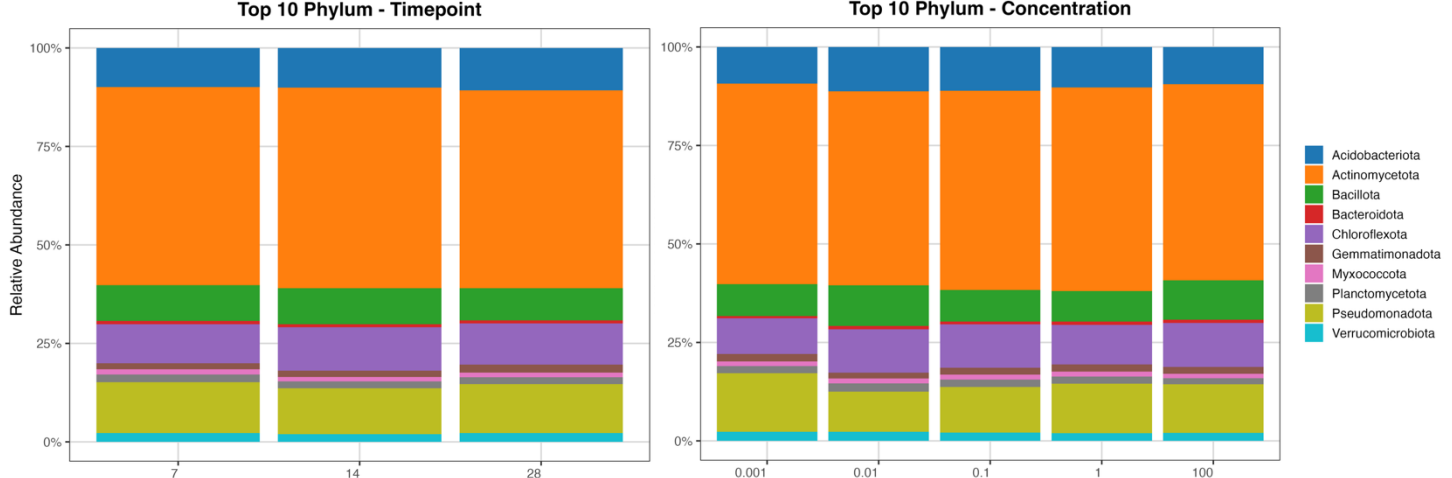


**Figure 34** - Top 10 phyla in DDAC-C10-treated soil across timepoints (left) and concentrations (right).

The plots above show the stability of the effect that DDAC-C10 has on the most abundant taxa throughout time and concentration range.

## Heatmap – Genera across treatments

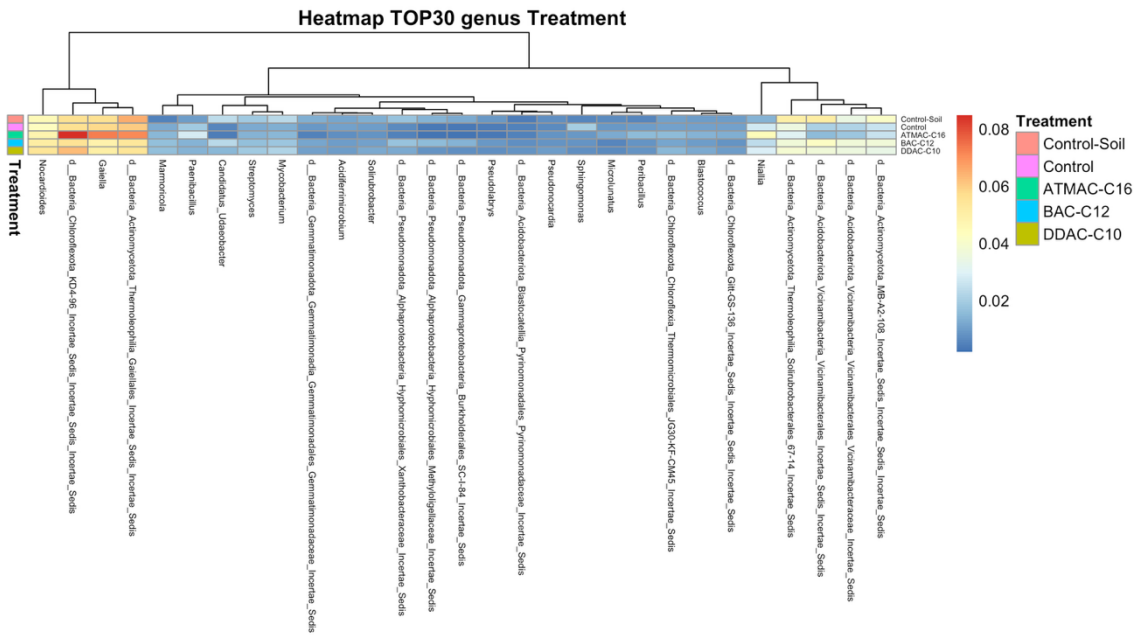


**Figure 35** - Heatmap of the top 30 bacterial genera based on relative abundance across treatments. Bacterial genera are shown along the bottom axis, and treatments are indicated on the right.

The top 30 genera of each treatment were compared (Figure 35). It was identified a high relative abundance of a not-assigned genus from *Chloroflexota*-KD4-96 Order and the *Gaiella* genus on ATMAC-C16-treated soil. Overall, the consistent color patterns in the heatmap suggest that soil microbial composition remained stable across treatments for the 30 most abundant genera.

## DIFFERENTIAL ABUNDANCES ANALYSIS – DESEQ2

To better understand the fluctuation in bacterial composition throughout the concentration range, DESeq2 was performed on each chemical compound.

### ATMAC-C16

To verify the bacterial composition on the statistically significant downfall depicted in the alpha-diversity plot (Figure 11), differences between control (0) and 1 mg/kg, and comparison between control and 100 mg/kg were investigated.

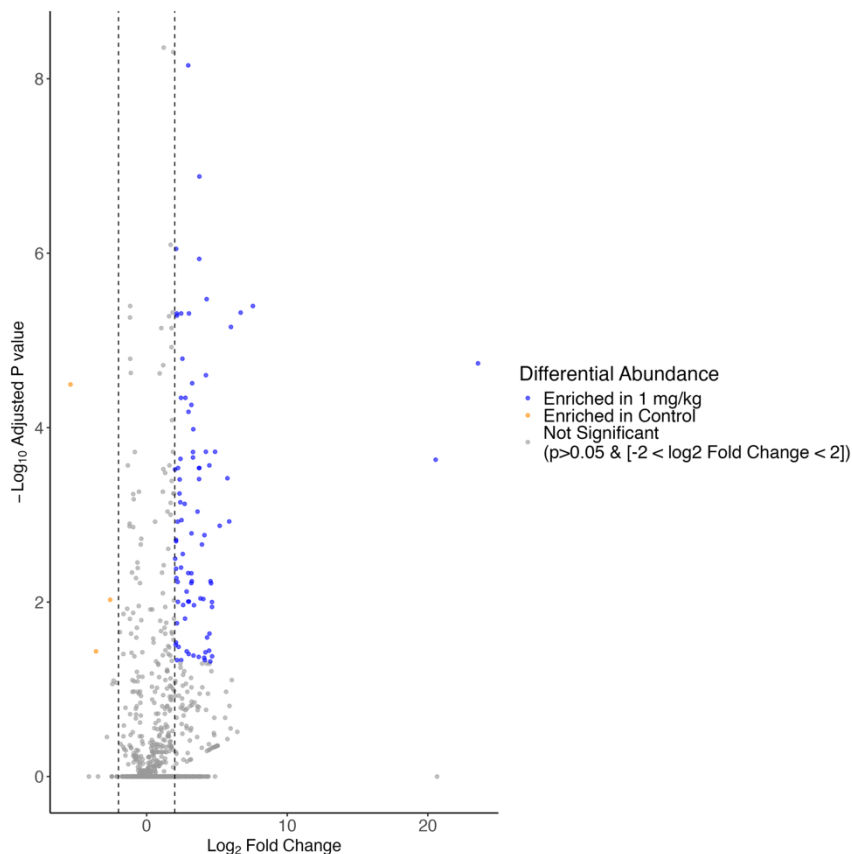


**Figure 36** - Volcano plot of ATMCA-C16 treated soil, comparing control and 1 mg/kg.

The volcano plot above illustrates the number of taxa that increased (blue dots) and decreased (orange dots) over the concentration downfall between 0 and 1 mg/kg of ATMAC-C16. To identify which genera increased or decreased, the heatmap of Log2 Fold Change shown below was used.



**Figure 37 - Heatmap of genus-level log<sub>2</sub> fold changes (sorted by value).** Bacterial genera are listed on the right, and comparisons are shown on the bottom axis. Color scale represents log<sub>2</sub> fold change (0-1mg/kg) – ATMAC-C16.

Some genera were identified (Figure 37): *Rikenella* and *Mucispirillum* had the highest Log2 Fold Change (dark orange lines) ( $p\text{-adj}<0.05$ ), and *Embleya*, followed by *Pseudalkalibacillus* and *Thermoslavimicrobium*, had the lowest Log2 Fold Change (blue lines) ( $p\text{-adj}<0.05$ ), representing a decrease in their abundances over the concentration spectrum.

A more focused look at the highest concentration, 100 mg/kg, allowed for more taxa to be identified (Figure 38).

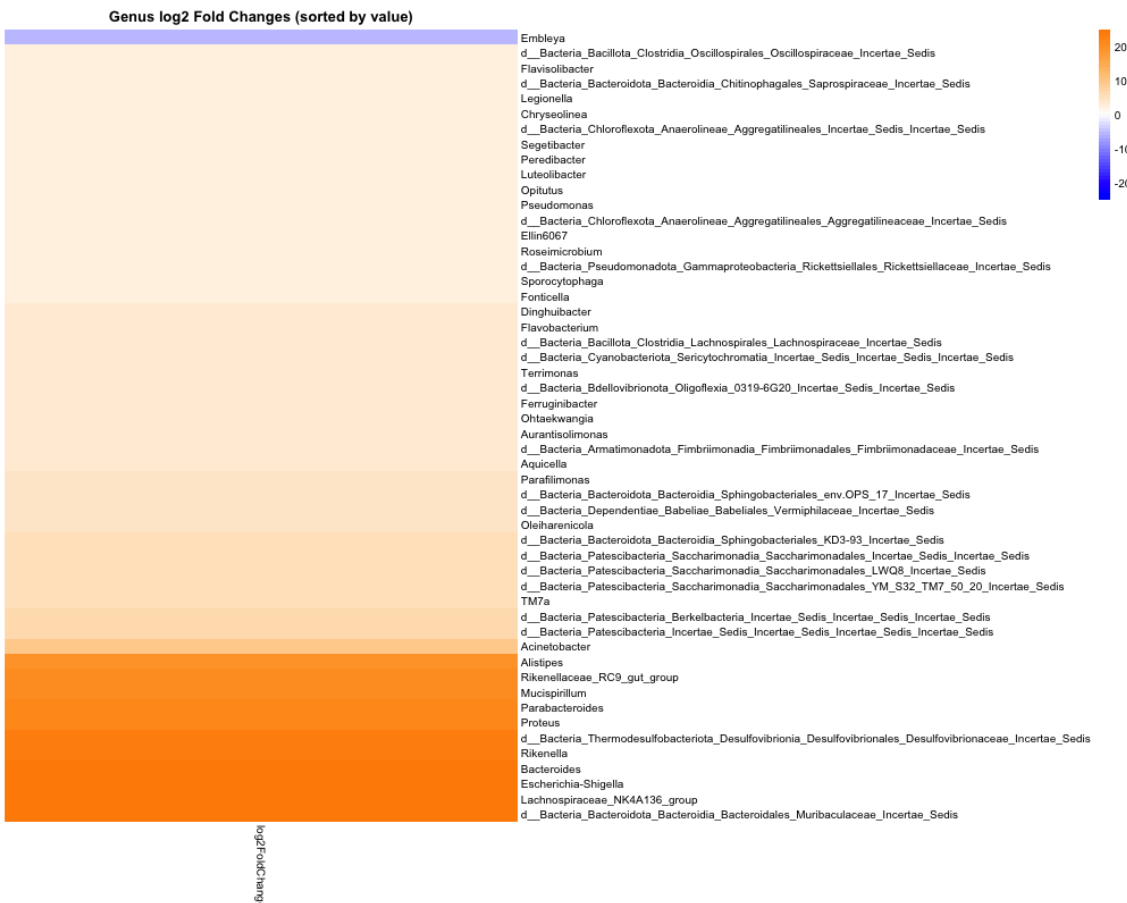


**Figure 38** - Heatmap of genus-level log<sub>2</sub> fold changes (sorted by value). Bacterial genera are listed on the right, and comparisons are shown on the bottom axis. Color scale represents log<sub>2</sub> fold change (0-100mg/kg) – ATMAC-C16.

Several taxa had very high Log2 Fold change values, showing an increase in abundances of some of the following taxa besides the previously identified: *Bacteroides*, *Escherichia-Shigella*, *Proteus*, *Parabacteroides*, *Alistipes* (orange lines) (p-adj<0.05). The genus *Embleya* continued to have its abundance reduced with the increase of the dosage of ATMAC-C16.

## BAC-C12

Again, the bacterial composition shifts observed in alpha diversity PCoA (Figure 14) indicated a similar response between lower concentrations (0-0.001-0.01 mg/kg). In this way, the transition between 0.01 mg/kg and 0.1 mg/kg was tackled: alterations in taxa abundances between 0-100 mg/kg and 0-0.001 mg/kg were observed.

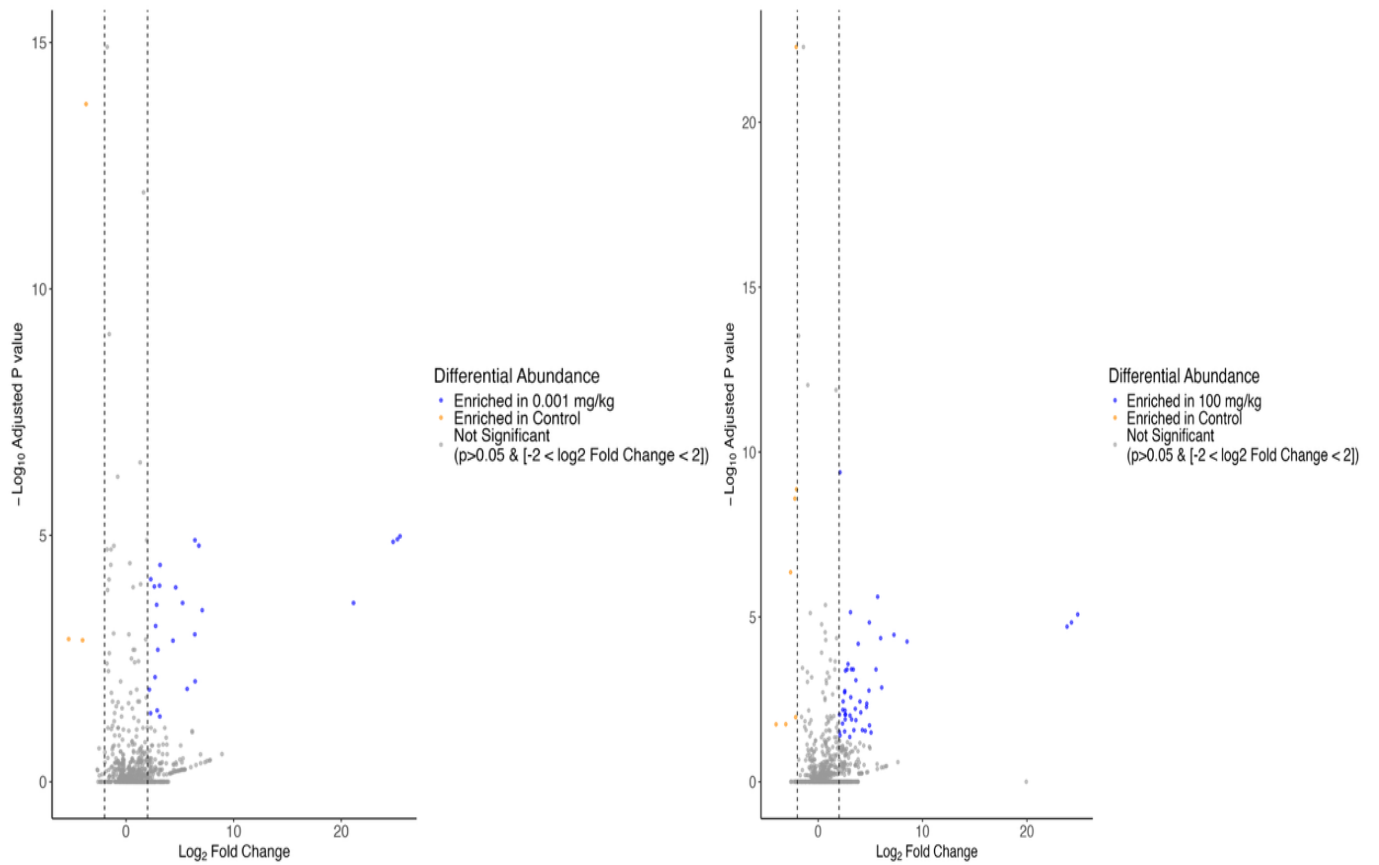


**Figure 39** - Volcano plots of BAC-C12 treated soil, comparing control and 0.001 mg/kg (left) and 100 mg/kg (right).

Since the difference in bacterial composition between the control (0) and the addition of 0.001 mg/kg is not statistically significant (Figure 39 – left), a contrast was observed regarding the number of taxa abundances that increased and decreased after the 0.1 mg/kg transition (Figure 39 - right). To identify which genera increased or decreased, the heatmap of Log2 Fold Change below was used.



**Figure 40** - Heatmap of genus-level log<sub>2</sub> fold changes (sorted by value). Bacterial genera are listed on the right, and comparisons are shown on the bottom axis. Color scale represents log<sub>2</sub> fold change (0-100mg/kg) – BAC-C12.

From the heatmap displayed above, *Embleya*, a not-assigned *Azospirillales* (taxonomic rank: Order), and the *mle1-7* genera had the lowest Log2 Fold Change values (blue lines), indicating a decrease in their abundance when 100 mg/kg of BAC-C12 is added to the soil. On the other hand, *Escherichia-Shigella*, a not-assigned *Muribaculaceae* (taxonomic rank: Family) genus, *Bacteroides*, and *Defluvitoga* genera were overrepresented (orange lines) (p-adj < 0.05).

## *DDAC-C10*

Aligning with alpha diversity results, the dichotomy presence/absence of DDAC-C10 was considered.

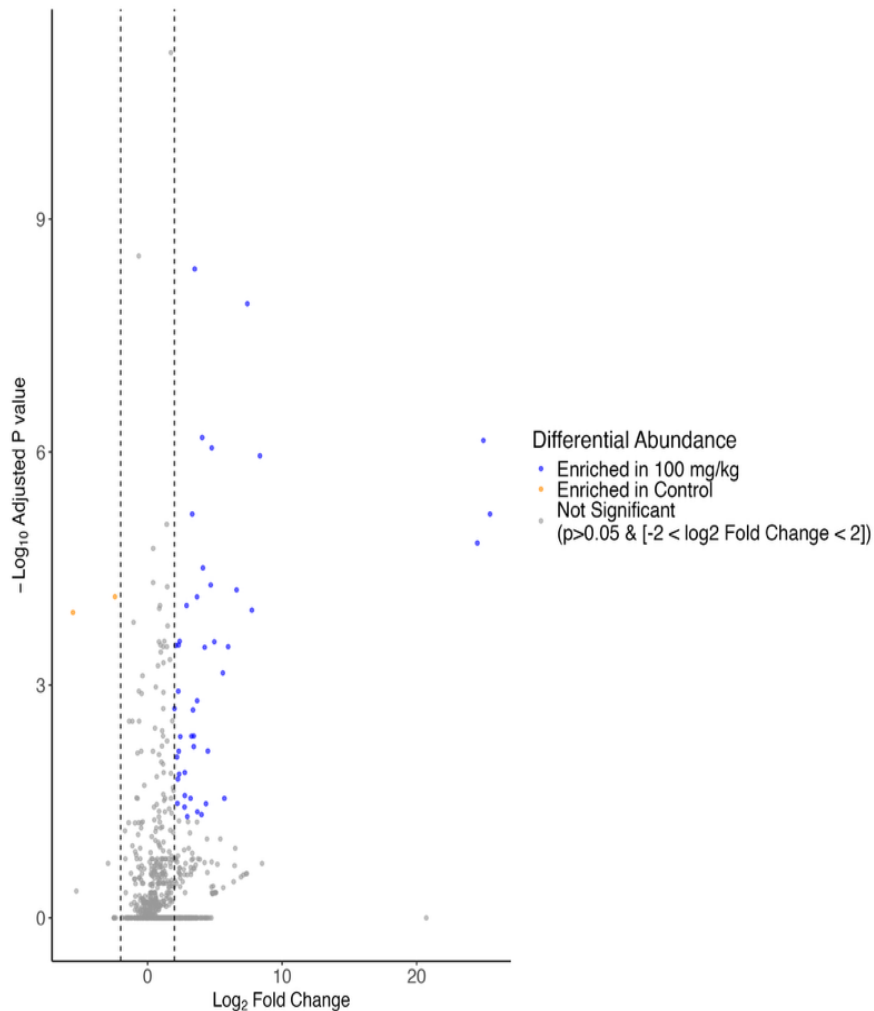


**Figure 41** - Volcano plot of DDAC-C10 treated soil, comparing control and 100 mg/kg.

The volcano plot above represents the comparison of the absence (0 mg/kg – control) and the presence of the highest concentration, 100 mg/kg. It was noticed that a higher number of taxa increased (blue dots) ( $\text{Log}_2 \text{ Fold Change} > 2$ ) than the number of taxa that decreased (orange dots) ( $\text{Log}_2 \text{ Fold Change}$  lower than -2) ( $p\text{-adj} < 0.05$ ).

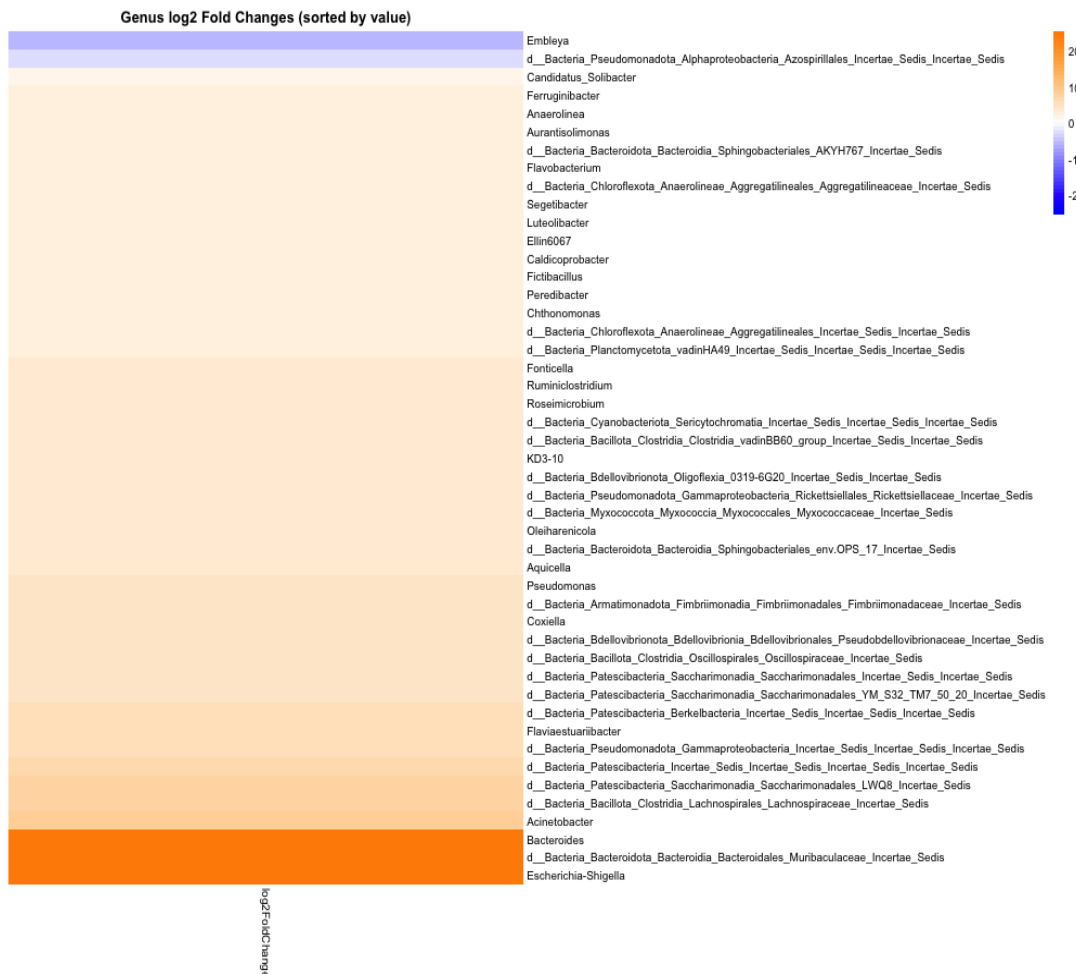


**Figure 42** - Heatmap of genus-level log<sub>2</sub> fold changes (sorted by value). Bacterial genera are listed on the right, and comparisons are shown on the bottom axis. Color scale represents log<sub>2</sub> fold change (0-100mg/kg) – DDAC-C10.

Again, the same taxa described for the previous compounds were identified. There were three genera with the highest Log2 Fold change values: *Escherichia-Shigella*, a not-assigned *Muribaculaceae* (taxonomic rank: Family) genus, and *Bacteroides* (orange lines). The two orange dots in the volcano plot represented *Embleya* and not-assigned *Azospirillales* (taxonomic rank: Order) genera, which indicated a decrease in the abundance of these taxa (blue lines) ( $p\text{-adj}<0.05$ ).

## FUNCTIONAL PREDICTION – FAPROTAX

To associate bacterial composition, especially regarding the statistical differences in the shifts of the identified taxa for each compound shown by differential abundance analysis, the FAPROTAX tool was used to match potential functions to the bacterial community.

### ATMAC-C16

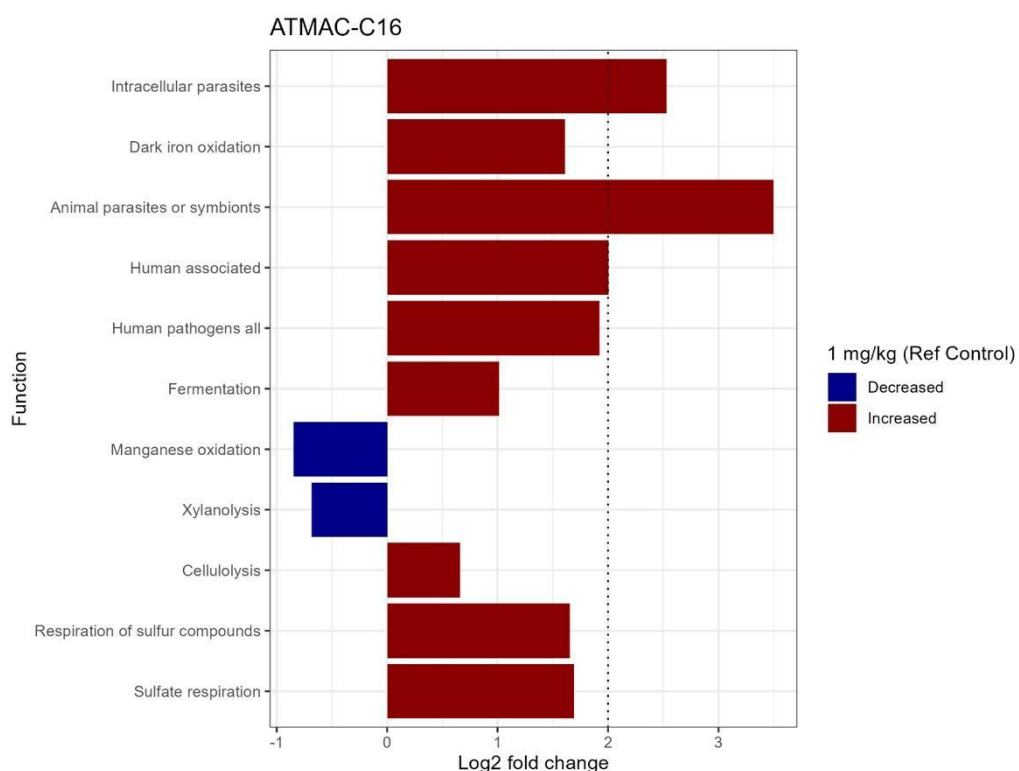


**Figure 43** - Functional changes in ATMAC-C16-treated soil relative to control (1 mg/kg), shown as log<sub>2</sub>fold changes. Red bars represent increased functions; blue bars represent decreased functions.

This chemical compound was associated with the following functions (Figure 43): sulfate and sulfur compounds respiration, cellulolysis (lysis of cellulose), xylanolysis (lysis of xylan), oxidation of manganese, fermentation, ferrous iron anaerobic oxidation (“dark\_iron\_oxidation”), and even the identification of potential human and animal pathogens ( $p\text{-adj}<0.05$ ).

## BAC-C12

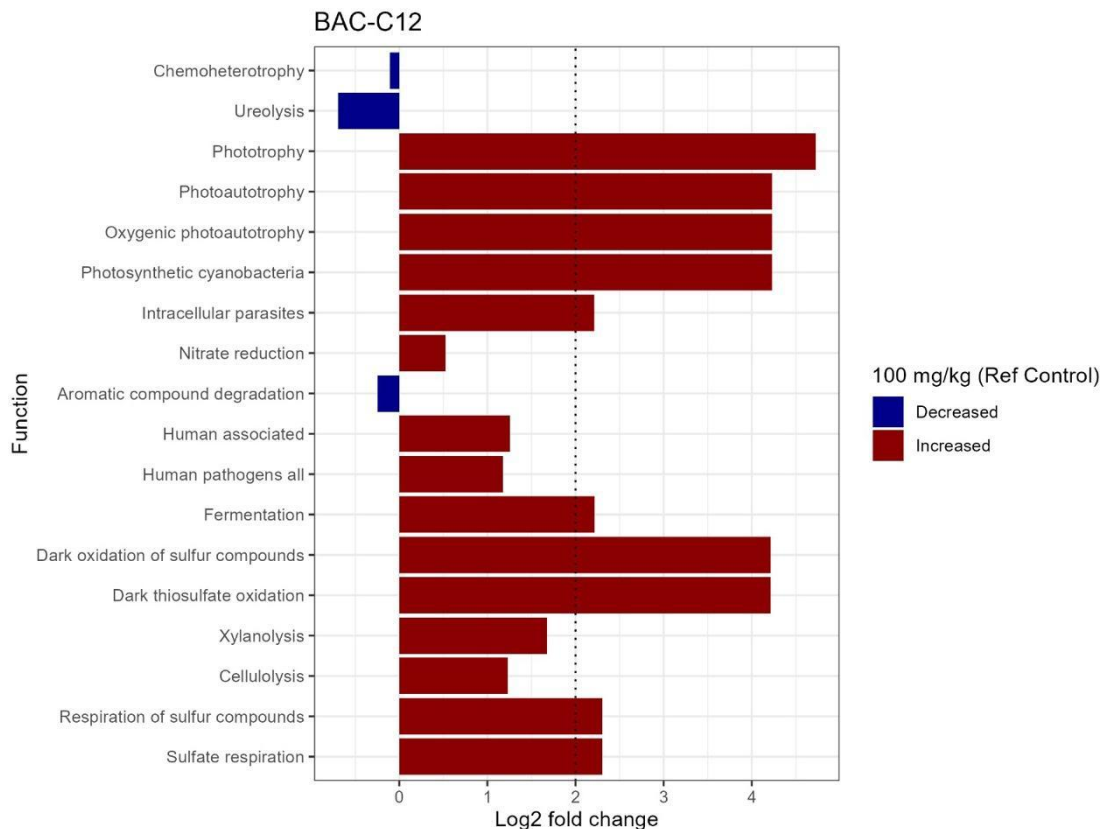


**Figure 44** - Functional changes in BAC-C12-treated soil relative to control (100 mg/kg), shown as log<sub>2</sub> fold changes. Red bars represent increased functions; blue bars represent decreased functions.

The following functions were predicted in the presence of BAC-C12 (Figure 44): sulfate and sulfur compounds respiration, thiosulfate and sulfur compounds anaerobic oxidation, photosynthesis by cyanobacteria, photo and photoautotrophy, (all, Log 2 Fold Change >2), and three downregulated functions (Log 2 Fold Change <0), ureolysis, aromatic compound degradation (p-adj<0.05).

## DDAC-C10

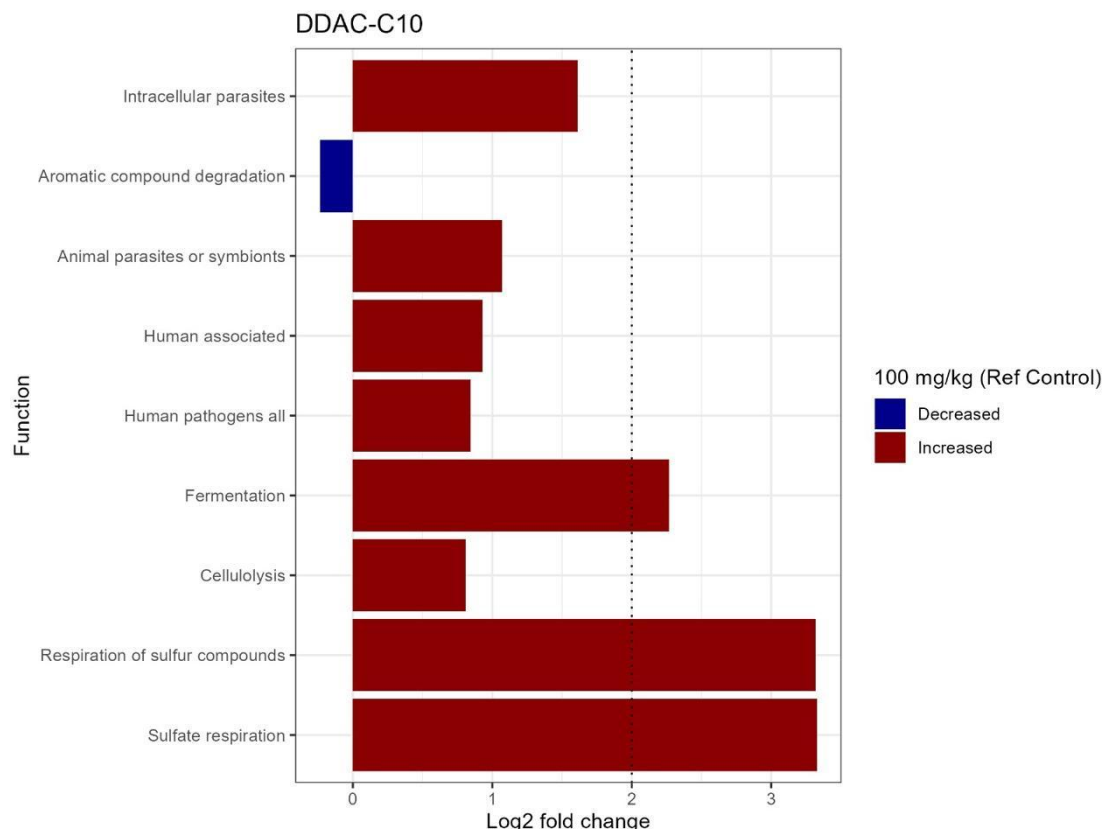


**Figure 45** - Functional changes in DDAC-C10-treated soil relative to control (100 mg/kg), shown as log<sub>2</sub> fold changes. Red bars represent increased functions; blue bars represent decreased functions.

The bar plot above shows the following functions predicted on soil treated with DDAC-C10: sulfate and sulfur compounds respiration, and fermentation ( $p\text{-adj}<0.05$ ) ( $\text{Log } 2$  Fold Change  $> 2$ ), and aromatic compound degradation ( $\text{Log } 2$  Fold Change  $< 0$ ).

## Discussion

As previously mentioned, QACs are contaminants of growing concern, especially after the COVID-19 pandemic (Hora et al., 2020; Li et al., 2025). These ubiquitous contaminants reach the soil ecosystems through several ways, such as pesticides, contaminated wastewater and manure, and application of contaminated sewage sludges (Yang et al., 2023; Zeng et al., 2024). This study addressed the QACs contamination issue in soil by understanding how three different compounds from three different QAC's subgroups altered the soil bacterial community. To achieve this, a lab-based microcosm experiment was developed to simulate QAC's introduction into soil.

Although Danish soil is, overall, considered poor in organic matter, due to being highly leached (Adhikari et al., 2013), the number of identified taxa after sequencing, 38772, is appropriate for the type of soil used, from a research agricultural field, and the number of samples used, 252. Nonetheless, low DNA amount in each sample was a setback for DNA extraction, but tailored procedures were taken across the study to handle the low-biomass microbiome set by (Fierer et al., 2025) study.

The soil bacterial community showed different patterns between the different QACs. First, a closer look at alpha-diversity was taken to dissect bacterial composition across treatments. It was shown that introducing the sand, required to perform the spiking of the soil, didn't alter bacterial composition, as control and control-soil had no significant differences in Chao1, Shannon or Simpson measurements (Figure 7). It was also noticed that the control used for the comparisons, the control with the sand, had an increase of richness at time point 14 (Figure 8), although not statistically significant. This could be explained by the fact that bacteria increase the number of generations over time. However, such an explanation doesn't align with the decrease at time point 28. Another factor that should be taken into consideration is that the samples were independent by time point: T7 samples were collected after 7 days, while T14 and T28 samples remained in incubation. Subsequently, T14 samples were collected after 14 days, followed by T28 at 28 days. No repeated measurements were made on the same samples over time. Even though bacterial richness and evenness were similar between controls, bacterial structure varied, as predicted (Figure 18). The soil microbiome is sensitive to perturbations such

as the introduction of sand, which disrupts biofilms and cell aggregates (Ossowicki et al., 2021). Nonetheless, sand didn't seem to introduce a different set of bacterial taxa, as the most abundant taxa were very similar between controls (Figure 28).

In the case of ATMAC-C16, introducing this molecule into the soil had an impact on soil bacteria (Figure 9). However, no corresponding effect was observed over time (Figure 10). Besides not being time-dependent, the ATMAC-C16 effect is dose-dependent (Figure 11). As expected, the higher the concentration, the lower the bacterial richness. Also, the decrease of dominant taxa in the system increased the diversity, as shown by the Simpson index plot, which could mean the most abundant taxa might be sensitive to ATMAC-C16. This behavior quickly changes when the system encounters the highest concentration, 100 mg/kg, which could explain the nonsignificant value of the Chao1 index (Chao1, *p*-value = 0.07354). It would be expected to have a high bactericidal effect, and not a “re-gain” in bacterial richness. Such an occurrence may be explained by contamination or even the appearance of an opportunistic effect, where, in a destabilized ecosystem, some bacteria may benefit due to a lack of nutrition competition, as seen in the gut microbiome (Wang et al., 2018). Nevertheless, ATMAC-C16 still caused an impact on bacterial structure (confirmed by ANOSIM *p*-value<0.05) (Figure 19), but not on timepoint effect (*p*-value = 0.0676) (Figure 20). At the concentration level (Figure 21), the clustering of the low concentrations and the slightly distance from the absence (control) of ATMAC-C16, validates the alpha diversity results. On this matter, compared to controls, a different phylum was identified in the top 10, *Thermodesulfobacteriota*. Also, the phyla *Actinomycetota* and *Bacillota* were the most represented taxa (Figure 29). No major differences in the top 10 phyla were noticed across time and dose (Figure 30). However, when looking at the top 30 genera (Figure 35), a high relative abundance of a not-assigned genus from *Chloroflexota-KD4-96* (taxonomic rank: Order) and the *Gaiella* genus was noticed.

This information served as a cue to observe which and how taxa behave in the presence of ATMAC-C16. For that, DESeq2 analysis allowed for evaluation of the downfall presented in alpha diversity plots. Comparisons between absence (control) and 1 mg/kg, showed a predominance of taxa showing elevated abundance (Figure 36). These taxa were identified. *Rikenella* and *Mucispirillum*, bacteria associated with the human gut microbiome (Bomar et al., 2011; Coelho et al., 2020; Herp et al., 2019; Loy et al., 2017),

were the ones with the highest increase in abundance (Log 2 Fold change >>) (Figure 37). To the opposite effect, *Embleya*, known for its biosynthetic potential (Hashizume et al., 2021), *Pseudalkalibacillus*, and the thermophilic bacteria *Thermoflavimicrobium* (Goodfellow & Jones, 2015), had a disadvantage in the presence of ATMAC-C16. To tackle the abnormal increase of bacterial abundances in 100 mg/kg, a comparison between the absence (control) and 100 mg/kg was investigated. The increase of diversity might be due to the presence of *Bacteroides*, *Escherichia-Shigella*, *Proteus*, *Parabacteroides*, *Alistipes*, which are the bacteria with higher increase (Log 2-fold Change >>), and *Embleya* is still reduced (Figure 38). The FAPROTAX, a function prediction tool, partially explains these statistical differences. Among the identified upregulated functions (Log 2-fold Change >>) (Figure 43), fermentation and sulfur compounds respiration can be explained by the anaerobic *Rikenella*, a bacterium that produces desulfatases, enzymes that remove or make it accessible sulfate ions (Bomar et al., 2011). The observed ATMAC-C16 impact on the bacterial community can also be clarified by the valorization of *Mucispirillum*. The increase of *Mucispirillum* might be due to ATMAC-C16 degradation in the soil, which yields nitrate as a byproduct, and it's used as an electron acceptor molecule (nitrate reduction) (Loy et al., 2017). The upregulation of the fermentation function suggests an anoxic condition in soil. This lack of oxygen is detrimental in the soil, since it potentiates the denitrification process (reduction of oxidized nitrogen compounds), jeopardizing nitrogen assimilation in soil, and consequently soil fertilization (Rohe et al., 2021).

Concerning BAC-C12, a widespread use disinfectant that started to be commercialized in the medical field in the 1930s (Heyde et al., 2021), presented a different pattern in the soil bacteria. The results showed that BAC-C12 harms the bacterial community (Figure 12), not on the timeline effect but rather on the dose-dependent effect (Figure 13). The alpha diversity boxplots displayed an initial impact until 0.1 mg/kg, when compared to the control. After 0.1 mg/kg, a bigger decline in richness and diversity took place. However, such decline seemed to stabilize as the concentration increased until the highest dose, 100 mg/kg. This decreasing sigmoid response pattern (Godeau et al., 2020) might be due to loss of sensitive bacteria on the 0.1-1mg/kg transition, retaining primarily the ones that resist BAC-C12. In this way, 0.01 mg seems to be the lowest observed dose where no statistically significant effects occurred. Overall, adding BAC-

C12 to the soil is detrimental to the bacterial structure (Figure 22). Also, time plays a role in such effect (Figure 23), where a bigger dissimilarity between timepoint 28 and other timepoints, suggesting the longer the exposure, the higher the impact on bacterial structure. In terms of the dosage response, a clear distinction between a soil with the lowest concentration, 0.001 mg/kg, and a soil with the highest concentration, 100 mg/kg, sets the shift in community structure (Figure 24). On this matter, the top 10 phyla are equal to the control one (Figure 31), and no observed differences appear for either time point and concentration (Figure 32).

To better understand the transition of the BAC-C12 effect, between 0.01 mg/kg and 0.1 mg/kg, differential analysis was considered. There was a noticeably higher number of taxa with increased or decreased abundances in the 0–100 mg/kg comparison than in the 0–0.001 mg/kg comparison (Figure 39). This information aligns with the effect that happens on the suggested threshold. It was also noticed a decrease in *Embleya* abundances, the same taxa seen in ATMAC-C16 impact. In contrast, BAC-C12 seems to benefit a well-known pathogens, *Escherichia-Shigella* (two distinct, closely related genera), a not-assigned genus of the gut-friendly *Muribaculaceae* family, the human gut-residence pathogen *Bacteroides*, and the thermophilic anaerobic *Defluviitoga* (Ben Hania et al., 2012) (Figure 40). These mentioned taxa can partly justify the predicted functions (Figure 44): *Muribaculaceae*, known for its capacity on polysaccharide degradation, can perform the predicted functions, ureolysis and xylanolyis (Zhu et al., 2024). Far more relevant, the *Defluviitoga* genus reduces thiosulfate and elemental sulfur, a proton-consuming reaction, which can lead to an increase in soil pH, destabilizing nutrient assimilation in the soil ecosystem (Tran et al., 2021).

Finally, DDAC-C10, a widely applied biocidal agent in wood preservation (Terzi et al., 2011), disturbs soil bacteria. However, at first glance, the similarity in bacterial richness and evenness with the control group (Chao1, *p*-value = 0.5734, Shannon, *p*-value = 0.2912; Simpson, *p*-value = 0.1884) shown in alpha diversity plots (Figure 15), implies the presence of outliers that might be driving this effect. Even time exposure didn't present any significant differences (Figure 16), bacterial richness decreased (Chao1, *p*-value = 0.004935) at the highest concentration, 100 mg/kg (Figure 17), which suggests a step-change pattern. Nonetheless, the structure of the community was affected (Figure 25), especially after long exposure, shown by the clustering at timepoint 28 days (Figure

26), and at the highest concentration (Figure 27). These results suggest a concentration-dependent effect of DDAC-C10, with significant disruption at higher doses and community resilience at lower ones. Once again, the top 10 phyla are equal to the control one (Figure 33), and no observed differences appear for either time point and concentration (Figure 34).

To assign the pattern observed on 100 mg/kg, differential abundance analysis was performed between the control and 100 mg/kg (Figure 41). Curiously, some taxa described in ATMAC-C16, *Escherichia-Shigella*, a not-assigned *Muribaculaceae* (taxonomic rank: Family) genus, and *Bacteroides* (Log 2-Fold change >> 2) and Embleya (Log 2-Fold change >> 2), had the same effect in the presence of DDAC-C10 (Figure 42). This also aligns with the fact that the predicted functions ( $p\text{-adj} < 0.05$ ), such as fermentation, sulfur respiration, xylanolysis, etc., are also represented (Figure 45).

In the end, the effects of three compounds on soil bacterial community composition and diversity were assessed individually. Even though some hypotheses weren't met, like bacterial composition changing overtime, study objectives were fulfilled. It was also noticed that three different dose-dependence patterns: ATMAC-C16 reduced bacterial richness and diversity as the concentration increased (not considering the 100 mg/kg effect); BAC-C12 followed a decreasing sigmoid response, and DDAC-C10 had a greater impact at the highest concentration. Curiously, the FAPROTAX predicted functions were similar between ATMAC-C16 and DDAC-C10, which could be due to the similarity in the chemical structure of both compounds (Mongelli et al., 2025). By compromising the mentioned functions, some ecosystem services provided by soil, like carbon sequestering and nutrient assimilation, might not be met, posing a serious risk for soil health and soil productivity, especially in soil from agricultural fields. Additionally, metabarcoding only allows to do a estimation in soil functions and future studies should cross data with soil physicochemical analysis, enzyme activity, metabolomics or metatranscriptomics, or even replace, whenever it's possible, with metagenomics, where more information from the bacterial community can be obtained through the bacterial community genomes, instead of just one selected region of one gene such 16S rRNA (Semenov, 2021).

## **Final remarks and future steps**

In this research, the conception of a semi-automated DNA extraction using magnetic beads was successfully developed, laying the foundation for establishing a standardized and scalable laboratory workflow for high-throughput soil microbiome studies. However, handling low-biomass soil samples emerged as a key challenge, often resulting in suboptimal DNA yields for 16S rRNA gene metabarcoding. To address this, it is recommended that metabarcoding approaches be complemented with other environmental genomic techniques, such as metagenomics, qPCR, or targeted functional gene analyses, especially when working with degraded or nutrient-poor soils.

This study provided novel insights, helping to fill the knowledge gap on the effects of quaternary ammonium compounds (QACs) on the soil microbiome. Specifically, distinct effects were registered for ATMAC-C16, BAC-C12, and DDAC-C10. All compounds showed a dose-response effect for the bacterial richness, diversity, and structure. Time-dependent shifts were observed for community structure under exposure to BAC-C12 and DDAC-C10, suggesting that their microbial impact persists or evolves over the 28-day incubation period. Furthermore, differences in the impact patterns and predicted functions across ATMAC-C16 and DDAC-C10 highlighted the potential influence of their chemical structures on microbial sensitivity and resilience. This last result highlights the need to explore radical group chain length and its contribution to ecotoxicological effects.

Although no clear toxicity thresholds could be determined for ATMAC-C16 and DDAC-C10, high concentrations, like 100 mg/kg, significantly disrupted microbial community structure and function. Conversely, BAC-C12 exhibited a threshold of 0.01 mg/kg, beyond which ecological effects were noted. Nonetheless, future studies should apply more robust ecotoxicological indices such as EC, NOEC, LOEC, etc. (ECHA, 2008), to define critical concentrations for risk assessment.

Importantly, these findings contribute to the goals of the SYBERAC project by raising awareness among key stakeholders, including the drinking water company of Copenhagen (HOFOR), the food industry (e.g., Daily Arla), and the Danish and regulatory bodies such as the Danish Environmental Protection Agency (EPA). In a broader context, this study provides a scientific basis to inform the development of upcoming EU directives on soil protection. Overall, QACs contamination on wastewater

streams poses a silent risk for soil health when contaminated sewage sludge is applied. Under the One Health framework, the evidence that QAC-contaminated sewage sludge may impair soil microbial ecosystems points to a hidden risk for both environmental and public health.

## References

- Aislabie, J., Deslippe, J. R., & Dymond, J. (2013). Soil microbes and their contribution to soil services. *Ecosystem Services in New Zealand—Conditions and Trends.*, 1(12), 143–161.
- An, J., Gao, J., Zhao, J., Cui, Y., Zeng, L., Xu, H., & Wang, Q. (2024). Quaternary ammonium compounds inhibited phosphorus removal performance and aggravated the spread of resistance genes in enhanced biological phosphorus removal systems. *Chemical Engineering Journal*, 502, 157945. <https://doi.org/10.1016/j.cej.2024.157945>
- Arnold, W. A., Blum, A., Branyan, J., Bruton, T. A., Carignan, C. C., Cortopassi, G., Datta, S., DeWitt, J., Doherty, A.-C., Halden, R. U., Harari, H., Hartmann, E. M., Hrubec, T. C., Iyer, S., Kwiatkowski, C. F., LaPier, J., Li, D., Li, L., Muñiz Ortiz, J. G., ... Zheng, G. (2023). Quaternary Ammonium Compounds: A Chemical Class of Emerging Concern. *Environmental Science & Technology*, 57(20), 7645–7665. <https://doi.org/10.1021/acs.est.2c08244>
- Banerjee, S., & van der Heijden, M. G. A. (2023). Soil microbiomes and one health. *Nature Reviews Microbiology*, 21(1), 6–20. <https://doi.org/10.1038/s41579-022-00779-w>
- Ben Hania, W., Godbane, R., Postec, A., Hamdi, M., Ollivier, B., & Fardeau, M.-L. (2012). Defluviitoga tunisiensis gen. Nov., sp. Nov., a thermophilic bacterium isolated from a mesothermic and anaerobic whey digester. *International Journal of Systematic and Evolutionary Microbiology*, 62(Pt\_6), 1377–1382. <https://doi.org/10.1099/ijss.0.033720-0>
- Bobic, L., Harbolic, A., & Warner, G. R. (2024). Reproductive & developmental toxicity of quaternary ammonium compounds. *Biology of Reproduction*, 111(4), 742–756. <https://doi.org/10.1093/biolre/ioae107>
- Bomar, L., Maltz, M., Colston, S., & Graf, J. (2011). Directed Culturing of Microorganisms Using Metatranscriptomics. *mBio*, 2(2), e00012-11. <https://doi.org/10.1128/mBio.00012-11>
- Brevik, E., Slaughter, L., Ram Singh, B., Steffan, J., Collier, D., Barnhart, P., & Pereira, P. (2020). *Soil and Human Health: Current Status and Future Needs. Air, Soil and Water Research*(13), 1–13. <https://doi.org/10.1177/1178622120934441>
- Callahan, B. J., McMurdie, P. J., Rosen, M. J., Han, A. W., Johnson, A. J. A., & Holmes, S. P. (2016). DADA2: High-resolution sample inference from Illumina amplicon data. *Nature Methods*, 13(7), 581–583. <https://doi.org/10.1038/nmeth.3869>

- Caporaso, J. G., Kuczynski, J., Stombaugh, J., Bittinger, K., Bushman, F. D., Costello, E. K., Fierer, N., Peña, A. G., Goodrich, J. K., Gordon, J. I., Huttley, G. A., Kelley, S. T., Knights, D., Koenig, J. E., Ley, R. E., Lozupone, C. A., McDonald, D., Muegge, B. D., Pirrung, M., ... Knight, R. (2010). QIIME allows analysis of high-throughput community sequencing data. *Nature Methods*, 7(5), 335–336. <https://doi.org/10.1038/nmeth.f.303>
- Caporaso, J. G., Lauber, C. L., Walters, W. A., Berg-Lyons, D., Lozupone, C. A., Turnbaugh, P. J., Fierer, N., & Knight, R. (2011). Global patterns of 16S rRNA diversity at a depth of millions of sequences per sample. *Proceedings of the National Academy of Sciences of the United States of America*, 108(Suppl 1), 4516–4522. <https://doi.org/10.1073/pnas.1000080107>
- Chacon, L., Rojas-Jimenez, K., & Arias-Andres, M. (2023). Bacterial communities in residential wastewater treatment plants are physiologically adapted to high concentrations of quaternary ammonium compounds. *CLEAN – Soil, Air, Water*, 51(11), 2300056. <https://doi.org/10.1002/clen.202300056>
- Chen, Q., Palanisamy, V., Wang, R., Bosilevac, J. M., & Chitlapilly Dass, S. (2024). Salmonella-induced microbiome profile in response to sanitation by quaternary ammonium chloride. *Microbiology Spectrum*, 12(2), e02346-23. <https://doi.org/10.1128/spectrum.02346-23>
- Clara, M., Scharf, S., Scheffknecht, C., & Gans, O. (2007). Occurrence of selected surfactants in untreated and treated sewage. *Water Research*, 41(19), 4339–4348. <https://doi.org/10.1016/j.watres.2007.06.027>
- Coelho, J. J., Hennessy, A., Casey, I., Bragança, C. R. S., Woodcock, T., & Kennedy, N. (2020). Biofertilisation with anaerobic digestates: A field study of effects on soil microbial abundance and diversity. *Applied Soil Ecology*, 147, 103403. <https://doi.org/10.1016/j.apsoil.2019.103403>
- Creamer, R. E., Barel, J. M., Bongiorno, G., & Zwetsloot, M. J. (2022). The life of soils: Integrating the who and how of multifunctionality. *Soil Biology and Biochemistry*, 166, 108561. <https://doi.org/10.1016/j.soilbio.2022.108561>
- ECHA. (2008). *Guidance on information requirements and chemical safety assessment. Chapter R.10: Characterisation of dose [concentration]-response for environment.* [https://echa.europa.eu/documents/10162/13632/information\\_requirements\\_r10\\_en.pdf/bb902be7-a503-4ab7-9036-d866b8ddce69](https://echa.europa.eu/documents/10162/13632/information_requirements_r10_en.pdf/bb902be7-a503-4ab7-9036-d866b8ddce69)

ECHA CHEM. (n.d.). *Benzododecinium chloride* 100.004.865 | 01fa4790-2920-4461-8a6f-2d15c8c94038—ECHA CHEM. Retrieved 2 December 2024, from [https://chem.echa.europa.eu/100.004.865/dossier-view/01fa4790-2920-4461-8a6f-2d15c8c94038/85e03a2b-b992-4ab9-bf28-ff579add1f6c\\_9e5ade28-a0a5-4fb5-94a9-2cc47e88acca?searchText=Benzododecinium%20chloride](https://chem.echa.europa.eu/100.004.865/dossier-view/01fa4790-2920-4461-8a6f-2d15c8c94038/85e03a2b-b992-4ab9-bf28-ff579add1f6c_9e5ade28-a0a5-4fb5-94a9-2cc47e88acca?searchText=Benzododecinium%20chloride)

EMP. (n.d.). *16S Illumina Amplicon Protocol: Earthmicrobiome*. Retrieved 2 July 2025, from <https://earthmicrobiome.org/protocols-and-standards/16s/>

Ertekin, E., Hatt, J. K., Konstantinidis, K. T., & Tezel, U. (2016). Similar Microbial Consortia and Genes Are Involved in the Biodegradation of Benzalkonium Chlorides in Different Environments. *Environmental Science & Technology*, 50(8), 4304–4313. <https://doi.org/10.1021/acs.est.5b05959>

Estaki, M., Jiang, L., Bokulich, N. A., McDonald, D., González, A., Kosciolak, T., Martino, C., Zhu, Q., Birmingham, A., Vázquez-Baeza, Y., Dillon, M. R., Bolyen, E., Caporaso, J. G., & Knight, R. (2020). QIIME 2 Enables Comprehensive End-to-End Analysis of Diverse Microbiome Data and Comparative Studies with Publicly Available Data. *Current Protocols in Bioinformatics*, 70(1). <https://doi.org/10.1002/cpbi.100>

European Comission. (2021). *EU Soil Strategy for 2030 Reaping the benefits of healthy soils for people, food, nature and climate*. <https://eur-lex.europa.eu/legal-content/EN/TXT/PDF/?uri=CELEX:52021DC0699>

FAO (Ed.). (2006). *Guidelines for soil description* (4. ed). Food and Agriculture Organization of the United Nations.

FAO. (2020). *State of knowledge of soil biodiversity—Status, challenges and potentialities*. <https://doi.org/10.4060/cb1928en>

FAO (2022). Global assessment of soil pollution: Report. Food and Agriculture Organization of the United Nations and United Nations Environment Programme. Rome. <https://openknowledge.fao.org/items/3cba5eed-e9a0-45f0-937b-35f26f2f2723>

Fierer, N., Leung, P. M., Lappan, R., Eisenhofer, R., Ricci, F., Holland, S. I., Dragone, N., Blackall, L. L., Dong, X., Dorador, C., Ferrari, B. C., Goordial, J., Holmes, S. P., Inagaki, F., Korem, T., Li, S. S., Makhalaanyane, T. P., Metcalf, J. L., Nagarajan, N., ... Greening, C. (2025). Guidelines for preventing and reporting contamination in low-biomass microbiome studies. *Nature Microbiology*. <https://doi.org/10.1038/s41564-025-02035-2>

- Fierer, N., Wood, S. A., & Bueno de Mesquita, C. P. (2021). How microbes can, and cannot, be used to assess soil health. *Soil Biology and Biochemistry*, 153, 108111. <https://doi.org/10.1016/j.soilbio.2020.108111>
- Galan, M., Razzauti, M., Bard, E., Bernard, M., Brouat, C., Charbonnel, N., Dehne-Garcia, A., Loiseau, A., Tatard, C., Tamisier, L., Vayssier-Taussat, M., Vignes, H., & Cosson, J.-F. (2016). 16S rRNA Amplicon Sequencing for Epidemiological Surveys of Bacteria in Wildlife. *mSystems*, 1(4), 10.1128/msystems.00032-16. <https://doi.org/10.1128/msystems.00032-16>
- Godeau, U., Bouget, C., Piffady, J., Pozzi, T., & Gosselin, F. (2020). Lack of definition of mathematical terms in ecology: The case of the sigmoid class of functions in macro-ecology. *Ecology and Evolution*, 10(24), 14209–14220. <https://doi.org/10.1002/ece3.7016>
- Goodfellow, M., & Jones, A. L. (2015). *Thermoflavimicrobium*. In W. B. Whitman (Ed.), *Bergey's Manual of Systematics of Archaea and Bacteria* (1st edn, pp. 1–4). Wiley. <https://doi.org/10.1002/9781118960608.gbm00576>
- Hakimzadeh, A., Abdala Asbun, A., Albanese, D., Bernard, M., Buchner, D., Callahan, B., Caporaso, J. G., Curd, E., Djemiel, C., Brandström Durling, M., Elbrecht, V., Gold, Z., Gweon, H. S., Hajibabaei, M., Hildebrand, F., Mikryukov, V., Normandea, E., Özkurt, E., M. Palmer, J., ... Anslan, S. (2024). A pile of pipelines: An overview of the bioinformatics software for metabarcoding data analyses. *Molecular Ecology Resources*, 24(5), e13847. <https://doi.org/10.1111/1755-0998.13847>
- Hashizume, H., Harada, S., Sawa, R., Iijima, K., Kubota, Y., Shibuya, Y., Nagasaka, R., Hatano, M., & Igarashi, M. (2021). New chloptosins B and C from an Embleya strain exhibit synergistic activity against methicillin-resistant *Staphylococcus aureus* when combined with co-producing compound L-156,602. *The Journal of Antibiotics*, 74(1), 80–85. <https://doi.org/10.1038/s41429-020-0361-y>
- Halleux, V. (2024). *Soil monitoring and resilience directive*. European Parliamentary Research Service. [https://www.europarl.europa.eu/thinktank/en/document/EPRS\\_BRI\(2024\)757627](https://www.europarl.europa.eu/thinktank/en/document/EPRS_BRI(2024)757627)
- Hemkemeyer, M., Schwalb, S. A., Heinze, S., Joergensen, R. G., & Wichern, F. (2021). Functions of elements in soil microorganisms. *Microbiological Research*, 252, 126832. <https://doi.org/10.1016/j.micres.2021.126832>
- Herp, S., Brugiroux, S., Garzetti, D., Ring, D., Jochum, L. M., Beutler, M., Eberl, C., Hussain, S., Walter, S., Gerlach, R. G., Ruscheweyh, H. J., Huson, D., Sellin, M. E., Slack, E., Hanson, B., Loy, A.,

- Baines, J. F., Rausch, P., Basic, M., ... Stecher, B. (2019). *Mucispirillum schaedleri* Antagonizes *Salmonella* Virulence to Protect Mice against Colitis. *Cell Host & Microbe*, 25(5), 681-694.e8. <https://doi.org/10.1016/j.chom.2019.03.00>
- Heyde, B. J., Anders, A., Siebe, C., Siemens, J., & Mulder, I. (2021). Quaternary alkylammonium disinfectant concentrations in soils rise exponentially after long-term wastewater irrigation. *Environmental Research Letters*, 16(6), 064002. <https://doi.org/10.1088/1748-9326/abf0cf>
- Heyde, B. J., Barthel, A., Siemens, J., & Mulder, I. (2020). A fast and robust method for the extraction and analysis of quaternary alkyl ammonium compounds from soil and sewage sludge. *PLOS ONE*, 15(8), e0237020. <https://doi.org/10.1371/journal.pone.0237020>
- Hora, P. I., Pati, S. G., McNamara, P. J., & Arnold, W. A. (2020). Increased Use of Quaternary Ammonium Compounds during the SARS-CoV-2 Pandemic and Beyond: Consideration of Environmental Implications. *Environmental Science & Technology Letters*, 7(9), 622–631. <https://doi.org/10.1021/acs.estlett.0c00437>
- Hu, Q., Zhang, L., Yang, R., Tang, J., & Dong, G. (2024). Quaternary ammonium biocides promote conjugative transfer of antibiotic resistance gene in structure- and species-dependent manner. *Environment International*, 189, 108812. <https://doi.org/10.1016/j.envint.2024.108812>
- Huber, W., Carey, V. J., Gentleman, R., Anders, S., Carlson, M., Carvalho, B. S., Bravo, H. C., Davis, S., Gatto, L., Girke, T., Gottardo, R., Hahne, F., Hansen, K. D., Irizarry, R. A., Lawrence, M., Love, M. I., MacDonald, J., Obenchain, V., Oleś, A. K., ... Morgan, M. (2015). Orchestrating high-throughput genomic analysis with Bioconductor. *Nature Methods*, 12(2), 115–121. <https://doi.org/10.1038/nmeth.3252>
- Hudcová, H., Vymazal, J., & Rozkošný, M. (2019). Present restrictions of sewage sludge application in agriculture within the European Union. *Soil and Water Research*, 14(2), 104–120. <https://doi.org/10.17221/36/2018-SWR>
- Imfeld, G., Besaury, L., Maucourt, B., Donadello, S., Baran, N., & Vuilleumier, S. (2018). Toward Integrative Bacterial Monitoring of Metolachlor Toxicity in Groundwater. *Frontiers in Microbiology*, 9, null. <https://doi.org/10.3389/fmicb.2018.02053>
- Jansen, K., Mohr, C., Lügger, K., Heller, C., Siemens, J., & Mulder, I. (2023). Widespread occurrence of quaternary alkylammonium disinfectants in soils of Hesse, Germany. *Science of The Total Environment*, 857, 159228. <https://doi.org/10.1016/j.scitotenv.2022.159228>

- Jennings, M. C., Buttaro, B. A., Minbiole, K. P. C., & Wuest, W. M. (2015). Bioorganic Investigation of Multicationic Antimicrobials to Combat QAC-Resistant *Staphylococcus aureus*. *ACS Infectious Diseases*, 1(7), 304–309. <https://doi.org/10.1021/acsinfecdis.5b00032>
- Jensen, J., Toft Ingvertsen, S., & Magid, J. (2012). Risk evaluation of five groups of persistent organic contaminants in sewage sludge. Miljøstyrelsen Strandgade 29 1401.
- Kaj, L., Wallberg, P., & Brorström-Lundén, E. (2014). Quaternary ammonium compounds: Analyses in a Nordic cooperation on screening. Nordic Council of Ministers.
- Kang, H. I., & Shin, H. S. (2016). Rapid and Sensitive Determination of Benzalkonium Chloride Biocide Residues in Soil Using Liquid Chromatography–Tandem Mass Spectrometry after Ultrasonically Assisted Extraction. *Bulletin of the Korean Chemical Society*, 37(8), 1219–1227. <https://doi.org/10.1002/bkcs.10842>
- Khan, A. H., Macfie, S. M., & Ray, M. B. (2017). Sorption and leaching of benzalkonium chlorides in agricultural soils. *Journal of Environmental Management*, 196, 26–35. <https://doi.org/10.1016/j.jenvman.2017.02.065>
- Kikuchi, Y., & Graf, J. (2007). Spatial and Temporal Population Dynamics of a Naturally Occurring Two-Species Microbial Community inside the Digestive Tract of the Medicinal Leech. *Applied and Environmental Microbiology*, 73(6), 1984–1991. <https://doi.org/10.1128/AEM.01833-06>
- Knight, C. G., Nicolitch, O., Griffiths, R. I., Goodall, T., Jones, B., Weser, C., Langridge, H., Davison, J., Dellavalle, A., Eisenhauer, N., Gongalsky, K. B., Hector, A., Jardine, E., Kardol, P., Maestre, F. T., Schädler, M., Semchenko, M., Stevens, C., Tsiafouli, M. A., ... de Vries, F. T. (2024). Soil microbiomes show consistent and predictable responses to extreme events. *Nature*, 636(8043), 690–696. <https://doi.org/10.1038/s41586-024-08185-3>
- Landecker, H. (2019). Antimicrobials before antibiotics: War, peace, and disinfectants. *Palgrave Communications*, 5(1), 1–11. <https://doi.org/10.1057/s41599-019-0251-8>
- Larsson, Y., Mongelli, A., Kisielius, V., & Bester, K. (2024). Microbial biofilm metabolism of benzalkonium compounds (benzyl dimethyl dodecyl ammonium & benzyl dimethyl tetradecyl ammonium chloride). *Journal of Hazardous Materials*, 463, 132834. <https://doi.org/10.1016/j.jhazmat.2023.132834>
- Li, D., Gao, J., Dai, H., Wang, Z., Cui, Y., Zhao, Y., & Zhou, Z. (2022). Fates of quaternary ammonium compound resistance genes and the corresponding resistant strain in partial nitrification/anammox

- system under pressure of hexadecyl trimethyl ammonium chloride. *Water Research*, 217, 118395.  
<https://doi.org/10.1016/j.watres.2022.118395>
- Li, J., Chen, H., Zi, F., Wu, Z., Li, W., Duan, Q., Song, H., Huang, J., Zhao, Q., Hu, X., & Tian, S. (2025). Impacts of quaternary ammonium compounds on the ecological risks of cadmium, enzyme activities, and bacterial community in soils. *Environmental Technology & Innovation*, 37, 104047.  
<https://doi.org/10.1016/j.eti.2025.104047>
- Liu, C., Goh, S. G., You, L., Yuan, Q., Mohapatra, S., Gin, K. Y.-H., & Chen, B. (2023). Low concentration quaternary ammonium compounds promoted antibiotic resistance gene transfer via plasmid conjugation. *Science of The Total Environment*, 887, 163781.  
<https://doi.org/10.1016/j.scitotenv.2023.163781>
- Loos, R., Marinov, D., Sanseverino, I., Napierska, D., Lettieri, T., & European Commission (Eds). (2018). *Review of the 1st Watch List under the Water Framework Directive and recommendations for the 2nd Watch List*. Publications Office. <https://doi.org/10.2760/614367>
- Lori, M., Leitao, R., David, F., Imbert, C., Corti, A., Cunha, L., Symanczik, S., Bünenmann, E. K., Creamer, R., & Vazquez, C. (2025). Response of soil biota to agricultural management practices: A systematic quantitative meta-data-analysis and method selection framework. *Soil Biology and Biochemistry*, 207, 109815. <https://doi.org/10.1016/j.soilbio.2025.109815>
- Louca, S., Parfrey, L. W., & Doebeli, M. (n.d.). *Decoupling function and taxonomy in the global ocean microbiome*.
- Louca, S., Parfrey, L. W., & Doebeli, M. (2025). FAPROTAX. *Functional Annotation of Prokaryotic Taxa (FAPROTAX)*. <http://www.loucalab.com/archive/FAPROTAX/lib/php/index.php?section=Home>
- Love, M. I., Huber, W., & Anders, S. (2014). Moderated estimation of fold change and dispersion for RNA-seq data with DESeq2. *Genome Biology*, 15(12). <https://doi.org/10.1186/s13059-014-0550-8>
- Loy, A., Pfann, C., Steinberger, M., Hanson, B., Herp, S., Brugiroux, S., Gomes Neto, J. C., Boekschoten, M. V., Schwab, C., Urich, T., Ramer-Tait, A. E., Rattei, T., Stecher, B., & Berry, D. (2017). Lifestyle and Horizontal Gene Transfer-Mediated Evolution of *Mucispirillum schaedleri*, a Core Member of the Murine Gut Microbiota. *mSystems*, 2(1), e00171-16.  
<https://doi.org/10.1128/mSystems.00171-16>
- Lu, Z., K. Mahony, A., A. Arnold, W., W. Marshall, C., & J. McNamara, P. (2024). Quaternary ammonia compounds in disinfectant products: Evaluating the potential for promoting antibiotic resistance

- and disrupting wastewater treatment plant performance. *Environmental Science: Advances*, 3(2), 208–226. <https://doi.org/10.1039/D3VA00063J>
- Maki, K. A., Wolff, B., Varuzza, L., Green, S. J., & Barb, J. J. (2023). Multi-amplicon microbiome data analysis pipelines for mixed orientation sequences using QIIME2: Assessing reference database, variable region and pre-processing bias in classification of mock bacterial community samples. *PLOS ONE*, 18(1), e0280293. <https://doi.org/10.1371/journal.pone.0280293>
- Malizia, W. F., Gangarosa, E. J., & Goley, A. F. (1960). Benzalkonium Chloride as a Source of Infection. *New England Journal of Medicine*. <https://www.nejm.org/doi/abs/10.1056/NEJM196010202631608>
- Mattoo, R., & Mallikarjuna, S. (2023). Soil Microbiome Influences Human Health In the Context of Climate Change. *Future Microbiology*, 18(12), 845–859. <https://doi.org/10.2217/fmb-2023-0098>
- McMurdie, P. J., & Holmes, S. (2013). phyloseq: An R Package for Reproducible Interactive Analysis and Graphics of Microbiome Census Data. *PLOS ONE*, 8(4), e61217. <https://doi.org/10.1371/journal.pone.0061217>
- Mohapatra, S., Yutao, L., Goh, S. G., Ng, C., Luhua, Y., Tran, N. H., & Gin, K. Y.-H. (2023). Quaternary ammonium compounds of emerging concern: Classification, occurrence, fate, toxicity and antimicrobial resistance. *Journal of Hazardous Materials*, 445, 130393. <https://doi.org/10.1016/j.jhazmat.2022.130393>
- Mongelli, A., Larsson, Y., Koning, J. T., & Bester, K. (2025). Removal of Quaternary Ammonium Compounds (QACs) in Wastewater Treatment: Resolving the Contributions of Biodegradation and Sorption. *ACS ES&T Water*, 5(7), 3831–3842. <https://doi.org/10.1021/acsestwater.5c00196>
- Mulder, I., Siemens, J., Sentek, V., Amelung, W., Smalla, K., & Jechalke, S. (2018). Quaternary ammonium compounds in soil: Implications for antibiotic resistance development. *Reviews in Environmental Science and Bio/Technology*, 17(1), 159–185. <https://doi.org/10.1007/s11157-017-9457-7>
- Nadagouda, M. N., Vijayasarathy, P., Sin, A., Nam, H., Khan, S., Parambath, J. B. M., Mohamed, A. A., & Han, C. (2022). Antimicrobial activity of quaternary ammonium salts: Structure-activity relationship. *Medicinal Chemistry Research*, 31(10), 1663–1678. <https://doi.org/10.1007/s00044-022-02924-9>
- Natural England. (2008). *Natural England Technical Information Note TIN037—Soil texture*.

- Neuenkamp, L., García de León, D., Hamer, U., Hözel, N., McGale, E., & Hannula, S. E. (2024). Comprehensive tools for ecological restoration of soils foster sustainable use and resilience of agricultural land. *Communications Biology*, 7(1), 1–13. <https://doi.org/10.1038/s42003-024-07275-2>
- Ni, B., Zhang, T.-L., Cai, T.-G., Xiang, Q., & Zhu, D. (2024). Effects of heavy metal and disinfectant on antibiotic resistance genes and virulence factor genes in the platsphere from diverse soil ecosystems. *Journal of Hazardous Materials*, 465, 133335. <https://doi.org/10.1016/j.jhazmat.2023.133335>
- Nowak-Lange, M., Niedziałkowska, K., & Lisowska, K. (2022). Cosmetic Preservatives: Hazardous Micropollutants in Need of Greater Attention? *International Journal of Molecular Sciences*, 23(22), Article 22. <https://doi.org/10.3390/ijms232214495>
- Ossowicki, A., Raaijmakers, J. M., & Garbeva, P. (2021). Disentangling soil microbiome functions by perturbation. *Environmental Microbiology Reports*, 13(5), 582–590. <https://doi.org/10.1111/1758-2229.12989>
- Pena, S. A., Salas, J. G., Gautam, N., Ramos, A. M., & Frantz, A. L. (2023). Sublethal Exposure to Common Benzalkonium Chloride Leads to Antimicrobial Tolerance and Antibiotic Cross-Resistance in Commensal and Opportunistic Bacterial Species. *Applied Microbiology*, 3(2), 580–591. <https://doi.org/10.3390/applmicrobiol3020041>
- Pereira, A. P., Antunes, P., Bierge, P., Willems, R. J. L., Corander, J., Coque, T. M., Pich, O. Q., Peixe, L., Freitas, A. R., Novais, C., & from the ESCMID Study Group on Food- and Water-borne Infections (EFWISG). (2023). Unraveling Enterococcus susceptibility to quaternary ammonium compounds: Genes, phenotypes, and the impact of environmental conditions. *Microbiology Spectrum*, 11(5), e02324-23. <https://doi.org/10.1128/spectrum.02324-23>
- Peyneau, M., de Chaisemartin, L., Gigant, N., Chollet-Martin, S., & Kerdine-Römer, S. (2022). Quaternary ammonium compounds in hypersensitivity reactions. *Frontiers in Toxicology*, 4, 973680. <https://doi.org/10.3389/ftox.2022.973680>
- PubChem. (2024). *Benzethonium Chloride*. <https://pubchem.ncbi.nlm.nih.gov/compound/8478>
- Pulami, D., Schwabe, L., Blom, J., Schwengers, O., Wilharm, G., Kämpfer, P., & Glaeser, S. P. (2023). Genomic plasticity and adaptive capacity of the quaternary alkyl-ammonium compound and

- copper tolerant *Acinetobacter bohemicus* strain QAC-21b isolated from pig manure. *Antonie van Leeuwenhoek*, 116(4), 327–342. <https://doi.org/10.1007/s10482-022-01805-w>
- Putten, W. H. van der, Mudgal, S., Turbé, A., Toni, A. de, Lavelle, P., Benito, P., & Ruiz, N. (2010). *Soil biodiversity: Functions, threats and tools for policy makers*. <https://research.wur.nl/en/publications/soil-biodiversity-functions-threats-and-tools-for-policy-makers>
- Qiu, L., Zhang, Q., Zhu, H., Reich, P. B., Banerjee, S., van der Heijden, M. G. A., Sadowsky, M. J., Ishii, S., Jia, X., Shao, M., Liu, B., Jiao, H., Li, H., & Wei, X. (2021). Erosion reduces soil microbial diversity, network complexity and multifunctionality. *The ISME Journal*, 15(8), 2474–2489. <https://doi.org/10.1038/s41396-021-00913-1>
- R Core Team. (2024). *R: A Language and Environment for Statistical Computing*. [Computer software]. R Foundation for Statistical Computing. <https://www.R-project.org/>
- Rohe, L., Apelt, B., Vogel, H.-J., Well, R., Wu, G.-M., & Schlüter, S. (2021). Denitrification in soil as a function of oxygen availability at the microscale. *Biogeosciences*, 18(3), 1185–1201. <https://doi.org/10.5194/bg-18-1185-2021>
- Roux, S., & Emerson, J. B. (2022). Diversity in the soil virosphere: To infinity and beyond? *Trends in Microbiology*, 30(11), 1025–1035. <https://doi.org/10.1016/j.tim.2022.05.003>
- Sáez-Sandino, T., García-Palacios, P., Maestre, F. T., Plaza, C., Guirado, E., Singh, B. K., Wang, J., Cano-Díaz, C., Eisenhauer, N., Gallardo, A., & Delgado-Baquerizo, M. (2023). The soil microbiome governs the response of microbial respiration to warming across the globe. *Nature Climate Change*, 13(12), 1382–1387. <https://doi.org/10.1038/s41558-023-01868-1>
- Sarkar, B., Megharaj, M., Xi, Y., Krishnamurti, G. S. R., & Naidu, R. (2010). Sorption of quaternary ammonium compounds in soils: Implications to the soil microbial activities. *Journal of Hazardous Materials*, 184(1), 448–456. <https://doi.org/10.1016/j.jhazmat.2010.08.055>
- Saverina, E. A., Frolov, N. A., Kamanina, O. A., Arlyapov, V. A., Vereshchagin, A. N., & Ananikov, V. P. (2023). From Antibacterial to Antibiofilm Targeting: An Emerging Paradigm Shift in the Development of Quaternary Ammonium Compounds (QACs). *ACS Infectious Diseases*, 9(3), 394–422. <https://doi.org/10.1021/acsinfecdis.2c00469>

- Schlatter, D., Kinkel, L., Thomashow, L., Weller, D., & Paulitz, T. (2017). Disease Suppressive Soils: New Insights from the Soil Microbiome. *Phytopathology®*, 107(11), 1284–1297. <https://doi.org/10.1094/PHYTO-03-17-0111-RVW>
- Schulz, S., Brankatschk, R., Düming, A., Kögel-Knabner, I., Schloter, M., & Zeyer, J. (2013). The role of microorganisms at different stages of ecosystem development for soil formation. *Biogeosciences*, 10(6), 3983–3996. <https://doi.org/10.5194/bg-10-3983-2013>
- Seferyan, M. A., Saverina, E. A., Frolov, N. A., Detusheva, E. V., Kamanina, O. A., Arlyapov, V. A., Ostashevskaya, I. I., Ananikov, V. P., & Vereshchagin, Anatoly. N. (2023). Multicationic Quaternary Ammonium Compounds: A Framework for Combating Bacterial Resistance. *ACS Infectious Diseases*, 9(6), 1206–1220. <https://doi.org/10.1021/acsinfecdis.2c00546>
- Semenov, M. V. (2021). Metabarcoding and Metagenomics in Soil Ecology Research: Achievements, Challenges, and Prospects. *Biology Bulletin Reviews*, 11(1), 40–53. <https://doi.org/10.1134/S2079086421010084>
- Silva, V., Alaoui, A., Schlünssen, V., Vested, A., Graumans, M., Van Dael, M., Trevisan, M., Suciu, N., Mol, H., Beekmann, K., Figueiredo, D., Harkes, P., Hofman, J., Kandeler, E., Abrantes, N., Campos, I., Martínez, M. Á., Pereira, J. L., Goossens, D., ... Scheepers, P. T. J. (2021). Collection of human and environmental data on pesticide use in Europe and Argentina: Field study protocol for the SPRINT project. *PLOS ONE*, 16(11), e0259748. <https://doi.org/10.1371/journal.pone.0259748>
- Snyder, V. A., & Vázquez, M. A. (2005). STRUCTURE. In D. Hillel (Ed.), *Encyclopedia of Soils in the Environment* (pp. 54–68). Elsevier. <https://doi.org/10.1016/B0-12-348530-4/00533-6>
- Song, Y., Yao, S., Li, X., Wang, T., Jiang, X., Bolan, N., Warren, C. R., Northen, T. R., & Chang, S. X. (2024). Soil metabolomics: Deciphering underground metabolic webs in terrestrial ecosystems. *Eco-Environment & Health*, 3(2), 227–237. <https://doi.org/10.1016/j.eehl.2024.03.001>
- Tetro, J. A., Alderson, F. A., & Sattar, S. A. (2024). Is it time to re-evaluate exposure risks to quaternary ammonium compounds as disinfectants? *Current Research in Microbial Sciences*, 7, 100258. <https://doi.org/10.1016/j.crmicr.2024.100258>
- Tezel, U., & Pavlostathis, S. G. (2015). Quaternary ammonium disinfectants: Microbial adaptation, degradation and ecology. *Current Opinion in Biotechnology*, 33, 296–304. <https://doi.org/10.1016/j.copbio.2015.03.018>

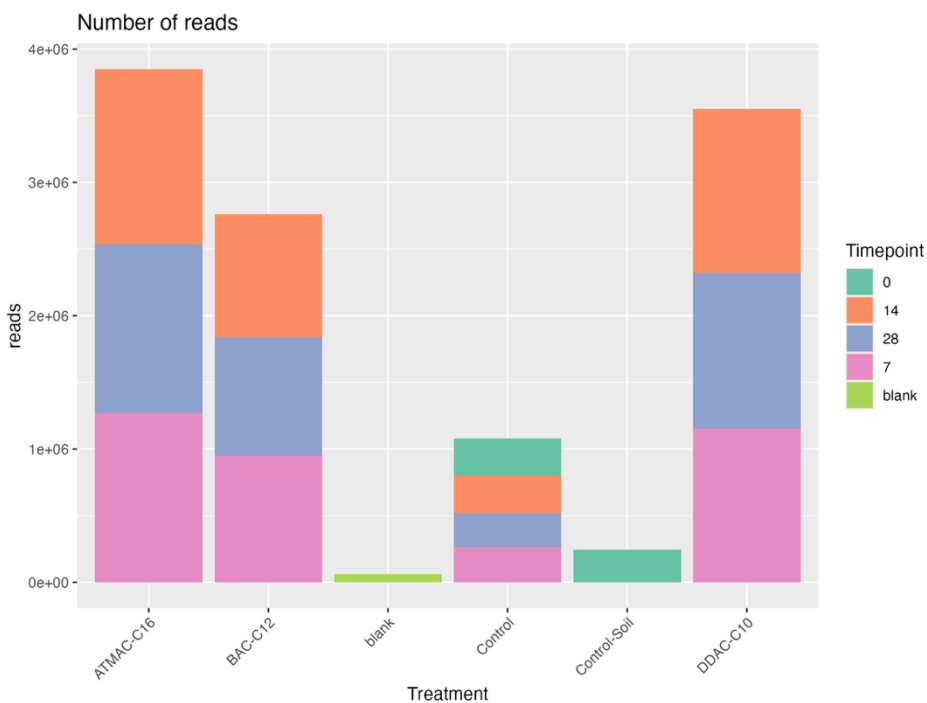
- Terzi, E., Kartal, S. N., White, R. H., Shinoda, K., & Imamura, Y. (2011). Fire performance and decay resistance of solid wood and plywood treated with quaternary ammonia compounds and common fire retardants. *European Journal of Wood and Wood Products*, 69(1), 41–51. <https://doi.org/10.1007/s00107-009-0395-0>
- Tran, T. T. T., Kannoorpatti, K., Padovan, A., & Thennadil, S. (2021). Effect of pH regulation by sulfate-reducing bacteria on corrosion behaviour of duplex stainless steel 2205 in acidic artificial seawater. *Royal Society Open Science*, 8(1), 200639. <https://doi.org/10.1098/rsos.200639>
- Wang, P., Wang, H., Qi, S., Wang, W., & Lu, H. (2025). Synergistic effects of quaternary ammonium compounds and antibiotics on the evolution of antibiotic resistance. *Water Research*, 275, 123206. <https://doi.org/10.1016/j.watres.2025.123206>
- WHO. (2022). *Strengthening WHO preparedness for and response to health emergencies—Strengthening collaboration on One Health*. [https://apps.who.int/gb/ebwha/pdf\\_files/WHA75/A75\\_19-en.pdf](https://apps.who.int/gb/ebwha/pdf_files/WHA75/A75_19-en.pdf)
- Wu, R. A., Feng, J., Yue, M., Liu, D., & Ding, T. (2024). Overuse of food-grade disinfectants threatens a global spread of antimicrobial-resistant bacteria. *Critical Reviews in Food Science and Nutrition*, 64(19), 6870–6879. <https://doi.org/10.1080/10408398.2023.2176814>
- Xu, H., Gao, J., Yuan, Y., Zeng, L., Wang, Y., Wang, H., & An, J. (2024). Insight into the responses of performance, bacterial community and three-fraction resistance genes to different quaternary ammonium compounds in nitrifying system under the stress of environmental ciprofloxacin. *Chemical Engineering Journal*, 496, 154241. <https://doi.org/10.1016/j.cej.2024.154241>
- Yang, K., Chen, M.-L., & Zhu, D. (2023). Exposure to benzalkonium chloride disinfectants promotes antibiotic resistance in sewage sludge microbiomes. *Science of The Total Environment*, 867, 161527. <https://doi.org/10.1016/j.scitotenv.2023.161527>
- Yang, R., Zhou, S., Zhang, L., & Qin, C. (2023). Pronounced temporal changes in soil microbial community and nitrogen transformation caused by benzalkonium chloride. *Journal of Environmental Sciences*, 126, 827–835. <https://doi.org/10.1016/j.jes.2022.04.004>
- Yang, Z., Peng, C., Cao, H., Song, J., Gong, B., Li, L., Wang, L., He, Y., Liang, M., Lin, J., & Lu, L. (2022). Microbial functional assemblages predicted by the FAPROTAX analysis are impacted by physicochemical properties, but C, N and S cycling genes are not in mangrove soil in the Beibu Gulf, China. *Ecological Indicators*, 139, 108887. <https://doi.org/10.1016/j.ecolind.2022.108887>

- Zeng, J., Li, Y., Jin, G., Su, J.-Q., & Yao, H. (2022). Short-Term Benzalkonium Chloride (C12) Exposure Induced the Occurrence of Wide-Spectrum Antibiotic Resistance in Agricultural Soils. *Environmental Science & Technology*, 56(21), 15054–15063. <https://doi.org/10.1021/acs.est.2c04730>
- Zeng, J.-Y., Li, W., Su, J.-Q., Wang, Y.-Z., Li, Y., & Yao, H. (2024). Manure application amplified the co-selection of quaternary ammonium disinfectant and antibiotic on soil antibiotic resistome. *Journal of Hazardous Materials*, 468, 133792. <https://doi.org/10.1016/j.jhazmat.2024.133792>
- Zhang, W., Chang, Y., Zhong, W., Zhang, A., & Lin, Y. (2023). Antifungal mechanisms of polymeric quaternary ammonium salts against conidia of *Fusarium oxysporum* f. Sp. *Cubense*, race 4. *European Journal of Plant Pathology*, 165(2), 317–331. <https://doi.org/10.1007/s10658-022-02608-5>
- Zhang, Y., Gao, J., Wang, Z., Zhao, Y., Liu, Y., Zhang, H., & Zhao, M. (2023). The responses of microbial metabolic activity, bacterial community and resistance genes under the coexistence of nanoplastics and quaternary ammonium compounds in the sewage environment. *Science of The Total Environment*, 879, 163064. <https://doi.org/10.1016/j.scitotenv.2023.163064>
- Zhao, J., Rodriguez, J., & Martens-Habbena, W. (2023). Fine-scale evaluation of two standard 16S rRNA gene amplicon primer pairs for analysis of total prokaryotes and archaeal nitrifiers in differently managed soils. *Frontiers in Microbiology*, 14, 1140487. <https://doi.org/10.3389/fmicb.2023.1140487>
- Zhao, M., Gao, J., Liu, Y., Wang, Z., Wu, Z., Zhang, H., & Zhang, Y. (2023). Short-term stress of quaternary ammonium compounds on intracellular and extracellular resistance genes in denitrification systems. *Chemical Engineering Journal*, 452, 139166. <https://doi.org/10.1016/j.cej.2022.139166>
- Zhu, Y., Zhu, D., Rillig, M. C., Yang, Y., Chu, H., Chen, Q., Penuelas, J., Cui, H., & Gillings, M. (2023). Ecosystem Microbiome Science. *mLife*, 2(1), 2–10. <https://doi.org/10.1002/mlf2.12054>
- Zhu, Y., Chen, B., Zhang, X., Akbar, M. T., Wu, T., Zhang, Y., Zhi, L., & Shen, Q. (2024). Exploration of the Muribaculaceae Family in the Gut Microbiota: Diversity, Metabolism, and Function. *Nutrients*, 16(16), 2660. <https://doi.org/10.3390/nu16162660>

## ATTACHMENTS

In this section, it's presented some complementary information that helped develop the methodology used above. Items are organized in chronological order to facilitate consultation.

### 1. Number of reads before filtering and normalization



One of three blanks showed high-level contamination, but it was dismissed following quality control evaluation.

### 2. DNA extraction kit

Since the SYBERAC project had a large number of samples, it was necessary to choose a quick and reliable way to extract DNA from soil. For that, a magnetic bead system extraction was preferred to conventional column-based DNA extraction since it can be automated in throughput equipment like Opentrons OT-2.

The process to select the DNA extraction kit was time-consuming, mainly because of the lower amount of DNA in the soil samples, even with the column-based DNA extraction

method (Table 1 – Test nº 1). Three kits were tested: NZY Mag Bacterial & Viral RNA/DNA Isolation Kit, RUO (recommended by NZYTech itself for the study), OMEGA Mag-Bind® Environmental DNA 96 Kit, and Norgen's Soil DNA Isolation Kit (Magnetic Bead System). Different volumes of buffers, homogenization conditions, magnetic bead types, etc., were tested. In the end, the kit selected was NorgenBiotek Soil DNA Isolation Kit (Magnetic Bead System), as mentioned before.

To better understand the reason for less DNA compared to the conventional method, column-based, a troubleshooting was done to the kit protocol, to see where DNA was being lost (Table 2). Since the biggest decrease of DNA amount was after the addition of Binding Buffer I and/or OSR solution (Table 2) (with the function of removing PCR inhibitors), it was hypothesized that the DNA was being co-pelleted with the soil debris, which was also confirmed (Table 2 – Test nº 4).

**Table 1** – Optimization of the kits protocol: comparison between modifications.

Test	Homogenization Buffers	Kit	Concentration Nanodrop	A260/A280	A260/A230	Concentration Qubit	Notes
1	NSL1/NS_enhancer/NSL3_(column kit)	NZYtech_column_kit	55.137(R1);44.438(R2);58.642(R3)	1.819(R1);1.836(R2);1.821(R3)	0.977(R1);1.881(R2);1.952(R3)	42.4(R1);34.2(R2);51.4(R3)	nothing_to_report
2	NSL1/NS_enhancer/NSL3_(column kit)	NZY_Mag_Bacterial_& Viral_RNA/DNA_Isolation_Kit, RUO	26.926(R1);32.878(R2);61.222(R3)	1.497(R1);1.470(R2);1.482(R3)	0.389(R1);0.304(R2);0.401(R3)	-	200ul_supernatant(50/50_plate/epp)
3	PBS	NZY_Mag_Bacterial_& Viral_RNA/DNA_Isolation_Kit, RUO	8.841(R1);9.401(R2);11.283(R3)	1.459(R1);1.384(R2);1.470(R3)	0.180(R1);0.384(R2);0.073(R3)	-	200ul_supernatant
4	NSL1/NS_enhancer/NSL3_(column kit)	NZYtech_column_kit	35.890(R1);30.215(R2);32.107(R3)	1.901(R1);1.723(R2);1.842(R3)	2.363(R1);1.882(R2);1.199(R3)	-	FastDNA™_Lysis_Matrix_A_(homogenization tubes)_&_500ul_supernatant(leftover)
5	PBS	NZYtech_column_kit	0.030(R1);1.706(R2);0.937(R3)	0.117(R1);1.635(R2);1.973(R3)	0.004(R1);0.786(R2);0.889(R3)	-	FastDNA™_Lysis_Matrix_A_(homogenization tubes)_&_500ul_supernatant(leftover)
6	NSL1/NS_enhancer/NSL3_(column kit)	NZY_Mag_Bacterial_& Viral_RNA/DNA_Isolation_Kit, RUO	91.742(R1);52.568(R2);89.718(R3)	1.505(R1);1.468(R2);1.471(R3)	0.594(R1);0.405(R2);0.542(R3)	-	adaptation_in_eppe_ndorf/200ul_supernatant
7	NSL1/NS_enhancer/NSL3_(column kit)	NZY_Mag_Bacterial_& Viral_RNA/DNA_Isolation_Kit, RUO	84.645(R1);30.230(R2);22.852(R3)	1.403(R1);1.433(R2);1.434(R3)	0.343(R1);0.474(R2);0.361(R3)	-	adaptation_in_eppe_ndorf/700ul_supernatant
8	kit_protocol	OMEGA_Mag-Bind®_Environmental_DNA_96_Kit	4.065(R1);3.054(R2);2.940(R3)	1.562(R1);2.823(R2);4.707(R3)	0.110(R1);0.009(R2);0.007(R3)	-	adaptation_in_eppe_ndorf
9	NSL1/NS_enhancer/NSL3_(column kit)	NZY_Mag_Bacterial_& Viral_RNA/DNA_Isolation_Kit, RUO	87.809(R1);98.645(R2);117.318(R3)	1.998(R1);1.808(R2);1.611(R3)	0.297(R1);0.206(R2);0.172(R3)	-	Shaker_Adaptation/Impurity_Guanidine_HCl

10	NSL1/NS_enhancer/NSL3_(column kit)	NZY_Mag_Bacterial_& Viral_RNA/DNA_Isolation_Kit, RUO	17.900(R1);48.798(R2);25.419(R3)	1.590(R1);1.602(R2);1.601(R3)	0.048(R1);0.109(R2);0.113(R3)	-	-
11	NSL1/NS_enhancer/NSL3_(column kit)	NZY_Mag_Bacterial_& Viral_RNA/DNA_Isolation_Kit, RUO	46.924(R1);82.285(R2);80.845(R3)	1.623(R1);1.518(R2);1.550(R3)	0.418(R1);0.275(R2);0.225(R3)	21.8(R1);17.0(R2);19.2(R3)	dry_beads/parafilm
12	NSL1/NS_enhancer/NSL3_(column kit)	NZY_Mag_Bacterial_& Viral_RNA/DNA_Isolation_Kit, RUO	46.924(R1);82.285(R2);80.845(R3)	1.623(R1);1.518(R2);1.550(R3)	0.418(R1);0.275(R2);0.225(R3)	21.8(R1);17.0(R2);19.2(R3)	dry_beads/parafilm
13	Lysis Buffer L and Lysis Additive A	Norgen's Soil DNA Isolation Kit (Magnetic Bead System)	4.408(R1);5.349(R2);5.065(R3)	1.146(R1);1.195(R2);1.198(R3)	1.234(R1);0.981(R2);0.866(R3)	-	BeadBlaster: 5.5m/s;2 cycles; 20s; 10s between cycles & 100ul elution buffer
14	Lysis Buffer L and Lysis Additive A	Norgen's Soil DNA Isolation Kit (Magnetic Bead System)	10.706(R1);9.950(R2);8.124(R3)	1.597(R1);1.742(R2);1.600(R3)	1.333(R1);1.318(R2);1.134(R3)	-	BeadBlaster: 6.0m/s;3 cycles; 30s; 1min between cycles & 50ul elution buffer
15	Lysis Buffer L and Lysis Additive A	Norgen's Soil DNA Isolation Kit (Magnetic Bead System)	10.261(R1);16.356(R2);13.727(R3)	1.643(R1);1.568(R2);1.645(R3)	0.911(R1);0.863(R2);0.975(R3)	-	BeadBlaster: 6.0m/s;3 cycles; 30s; 1min between cycles & 50ul elution buffer & 100mg sample
16	Lysis Buffer L and Lysis Additive A	Norgen's Soil DNA Isolation Kit (Magnetic Bead System)	12.586(R1);14.541(R2);13.823(R3)	1.678(R1);1.622(R2);1.608(R3)	1.077(R1);1.176(R2);1.351(R3)	-	BeadBlaster: 6.0m/s;3 cycles; 30s; 1min between cycles & 50ul elution buffer & no Binding Buffer I step
17	Lysis Buffer L and Lysis Additive A	Norgen's Soil DNA Isolation Kit (Magnetic Bead System)	13.883(R1);16.746(R2);20.466(R3)	1.646(R1);1.521(R2);1.510(R3)	1.092(R1);0.938(R2);0.892(R3)	-	BeadBlaster: 6.0m/s;3 cycles; 30s; 1min between cycles & 50ul elution buffer &

							skip binding buffer I and OSR buffer steps
18	Lysis Buffer L and Lysis Additive A	Norgen's Soil DNA Isolation Kit (Magnetic Bead System)	17.357(R1);16.168(R2);15.302(R3)	1.647(R1);1.688(R2);1.809(R3)	1.100(R1);1.261(R2);1.323(R3)	13.9(R1);13.7(R2);12.4(R3)	BeadBlaster: 6.0m/s;3 cycles; 30s; 1min between cycles & 50ul elution buffer & no OSR buffer step
19	NSL1/NS_enhancer/NSL3_(column kit)	NZY_Mag_Bacterial_& Viral_RNA/DNA_Isolation_Kit,_RUO	30.810(R1);62.777(R2);147.550(R3)	1.583(R1);1.467(R2);1.410(R3)	0.074(R1);0.230(R2);0.408(R3)	-	BeadBlaster: 6.0m/s;3 cycles; 30s; 1min between cycles
20	NSL1/NS_enhancer/NSL3_(column kit)	NZY_Mag_Bacterial_& Viral_RNA/DNA_Isolation_Kit,_RUO	20.283(R1);25.071(R2);47.786(R3)	1.745(R1);1.798(R2);1.650(R3)	0.030(R1);0.022(R2);0.040(R3)	-	BeadBlaster: 6.0m/s;3 cycles; 30s; 1min between cycles & lab-made tubes (aluminum oxide sand and zirconia beads)
21	NSL1/NS_enhancer/NSL3_(column kit)	NZY_Mag_Bacterial_& Viral_RNA/DNA_Isolation_Kit,_RUO	32.167(R1);30.337(R2);25.020(R3);12.642(R4);11.794(R5)	1.585(R1);1.649(R2);1.650(R3);1.595(R4);1.852(R5)	0.060(R1);0.778(R2);0.036(R3);0.694(R4);0.048(R5)	13.6(1R1);12.8(R2);8.54(R3);4.56(R4);6.78(R5)	BeadBlaster: 6.0m/s;3 cycles; 30s; 1min between cycles & lab-made tubes (aluminum oxide sand and zirconia beads) & kit Proteinase K (25ul-200ul buffer)
22	Lysis Buffer L and Lysis Additive A	Norgen's Soil DNA Isolation Kit (Magnetic Bead System)	22.1(R1);26.1(R2);28.3(R3);24.2(R4);22.6(R5)	1.68(R1);1.79(R2);1.77(R3);1.81(R4);1.78(R5)	1.24(R1);1.54(R2);0.940(R3);1.58(R4);1.33(R5)	12.7(1R1);28.2(R2);35.6(R3);30.6(R4);17.8(R5)	BeadBlaster: 6.0m/s;3 cycles; 30s; 1min between cycles & lab-made tubes (aluminum oxide sand and zirconia beads) &

							Proteinase K (50ul-400ul buffer)
23	NSL1/NS_enhancer/NSL3_(column kit)	NZY_Mag_Bacterial_& Viral_RNA/DNA_Isolation_Kit,_RUO	29.111(R1);24.186(R2);25.103(R3);28.527(R4);57.997*(R5)	1.566(R1);1.468(R2);1.460(R3);1.502(R4);1.873(R5)	0.077(R1);0.217(R2);0.100(R3);0.086(R4);0.070(R5)	-	BeadBlaster: 6.0m/s;3 cycles; 30s; 1min between cycles & lab-made tubes (aluminum oxide sand and zirconia beads) & kit Proteinase K (25ul-200ul buffer) & tissue magnetic beads
24	Lysis Buffer L and Lysis Additive A	Norgen's Soil DNA Isolation Kit (Magnetic Bead System)	3.893(R1);3.568(R2);3.786(R3);4.740(R4);3.435(R5)	1.568(R1);1.364(R2);1.178(R3);1.612(R4);1.146(R5)	0.844(R1);0.878(R2);0.824(R3);1.020(R4);0.971(R5)	-	BeadBlaster: 6.0m/s;3 cycles; 30s; 1min between cycles & lab-made tubes (aluminum oxide sand and zirconia beads) & Proteinase K (50ul-400ul buffer) & tissue magnetic beads

**Table 2** – Troubleshooting of Norgen’s Soil DNA Isolation Kit (Magnetic Bead System).

Test	Protocol_step	Buffers	Nanodrop_concentration	A260/A280	A260/A230	Notes
1	After homogenization	Lysis Buffer L and lysis Additive A	286.871(R1),257.505(R2),530 .631(R3)	1.447(R1),1.489(R2),1.4 80(R3)	0.207(R1),0.276(R2),0.2 27(R3)	Other soil samples used
2	After homogenization	Lysis Buffer L and lysis Additive A	157.788(R1),231.466(R2),304 .909(R3)	1.571(R1),1.565(R2),1.4 27(R3)	0.171(R1),0.167(R2),0.2 07(R3)	
3	After Binding Buffer centrifugation	Binding Buffer I	186.104(R1),253.408(R2),175 .424(R3)	1.494(R1),1.467(R2),1.5 00(R3)	0.172(R1),0.224(R2),0.1 63(R3)	-
4	Binding Buffer pellet	Binding Buffer I	460.876(R1),131.497(R2),91. 079(R3)	1.200(R1),1.437(R2),1.3 25(R3)	0.653(R1),0.471(R2),0.3 11(R3)	Dissolved in dH2O
5	After OSR centrifugation	OSR solution	118.143(R1),121.600(R2),117 .594(R3)	1.520(R1),1.512(R2),1.5 20(R3)	0.119(R1),0.122(R2),0.1 18(R3)	-
6	Before first washing	Beads, Binding Buffer B, 96% etOH	16.109(R1),35.486(R2),18.71 2(R3)	1.197(R1),1.317(R2),1.3 69(R3)	0.046(R1),0.091(R2),0.0 52(R3)	-
7	After first washing	WN solution	0.658(R1),3.324(R2),0.139(R 3)	0.938(R1),0.973(R2),0.5 96(R3)	0.122(R1),7.428(R2),- 0.035(R3)	-
8	After homogenization	NSL1/NS_enhancer/NSL3_(column kit)	281.538(R1),260.959(R2),281 .140(R3)	1.415(R1),1.367(R2),1.3 65(R3)	0.420(R1),0.411(R2),0.4 28(R3)	-
9	After first washing	Wash buffer	15.705(R1),16.902(R2),14.70 0(R3)	2.412(R1),2.560(R2),2.4 39(R3)	0.012(R1),0.013(R2),0.0 11(R3)	-

### 3. DNA concentration – NanoDrop™ One measurements

**Table 3** – First plate.

Sample Name	Nucleic Acid(ng/uL)	A260/A280	A260/A230
B	5.561	1.260	0.164
B	2.715	0.838	0.682
B	5.561	1.011	0.633
C1	11.420	1.378	0.735
C2	34.205	1.590	1.120
C3	18.723	1.432	0.991
C4	17.951	1.367	0.790
C5	12.580	1.367	0.753
C6	4.314	1.170	0.656
C7	1.354	0.735	0.305
C8	4.201	1.107	0.607
C9	4.567	1.283	0.646
C10	12.735	1.242	0.668
C11	7.828	1.360	0.642
C12	12.551	1.313	0.653
C13	32.728	1.012	0.798
C14	4.989	1.100	0.621
C15	7.006	1.374	0.643
C16	12.732	1.409	0.668
C17	10.218	1.389	0.563
C18	13.981	1.377	0.671
C19	13.430	1.293	0.695
C20	9.088	1.330	0.618
C21	10.234	1.431	0.695
C22	12.745	1.608	0.924
C23	9.502	1.601	0.858
C24	7.734	1.424	0.727
C25	5.783	1.398	0.712
AT1	7.073	1.523	0.648
AT2	10.859	1.301	0.650
AT3	11.697	1.392	0.676
AT4	6.078	1.319	0.584
AT5	4.374	1.639	0.753
AT6	10.791	1.498	0.783

AT7	4.699	1.533	0.539
AT8	5.634	1.360	0.691
AT9	9.959	1.432	0.692
AT10	9.108	1.363	0.673
AT11	10.826	1.284	0.630
AT12	17.324	1.311	0.646
AT13	29.588	1.385	0.809
AT14	28.514	1.275	0.712
AT15	8.977	1.231	0.625
AT16	4.343	1.185	0.371
AT17	47.066	1.228	0.731
AT18	9.680	1.371	0.557
AT19	49.207	1.256	0.748
AT20	46.290	1.240	0.737
AT21	7.462	1.604	0.876
AT22	6.946	1.385	0.640
AT23	4.919	1.235	0.608
AT24	5.252	1.272	0.642
AT25	4.860	1.229	0.784
AT26	6.484	1.169	0.726
AT27	5.223	1.318	0.653
AT28	3.802	1.439	0.894
AT29	7.796	1.692	0.912
AT30	6.920	1.319	0.799
AT31	3.282	1.331	1.121
AT32	5.574	1.271	0.892
AT33	8.377	1.323	0.768
AT34	4.819	1.164	0.679
AT35	6.156	1.368	0.765
AT36	11.882	1.307	0.630
AT37	15.125	1.393	0.762
AT38	14.684	1.317	0.774
AT39	17.746	1.415	0.749
AT40	13.755	1.410	0.752
AT41	26.453	1.421	0.755
AT42	17.531	1.428	0.743
AT43	31.198	1.359	0.714
AT44	14.264	1.390	0.652
AT45	7.486	1.393	0.741
AT46	10.383	1.319	0.665
AT47	8.549	1.477	0.599

AT48	10.183	1.547	0.931
AT49	11.372	1.383	0.761
AT50	9.799	1.458	1.041
AT51	4.393	1.629	0.181
AT52	6.992	1.339	0.712
AT53	13.123	1.391	0.912
AT54	6.184	1.227	0.671
AT55	17.389	1.525	0.976
AT56	13.383	1.527	0.985
AT57	14.300	1.548	0.951
AT58	5.836	1.373	0.826
AT59	17.194	1.531	0.940
AT60	16.365	1.508	0.927
AT61	18.048	1.384	0.718
AT62	16.837	1.497	0.852
AT63	11.972	1.325	0.790
AT64	13.029	1.431	0.929
AT65	22.039	1.356	0.762
AT66	18.617	1.469	0.894
AT67	5.396	1.380	0.653
AT68	17.785	1.321	0.705

**Table 4 – Second plate.**

Sample Name	Nucleic Acid(ng/uL)	A260/A280	A260/A230
B	15.884	1.492	0.701
B	10.816	1.454	0.698
B	12.210	1.303	0.666
AT69	26.267	1.546	0.918
AT70	23.069	1.539	0.858
AT71	24.443	1.613	0.913
AT72	22.525	1.582	0.956
AT73	28.925	1.730	1.083
AT74	25.446	1.550	0.942
AT75	21.319	1.659	1.058
BC1	20.418	1.654	1.132
BC2	22.619	1.674	1.031
BC3	26.118	1.696	1.079
BC4	16.475	1.637	0.872
BC5	34.745	1.653	1.034

BC6	23.299	1.665	1.001
BC7	27.963	1.680	1.012
BC8	16.971	1.745	1.262
BC9	18.862	1.615	0.956
BC10	22.382	1.542	0.876
BC11	24.892	1.716	1.174
BC12	20.694	1.685	1.001
BC13	19.856	1.644	1.034
BC14	25.595	1.640	0.982
BC15	24.000	1.632	1.012
BC16	31.643	1.678	1.170
BC17	22.120	1.666	1.173
BC18	28.672	1.670	1.206
BC19	33.101	1.709	1.273
BC20	30.202	1.665	1.200
BC21	27.374	1.667	1.166
BC22	23.253	1.578	1.006
BC23	19.303	1.652	1.151
BC24	11.676	1.665	1.087
BC25	25.183	1.742	1.370
BC26	16.551	1.657	0.975
BC27	16.574	1.721	1.093
BC28	12.442	1.648	1.060
BC29	24.360	1.589	1.177
BC30	20.472	1.599	1.130
BC31	37.767	1.573	0.895
BC32	31.242	1.471	0.776
BC33	27.304	1.546	0.823
BC34	23.170	1.471	0.838
BC35	53.995	1.592	0.905
BC36	45.613	1.498	0.865
BC37	54.206	1.531	0.888
BC38	51.838	1.592	0.931
BC39	20.621	1.674	1.300
BC40	29.007	1.700	1.341
BC41	15.426	1.690	1.456
BC42	22.734	1.718	1.304
BC43	24.420	1.643	1.268
BC44	22.849	1.687	1.286
BC45	27.398	1.684	1.318
BC46	22.770	1.611	1.180

BC47	20.914	1.605	1.081
BC48	18.352	1.685	1.263
BC49	19.669	1.660	1.223
BC50	20.259	1.572	1.065
BC51	28.415	1.578	1.095
BC52	34.972	1.610	1.167
BC53	29.007	1.499	0.872
BC54	27.383	1.639	1.139
BC55	27.180	1.565	1.084
BC56	30.319	1.648	1.121
BC57	18.164	1.819	1.255
BC58	27.483	1.693	1.058
BC59	32.499	1.657	1.174
BC60	32.082	1.716	1.172
BC61	30.243	1.616	1.090
BC62	31.206	1.656	1.144
BC63	25.740	1.637	1.086
BC64	31.871	1.690	1.173
BC65	22.333	1.748	1.318
BC66	28.607	1.640	1.137
BC67	42.425	1.672	1.378
BC68	35.835	1.581	1.009
BC69	27.696	1.512	0.993
BC70	38.151	1.624	1.173
BC71	17.771	1.661	1.147
BC72	21.026	1.554	1.014
BC73	38.706	1.716	1.457
BC74	22.642	1.572	1.027
BC75	21.171	1.868	1.769
DD1	30.561	1.620	1.108
DD2	30.510	1.667	1.303
DD3	32.012	1.734	1.325
DD4	49.058	1.461	0.982
DD5	51.354	1.515	0.881
DD6	18.421	1.601	1.031
DD7	46.098	1.527	0.961
DD8	48.160	1.427	0.960
DD9	52.204	1.496	0.985
DD10	73.113	1.393	0.949
DD11	83.793	1.315	0.945

**Table 5** – Third plate.

Sample Name	Nucleic Acid(ng/uL)	A260/A280	A260/A230
B	8.723	1.383	0.624
B	7.896	1.118	0.694
B	6.917	1.120	0.681
DD12	18.917	1.546	0.906
DD13	23.721	1.598	0.968
DD14	10.636	1.519	0.761
DD15	18.631	1.526	0.806
DD16	17.460	1.521	0.833
DD17	5.899	1.251	0.835
DD18	14.185	1.493	0.812
DD19	10.012	1.565	0.808
DD20	13.255	1.460	0.737
DD21	36.530	1.566	0.897
DD22	11.221	1.429	0.717
DD23	14.461	1.585	0.835
DD24	11.358	1.609	0.875
DD25	12.334	1.439	0.721
DD26	16.857	1.544	0.853
DD27	11.025	1.567	0.989
DD28	24.136	1.498	0.839
DD29	25.639	1.537	0.928
DD30	13.553	1.552	0.926
DD31	17.311	1.535	0.940
DD32	17.228	1.520	0.851
DD33	14.170	1.473	0.775
DD34	9.134	1.850	1.542
DD35	45.746	1.495	0.840
DD36	23.354	1.464	0.821
DD37	15.672	1.888	1.820
DD38	14.971	1.425	0.780
DD39	15.612	1.618	0.939
DD40	20.216	1.531	0.818
DD41	21.319	1.478	0.794
DD42	22.598	1.528	0.796
DD43	22.316	1.502	0.865
DD44	31.654	1.525	0.803
DD45	21.767	1.491	0.822

DD46	13.546	1.573	0.999
DD47	19.597	1.529	0.884
DD48	26.274	1.480	0.871
DD49	102.792	1.305	0.750
DD50	95.608	1.328	0.759
DD51	112.800	1.380	0.780
DD52	75.822	1.298	0.806
DD53	101.753	1.339	0.783
DD54	77.997	1.296	0.805
DD55	109.583	1.325	0.803
DD56	93.095	1.282	0.810
DD57	43.280	1.452	0.861
DD58	32.005	1.407	0.807
DD59	25.073	1.435	1.011
DD60	50.400	1.421	0.830
DD61	39.733	1.413	0.878
DD62	28.060	1.416	0.880
DD63	108.644	1.323	0.800
DD64	44.989	1.416	0.857
DD65	25.574	1.517	0.980
DD66	16.108	1.425	0.920
DD67	22.392	1.473	0.885
DD68	37.560	1.493	0.943
DD69	24.560	1.387	0.800
DD70	24.917	1.497	0.883
DD71	32.315	1.532	1.100
DD72	56.933	1.471	0.908
DD73	50.518	1.323	0.838
DD74	52.772	1.315	0.802
DD75	52.412	1.305	0.822

#### 4. Proof of amplification of extracts (gel)

Briefly, to confirm that the DNA extracted with the Norgen's kit is able to be amplified before sending to Novogene, a PCR of the 16SrRNA V4 region was done with the following conditions: 9ul of mastermix (40.4 µL deionized ultrapure water, 59,4 µL Qiagen Multiplex buffer (Galan et al., 2016), 3,6 µL of each forward and reverse primer – 515f/806R pair) and 1 µL of water or DNA sample. The PCR plate used was NG PCR EZtrieve microplates 96x20 µL, and it was prepared in a BioSan UVC/T-AR DNA/RNA UV Cleaner Box. Afterwards, the plate was sealed with EZtrieve Heat Seal (165°C per 1.5s) in a plate sealer NG PCR ISOGEN LifeScience, and it was set under these conditions in NextGenPCR: 94°C-3min (initial denaturation) and 35 cycles at 94 °C - 45 s, 50 °C - 60 s, and 72 °C - 90 s; a final extension of 10 min at 72 °C (Caporaso et al., 2011; EMP, n.d.; J. Zhao et al., 2023). Then, the PCR plate was centrifuged at 1000 rpm for 1min before retrieving the samples, where the plate was placed on top of the pipetting

anvil and pierced through the seal. To visualize the amplification, an electrophoresis gel was prepared and observed in the BioRad GelDoc Go Imaging System.

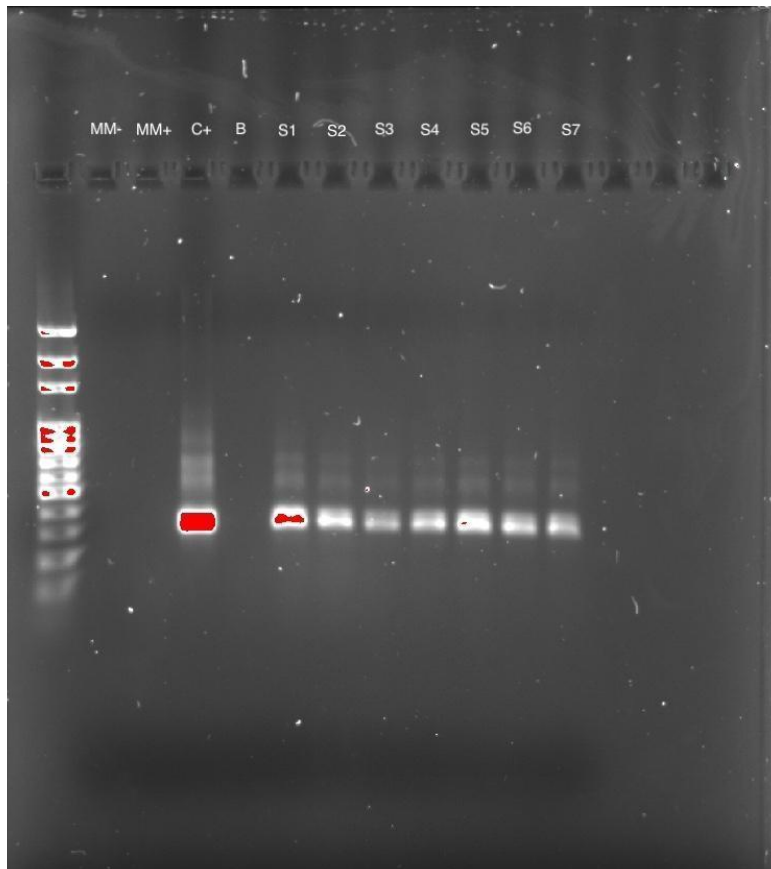


**Figure 1** – Electrophoresis gel of the OT-2 DNA extracts. The gel wells were loaded with: Qiagen Mastermix without primers (MM-) and with (MM+); a soil sample manually extracted as positive control (C+); a OT-2 extraction blank (B) and extracted DNA from the study samples (S1-S7).

## 5. Deck preparation OT-2

Section 2 of Norgen's Soil DNA isolation kit is done in Opentrons OT-2. The scripts were made using Opentrons Protocol Designer version 8.4.4 and are available at this GitHub repository: [https://github.com/MCS-micro/NorgenBiotek\\_Kit-OT2\\_Adaptation-Thesis](https://github.com/MCS-micro/NorgenBiotek_Kit-OT2_Adaptation-Thesis). The protocol was divided into three to minimize errors with the tip racks counted in the script. Every labware used was DNA-free. Every mixture of buffers and its addition to reservoirs was freshly made.

Specifications:

- Pipette: Right mount P300 8-Channel GEN2
- Opentrons OT-2 96 Filter Tip Rack 200  $\mu\text{L}$
- Modules used: Magnetic Module GEN2 and Heater-Shaker Module GEN1 with Opentrons 96 Deep Well Heater-Shaker Adapter
- Labware: NEST 1 Well Reservoir 195 mL (for discharge); NEST 12 Well Reservoir 15 mL (to place buffers) and NEST 96 Well Plate 100  $\mu\text{L}$  PCR Full Skirt (final DNA extracts)

Protocol 1: Addition of magnetic beads and first and second wash with Solution WN

Mix of magnetic beads:

Per column of a 15mL NEST 12 well reservoir. To the amount set by the kit manufacturer, it was multiplied by eight wells (number of wells per column in a 96-well plate) and by 15% extra volume for pipetting errors. To avoid potential cross-contamination between columns, the full volume of the mixture (5828  $\mu\text{L}$ ) was added to each 12-well plate, rather than reducing the number of wells used to six.

Binding Buffer B	$300 \times 8 \times 0.15 = 2760 \mu\text{L}$
96% EtOH	$320 \times 8 \times 0.15 = 2944 \mu\text{L}$
Magnetic beads	$20 \times 8 \times 0.15 = 184 \mu\text{L}$
Total	5828 $\mu\text{L}$

Solution WN:

Per column of a 15mL NEST 12 well reservoir. To the amount set by the kit manufacturer, it was multiplied by eight wells (number of wells per column in a 96-well plate) and by 15% extra volume for pipetting errors.

$1000 \mu\text{L} \times 8 \times 0.15 = 8800 \mu\text{L}$   
Two full reservoirs with 8800  $\mu\text{L}$  in each well.

Protocol 2: Addition of first and second wash 80% EtOH

Per column of a 15mL NEST 12 well reservoir. To the amount set by the kit manufacturer, it was multiplied by eight wells (number of wells per column in a 96-well plate) and by 15% extra volume for pipetting errors.

$$1000 \mu\text{L} \times 8 \times 0.15 = 8800 \mu\text{L}$$

Two full reservoirs with 8800  $\mu\text{L}$  in each well.

Protocol 3: Elution of DNA from the magnetic beads

Per column of a 15mL NEST 12 well reservoir. To the amount set by the kit manufacturer, it was multiplied by eight wells (number of wells per column in a 96-well plate) and by 15% extra volume for pipetting errors.

$$50 \mu\text{L} \times 8 \times 0.15 = 5520 \mu\text{L}$$

One well is filled with 5520  $\mu\text{L}$  in a single reservoir.

## 6. List of some R packages used in this study

Packages: phyloseq; ggplot2; dplyr; Biostrings; RcolorBrewer; DESeq2; microbiome; tidyR; tibble; devtools; devtools::install\_github("jbisanz/qiime2R")

## 7. Alpha-diversity

### Controls

Controls		
test-assumptions	p-value	result
		non-
Shapiro-Chao1	0.03009	normal
Leven-Chao1	0.1731	equal_var
		non-
Shapiro-Shannon	0.006858	normal
Levene-Shannon	0.1802	equal_var
		non-
Shapiro-Simpson	0.00265	normal
Levene-Simpson	0.02202	diff_var

stats - Wilcoxon rank sum exact test /Mann-Whitney		
Index	p-value	result
Chao1	0.6905	no_dif
Shannon	0.2222	no_dif
Simpson	0.6905	no_dif

## ATMAC-C16

ATMAC-C16			stats - Kruskal Wallis		
TREATMENT			TREATMENT		
test-assumptions	p-value	result	Index	p-value	result
Shapiro-Chao1	0.008138	non-normal	Chao1	0.08816	no_dif
Leven-Chao1	0.07909	equal_var	Shannon	0.03916	*
Shapiro-Shannon	0.000104	non-normal	Simpson	0.05197	no_dif
TIMEPOINT			TIMEPOINT		
test-assumptions	p-value	result	Index	p-value	result
Shapiro-Chao1	0.008138	non-normal	Chao1	0.2536	no_dif
Leven-Chao1	0.1496	equal_var	Shannon	0.353	no_dif
Shapiro-Shannon	0.000104	non-normal	Simpson	0.3479	no_dif
CONCENTRATION			CONCENTRATION		
test-assumptions	p-value	result	Index	p-value	result
Shapiro-Chao1	0.008138	non-normal	Chao1	0.07354	no_dif
Leven-Chao1	0.236	equal_var	Shannon	0.01364	*
Shapiro-Shannon	0.000104	non-normal	Simpson	0.0117	*
PLATE			PLATE		
test-assumptions	p-value	result	Index	p-value	result
Shapiro-Chao1	0.008138	non-normal	Chao1	0.01839	*
Leven-Chao1	0.3853	equal_var	Shannon	0.002064	*
Shapiro-Shannon	0.3.19e-14	non-normal	Simpson	0.0003268	*
CONCENTRATION					
test-assumptions	p-value	result			
Shapiro-Chao1	0.008138	non-normal			
Leven-Chao1	0.00289	diff_var			
Shapiro-Shannon	0.000104	non-normal			
Leven-Shannon	0.001113	diff_var			
Shapiro-Simpson	3.19e-14	non-normal			
PLATE					
test-assumptions	p-value	result			
Shapiro-Chao1	0.008138	non-normal			
Leven-Chao1	0.00289	diff_var			
Shapiro-Shannon	0.000104	non-normal			
Leven-Shannon	0.001113	diff_var			
Shapiro-Simpson	3.19e-14	non-normal			

Levene-Simpson	0.1032	equal_var
----------------	--------	-----------

DUNN test - Shannon				
Comparison	Z	P.unadj	P.adj Benjamini-Hochberg method.	results
0 - 0.001	0.384371106798037	2 0.70070341225168	0.808503937213479	no_dif
0 - 0.01	1.64231291086434	4 0.10052517280898	0.251312932022459	no_dif
0.001 -		0.20841280368414		
0.01	1.2579418040663	9 0.17965936324840	0.390774006907779	no_dif
0 - 0.1	1.34180459100406	8 0.33834850445129	0.384984349818017	no_dif
0.001 -		0.33834850445129		
0.1	0.957433484206019	7 0.76378945119908	0.507522756676946	no_dif
0.01 - 0.1	0.300508319860283	5 0.00061616506281	0.818345840570448 0.0092424759422339	no_dif
0 - 1	3.4243971332916	5594 0.00236557705339	1	*
0.001 - 1	3.04002602649356	788 0.07473549830588	0.0177418279004841	*
0.01 - 1	1.78208422242726	26 0.03728837957455	0.224206494917648	no_dif
0.1 - 1	2.08259254228754	02 0.139831423404563		no_dif
0 - 100	1.19504471386299	0.23206956067689	0.386782601128151	no_dif
0.001 -		0.41755313393276		
100	0.81067360706495	4 0.65468142662893	0.569390637181042	no_dif
0.01 -	-	0.65468142662893		
100	0.447268197001352	9 0.88332155509060	0.818351783286174	no_dif
0.1 - 100	0.146759877141068	6 0.02579046540742	0.883321555090606	no_dif
1 - 100	-2.22935241942861	38 0.128952327037119		no_dif
DUNN test - Simpson				
Comparison	Z	P.unadj	P.adj Benjamini-Hochberg method.	results
0 - 0.001	82138 1.4116902467	824 0.158041186386	0.824062395385525	no_dif
0 - 0.01	8552	827 0.263494184141	0.338659685114629	no_dif
0.001 -	1.1181704925			
0.01	0338 1.5584501239	2 0.119126582499	0.439156973568667	no_dif
0 - 0.1	2659	689 0.297816456249222		no_dif

0.001 -	1.2649303696	0.205896289523		no_dif
0.1	4445	103	0.386055542855819	
0.01 -	0.1467598771	0.883321555090		no_dif
0.1	41068	606	0.883321555090606	
	3.3964428709	0.000682678063		
0 - 1	7902	198312	0.0102401709479747	*
	3.1029231166	0.001916194138		
0.001 - 1	9688	47439	0.0143714560385579	*
	1.9847526241	0.047172000782		no_dif
0.01 - 1	935	877	0.176895002935789	
	1.8379927470	0.066063474072		no_dif
0.1 - 1	5243	1601	0.19819042221648	
	0.8665821316	0.386171007313		no_dif
0 - 100	90119	69	0.579256510970536	
0.001 -	0.5730623774	0.566602459815		no_dif
100	07981	541	0.708253074769427	
	-			
0.01 -	0.5451081150	0.585679161710		no_dif
100	95398	285	0.675783648127252	
	-			
	0.6918679922	0.489020232969		no_dif
0.1 - 100	36466	136	0.66684577223064	
	-			
	2.5298607392	0.011410780676		no_dif
1 - 100	889	1754	0.0570539033808771	

## BAC-C12

BAC-C12			stats - Kruskal Wallis		
TREATMENT			TREATMENT		
test-assumptions	p-value	result	Index	p-value	result
Shapiro-Chao1	0.0001656	non-normal	Chao1	0.01183	*
Leven-Chao1	0.5195	equal_var	Shannon	0.07852	no_dif
Shapiro-Shannon	2.584e-05	non-normal	Simpson	0.6768	no_dif
Levene-Shannon	0.846	equal_var	TIMEPOINT		
Shapiro-Simpson	1.329e-07	non-normal	Index	p-value	result
Levene-Simpson	0.08514	equal_var	Chao1	0.5817	no_dif
TIMEPOINT			Shannon	0.493	no_dif
test-assumptions	p-value	result	Simpson	0.5092	no_dif
Shapiro-Chao1	0.0001656	non-normal	CONCENTRATION		
Leven-Chao1	0.1977	equal_var	Index	p-value	result
Shapiro-Shannon	2.584e-05	non-normal	Chao1	9.854e-09	*
Levene-Shannon	0.1144	equal_var	Shannon	4.078e-08	*

Shapiro-Simpson	1.329e-07	non-normal	Simpson	1.178e-07	*
Levene-Simpson	0.1715	equal_var		PLATE	
CONCENTRATION			Index	p-value	result
test-assumptions	p-value	result	Chao1	0.01183	*
Shapiro-Chao1	0.0001656	non-normal	Shannon	0.07852	*
Leven-Chao1	0.007702	diff_var	Simpson	0.6768	no_dif
Shapiro-Shannon	2.584e-05	non-normal			
Levene-Shannon	0.004137	diff_var			
Shapiro-Simpson	1.329e-07	non-normal			
Levene-Simpson	0.02193	diff_var			
PLATE					
test-assumptions	p-value	result			
Shapiro-Chao1	0.0001656	non-normal			
Leven-Chao1	0.5195	equal_var			
Shapiro-Shannon	2.584e-05	non-normal			
Levene-Shannon	0.846	equal_var			
Shapiro-Simpson	1.329e-07	non-normal			
Levene-Simpson	0.08514	equal_var			

DUNN test - Chao1					
Comparis on	Z	P.unadj	P.adj Benjamini- Hochberg method.		result s
-					
	1.0902296915616				no_di
0 - 0.001	1	0.275611977244653	0.375834514424527		f
	0.2411084894799				no_di
0 - 0.01	71	0.809471033198006	0.867290392712149		f
0.001 -	1.3313381810415				no_di
0.01	8	0.183077760426952	0.274616640640428		f
		0.000624039304057			
0 - 0.1	3.420945089868	335	0.00133722708012286		*
0.001 -	4.5111747814296	6.44695701694601e			
0.1	1	-06	3.223478508473e-05		*
	3.1798366003880	0.001473581184753			
0.01 - 0.1	3	15	0.00245596864125526		*
		0.000182254332898	0.00068345374836776		
0 - 1	3.7424230758413	071	7		*
	4.8326527674029	1.34725655211711e			
0.001 - 1	1	-06	2.02088482817567e-05		*
	3.5013145863613	0.000462968995510			
0.01 - 1	2	491	0.00138890698653147		*
	0.3214779859732				no_di
0.1 - 1	95	0.74784819226768	0.9348102403346		f

	3.4349223936059	0.000592723546075		
0 - 100	7	154	0.00148180886518789	*
0.001 - 100	4.5251520851675	6.03520894820461e-06	4.52640671115346e-05	*
0.01 - 100	3.193813904126	0.0139773037379	0.001404065965312	*
0.1 - 100	693	-	0.00263262368496015	no_dif
1 - 100	26	0.3075006822353	0.988848088262581	f
		0.758462303818876	0.988848088262581	no_dif
		0.875148812098704		f

DUNN test - Shannon				
Comparison	Z	P.unadj	P.adj Benjamini-Hochberg method.	results
	-			
0 - 0.001	1.649301476	0.09908588733	0.1486288310068	
	44248	79155	73	no_dif
	-			
0 - 0.01	0.398348237	0.69037350749	0.8629668843727	
	954329	8212	65	no_dif
0.001 - 0.01	1.250953238	0.21095153848	0.2876611888448	
	48816	6209	3	no_dif
0 - 0.1	2.788437665	0.00529629386	0.0088271564424	
	6803	548941	8235	*
0.001 - 0.1	4.437739142	9.09086964295	4.5454348214774	
	12279	496e-06	8e-05	*
0.01 - 0.1	3.186785903	0.00143863223	0.0035965805853	
	63463	412543	1358	*
0 - 1	3.172808772	0.00150971927	0.0032351127297	
	47834	390536	972	*
0.001 - 1	4.822110248	1.42047393313	2.1307108996981	
	92082	213e-06	9e-05	*
0.01 - 1	3.571157010	0.00035540774	0.0013327790608	
	43267	9557885	4207	*
0.1 - 1	0.384371106	0.70070341225	0.8085039372134	
	798037	1682	79	no_dif
0 - 100	2.900254714	0.00372859532	0.0069911162301	
	93064	273588	2978	*
0.001 - 100	4.549556191	5.37591774286	4.0319383071492	
	37312	569e-06	7e-05	*
0.01 - 100	3.298602952	0.00097167241	0.0029150172444	
	88497	4825113	7534	*
0.1 - 100	0.111817049	0.91096846895	0.9109684689542	
	250338	4272	72	no_dif

	-	0.272554057	0.78519603193	0.8412814627822	
1 - 100		547699	0068	16	no_dif
<b>DUNN test - Simpson</b>					
Comparison	Z	P.unadj	P.adj	res	ult
-	2.683609182	0.0072832189	0.0156068977		
0 - 0.001	00811	6826405	891372	*	
-	1.495553033	0.1347701699	0.1837775044	no_	
0 - 0.01	72327	53663	82267	dif	
-	1.188056148	0.2348112893	0.2935141116	no_	
0.001 - 0.01	28484	15166	43958	dif	
-	1.740152828	0.0818321859	0.1227482789	no_	
0 - 0.1	95838	61448	42172	dif	
-	4.423762010	9.6996868253	4.8498434126		
0.001 - 0.1	9665	7887e-06	8944e-05	*	
-	3.235705862	0.0012134235	0.0030335587		
0.01 - 0.1	68165	1639596	909899	*	
-	2.089581107	0.0366554450	0.0687289595	no_	
0 - 1	86569	68468	033775	dif	
-	4.773190289	1.8133031150	2.7199546725		
0.001 - 1	8738	5282e-06	7922e-05	*	
-	3.585134141	0.0003369049	0.0012633937		
0.01 - 1	58896	94839947	306498	*	
-	0.349428278	0.7267678061	0.8385782379	no_	
0.1 - 1	907306	99101	22039	dif	
-	1.963786927	0.0495548067	0.0825913445	no_	
0 - 100	45906	166596	27766	dif	
-	4.647396109	3.3615129452	2.5211347089		
0.001 - 100	46717	0432e-06	0324e-05	*	
-	3.459339961	0.0005415009	0.0016245029		
0.01 - 100	18233	66876564	0062969	*	
-	0.223634098	0.8230420287	0.8818307451	no_	
0.1 - 100	500676	95912	38477	dif	
-	0.125794180	0.8998948485	0.8998948485	no_	
1 - 100	40663	42443	42443	dif	

## DDAC-C10

DDAC-C10	stats - Kruskal Wallis
TREATMENT	TREATMENT

test-assumptions	p-value	result	Index	p-value	result																	
Shapiro-Chao1	1.784e-06	non-normal	Chao1	0.5734	no_dif																	
Leven-Chao1	3.496e-06	diff_var	Shannon	0.2912	no_dif																	
Shapiro-Shannon	4.832e-06	non-normal	Simpson	0.1884	no_dif																	
TIMEPOINT																						
test-assumptions	p-value	result	Index	p-value	result																	
Shapiro-Chao1	1.249e-11	non-normal	Chao1	0.2319	no_dif																	
Levene-Simpson	0.002138	diff_var	Shannon	0.3818	no_dif																	
TIMEPOINT																						
test-assumptions	p-value	result	Index	p-value	result																	
Shapiro-Chao1	1.784e-06	non-normal	Chao1	0.004935	*																	
Leven-Chao1	0.3614	equal_var	Shannon	0.144	no_dif																	
Shapiro-Shannon	4.832e-06	non-normal	Simpson	0.3615	no_dif																	
Levene-Shannon	0.693	equal_var	CONCENTRATION																			
Shapiro-Simpson	1.249e-11	non-normal	Index	p-value	result	PLATE																
Levene-Simpson	0.6511	equal_var	Chao1	0.6875	no_dif	CONCENTRATION																
CONCENTRATION			Shannon	0.2313	no_dif	Index	p-value	result	Index	p-value	result											
test-assumptions	p-value	result	Simpson	0.08099	no_dif																	
Shapiro-Chao1	1.784e-06	non-normal	PLATE						Chao1	0.5734	no_dif											
Leven-Chao1	3.276e-05	diff_var	CONCENTRATION																			
Shapiro-Shannon	4.832e-06	non-normal	PLATE																			
Levene-Shannon	3.84e-05	diff_var	CONCENTRATION																			
Shapiro-Simpson	1.249e-11	non-normal	PLATE																			
Levene-Simpson	0.04513	diff_var	CONCENTRATION																			
PLATE						PLATE																
test-assumptions	p-value	result	CONCENTRATION																			
Shapiro-Chao1	1.784e-06	non-normal	PLATE																			
Leven-Chao1	1.463e-05	diff_var	CONCENTRATION																			
Shapiro-Shannon	4.832e-06	non-normal	PLATE																			
Levene-Shannon	2.435e-06	diff_var	CONCENTRATION																			
Shapiro-Simpson	1.249e-11	non-normal	PLATE																			
Levene-Simpson	0.003972	diff_var	CONCENTRATION																			

DUNN test - Chao1					
Comparis	on	Z	P.unadj	P.adj Benjamini-	result
		-		Hochberg method.	s
0 - 0.001	474	0.167729715912	0.86679591744704	0.866795917447046	no_dif
0 - 0.01	77	1.334848989136	0.18192577601522	0.341110830028541	no_dif

	-				
0.001 -	1.167119273224	0.24316220556371			no_di
0.01	29	7	0.405270342606195		f
	0.328470693661	0.74255579924076			no_di
0 - 0.1	927	2	0.79559549918653		f
	0.496200409574	0.61975302206876			no_di
0.001 - 0.1	401	1	0.774691277585952		f
	1.663319682798	0.09624846080111			no_di
0.01 - 0.1	69	51	0.206246701716675		f
	0.772255567013	0.43996307634611			no_di
0 - 1	68	6	0.599949649562886		f
	0.939985282926	0.34722510974342			no_di
0.001 - 1	153	5	0.520837664615138		f
	2.107104556150	0.03510851749571			no_di
0.01 - 1	45	13	0.105325552487134		f
	0.443784873351	0.65719812583756			no_di
0.1 - 1	753	4	0.758305529812574		f
	2.582338751235	0.00981332086149			
0 - 100	79	251	0.0490666043074626	*	
0.001 -	2.750068467148	0.00595828136674			
100	26	664	0.0446871102505998	*	
	3.917187740372	8.95879782693703			
0.01 - 100	56	e-05	0.00134381967404055	*	
	2.253868057573	0.02420446971422			no_di
0.1 - 100	86	81	0.0907667614283554		f
	1.810083184222	0.07028288828070			no_di
1 - 100	11	89	0.175707220701772		f

## 8. Beta-diversity: beta-dispersion and ANOSIM

ATMAC - ANOSIM				betadispersion	anova	permutations
	TREATMENT			Bray	0.01855	0.016
Distance	R	p-value	result			
Bray	0.323059	0.0023	*			
	TIMEPOINT					
Distance	R	p-value	result			
Bray	0.01594	0.0676	no_dif			
	CONCENTRATION					
Distance	R	p-value	result			
Bray	0.086538	1,00E-04	*			
	PLATE					
Distance	R	p-value	result			

Bray	0.26658	0.0431	*
------	---------	--------	---

BAC - ANOSIM				betadispersion	anova	permutations
TREATMENT				Bray	6.4082e-08	0.001
Distance	R	p-value	result			
Bray	0.761109	1,00E-04	*			
TIMEPOINT						
Distance	R	p-value	result			
Bray	0.026599	0.0174	*			
CONCENTRATION						
Distance	R	p-value	result			
Bray	0.29141258	1,00E-04	*			
PLATE						
Distance	R	p-value	result			
Bray	0.761109	1,00E-04	*			

DDAC - ANOSIM				betadispersion	anova	permutations
TREATMENT				Bray	2.377e-09	0.001
Distance	R	p-value	result			
Bray	0.71651	1,00E-04	*			
TIMEPOINT						
Distance	R	p-value	result			
Bray	0.024595	0.018	*			
CONCENTRATION						
Distance	R	p-value	result			
Bray	0.16481128	1,00E-04	*			
PLATE						
Distance	R	p-value	result			
Bray	0.426397	1,00E-04	*			

## 9. DESeq2 tables

### ATMAC-C16 (0-1mg/kg)

	baseMean	log2FoldChange	IfcSE	stat	pvalue	padj
Candidatus_Solibacter	15.9179 851178 621	3.18317 236252 373	0.68864 2632083 359	4.62238 643706 046	3.7935049 2550512e -06	5.4894247e 7455447e -05

d_Bacteria_Acidobacteriota_Blastocatellia_Blastocatellales_Blastocatellaceae_Incertae_Sedis	16.7952 766215 683	2.09043 115197 364	0.79751 0841753 038	2.62119 465031 797	0.0087622 21694892 59	0.0291284 66715453 8
d_Bacteria_Acidobacteriota_Holophagae_Subgroup_7_Incertae_Sedis_Incertae_Sedis	33.5939 059723 147	2.54431 944509 272	0.51441 6385702 099	4.94603 110594 955	7.5741861 1295302e -07	1.6202172 0329256e -05
d_Bacteria_Acidobacteriota_Subgroup_11_Incertae_Sedis_Incertae_Sedis_Incertae_Sedis	11.4740 242550 935	2.06618 271544 54	0.79557 3118577 872	2.59709 970987 809	0.0094014 62852083 29	0.0310437 56531711 3
d_Bacteria_Acidobacteriota_Subgroup_25_Incertae_Sedis_Incertae_Sedis_Incertae_Sedis	16.3377 097083 328	2.16070 236859 141	0.76483 4974476 407	2.82505 696090 923	0.0047272 21154467 97	0.0174871 63969911 6
d_Bacteria_Acidobacteriota_Vicinamibacteria_Subgroup_17_Incertae_Sedis_Incertae_Sedis	33.3432 976642 502	2.11741 963102 036	0.64773 6200306 412	3.26895 367283 582	0.0010794 59739083 85	0.0053109 41916292 55
d_Bacteria_Actinomycetota_Acidimicrobiia_Microtrichales_Microtrichaceae_Incertae_Sedis	3.71253 354629 403	2.99413 031995 82	1.20426 9944277 36	2.48626 176729 41	0.0129092 97040865 5	0.0393937 78231359 8
Embleya	4.57058 352945 032	- 5.41473 504610 198	1.13949 6053497 8	- 4.75186 818724 021	2.0154575 0683529e -06	3.1987261 0762245e -05
d_Bacteria_Armatimonadota_Fimbriimonadia_Fimbriimonadales_Fimbriimonadaceae_Incertae_Sedis	7.43859 583308 229	3.72882 414204 935	0.91302 8881614 237	4.08401 554116 972	4.4264068 4824856e -05	0.0003888 91458810 409
Pseudalkalibacillus	2.39424 028667 737	- 3.59989 421868 398	1.42627 3015269 23	- 2.52398 676841 296	0.0116032 29585862 9	0.0367312 49801103 8
Thermoflavimicrobium	8.21196 812801 171	- 2.59226 533140 326	0.84376 7335508 807	- 3.07225 134502 282	0.0021245 07535360 81	0.0094167 36102680 36
d_Bacteria_Bacillota_Clostridia_Incertae_Sedis_Incertae_Sedis_Incertae_Sedis	2.45207 022540 964	3.70605 194813 987	1.51628 7889885 57	2.44416 114700 985	0.0145189 39794227 3	0.0425197 52254522 9
d_Bacteria_Bacillota_Clostridia_Lachnospirales_Lachnospiraceae_Incertae_Sedis	17.5415 369148 915	3.01028 313128 652	0.98604 7227358 652	3.05287 926152 405	0.0022665 71137582 53	0.0098595 20571600 74
Rikenella	13.7389 992325 31	23.5671 804825 722	4.80403 5996378 09	4.90570 439112 866	9.3092641 4228175e -07	1.8320631 8320105e -05
Terrimonas	23.1982 246026 106	2.09364 513458 162	0.58268 2183016 779	3.59311 678922 802	0.0003267 46047676 422	0.0019368 56089840 96
Cytophaga	4.06521 443331 635	5.19502 869475 606	1.40102 9180237 46	3.70800 891804 091	0.0002088 95301248 374	0.0013347 59587197 41
Chryseolinea	14.4760 497937 345	3.31823 525496 779	0.74242 8083832 819	4.46943 660568 071	7.8425898 6021384e -06	0.0001042 85248952 033
Ohtaekwangia	8.30461 355069 589	2.85022 605044 126	1.12984 1332061 38	2.52267 815803 928	0.0116464 93839374 4	0.0367312 49801103 8
OLB12	2.71216 963517 021	4.65694 132468 859	1.89903 6646918 64	2.45226 511676 06	0.0141960 02601023 5	0.0418584 62303641 5
Flavobacterium	29.8162 584781 411	2.40762 134840 539	0.56508 0486804 427	4.26066 977116 955	2.0381519 339016e- 05	0.0002279 02443518 088

d_Bacteria_Bacteroidota_Bacteroidia_Sphingobacteriales_AKYH767_Incertae_Sedis	7.50390 158714 979	3.18495 474927 715	0.96201 9433549 698	3.31069 689260 349	0.0009306 39550829 896	0.0046721 90398043 97
d_Bacteria_Bdellovibrionota_Bdellovibrionia_Bdellovibrionales_Pseudobdellovibrionaceae_Incertae_Sedis	3.59756 521404 405	5.74561 352724 523	1.40366 8538129 46	4.09328 368569 255	4.2530684 5160019e -05	0.0003804 56305124 963
OM27_clade	33.0952 152934 613	2.15920 575594 319	0.41279 5387067 046	5.23069 255033 243	1.6887617 2449117e -07	5.1929423 0281033e -06
d_Bacteria_Bdellovibrionota_Oligoflexia_0319-6G20_Incertae_Sedis_Incertae_Sedis	23.1182 220663 659	3.73899 626327 717	0.66238 8857987 218	5.64471 491057 195	1.6545518 6239498e -08	1.1629135 947119e-06
Candidatus_Protochlamydia	2.58894 757124 23	4.44317 623950 835	1.75354 8579390 01	2.53381 987344 426	0.0112826 71204601 7	0.0360459 36575740 6
d_Bacteria_Chlamydiota_Chlamydii_Chlamydiales_Parachlamydiaceae_Incertae_Sedis	2.17048 612907 635	4.29947 262044 59	1.60546 7717449 01	2.67801 873168 618	0.0074059 07648223 88	0.0254804 65475008
Neochlamydia	3.97066 197087 903	3.82645 816017 577	1.23899 8323968 59	3.08834 813264 266	0.0020127 25367432 02	0.0090849 62208959 21
d_Bacteria_Chloroflexota_Anaerolineae_Aggreatiliniales_Aggreatilineaceae_Incertae_Sedis	21.9335 856639 373	2.97663 396487 12	0.65014 1099329 389	4.57844 299943 744	4.6844977 6939814e -06	6.5850654 3583968e -05
d_Bacteria_Chloroflexota_Anaerolineae_Aggreatiliniales_Incertae_Sedis_Incertae_Sedis	18.3284 375162 334	3.23842 435155 836	0.67962 1463577 396	4.76504 131360 408	1.8881495 8233365e -06	3.0965653 1502719e -05
Mucispirillum	4.63126 739274 772	20.5552 693262 447	4.83587 8166945 36	4.25057 634138 634	2.1322114 4130122e -05	0.0002331 21784248 934
d_Bacteria_Dependentiae_Babeliae_Babeliales_Babiliaceae_Incertae_Sedis	3.83522 852282 697	3.33191 197782 311	1.35261 3126477 37	2.46331 483304 502	0.0137658 97955133 4	0.0410474 04811670 4
d_Bacteria_Dependentiae_Babeliae_Babeliales_Vermiphilaceae_Incertae_Sedis	2.94882 411598 232	4.46822 292847 159	1.64378 3385620 15	2.71825 531731 23	0.0065627 17533731 57	0.0229834 81909824 9
d_Bacteria_Gemmatimonadota_BD2-11_terrestrial_group_Incertae_Sedis_Incertae_Sedis_Incertae_Sedis	5.47642 428432 167	2.73077 617944 23	0.94909 2120904 827	2.87725 092147 945	0.0040115 64669441 73	0.0154773 79146222 7
YC-ZSS-LKJ147	12.1940 926340 962	2.70282 777578 727	0.69620 1038149 018	3.88225 186071 72	0.0001034 93603098 717	0.0007488 06657714 25
d_Bacteria_MBNT15_Incertae_Sedis_Incertae_Sedis_Incertae_Sedis_Incertae_Sedis	1.57011 650460 38	4.52672 904981 259	1.89759 3952112 995	2.38550 984248 7	0.0170554 65986609 6	0.0479502 24373782
d_Bacteria_Methylomirabilota_Methylomirabilia_Rokubacteriales_Incertae_Sedis_Incertae_Sedis	23.2447 080509 023	3.29507 751969 852	0.77100 7102941 325	4.27373 172974 423	1.9222830 3108726e -05	0.0002199 44942161 612
d_Bacteria_Methylomirabilota_Methylomirabilia_Rokubacteriales_WX65_Incertae_Sedis	11.2197 345377 468	3.17770 428855 095	0.98693 6027706 604	3.21976 723854 65	0.0012829 47191932 19	0.0060525 72300705 42
d_Bacteria_Myxococcota_Myxococcia_Myxococcales_Myxococcaceae_Incertae_Sedis	9.87411 779538 081	3.93414 915171 962	1.10736 4437296 52	3.55271 401104 798	0.0003812 78736083 415	0.0021866 50868572 04
d_Bacteria_Myxococcota_Polyangiiia_Blfdi19_Incertae_Sedis_Incertae_Sedis	4.98535 864939 484	4.11154 769504 155	1.13201 2987556 15	3.63206 760014 103	0.0002811 59441251 903	0.0017077 83272789 34
d_Bacteria_Myxococcota_Polyangiiia_Haliangiales_Haliangiaceae_Incertae_Sedis	117.024 360865 562	2.10095 216090 717	0.36753 3367395 587	5.71635 760800 42	1.0883158 3932787e -08	8.9241898 8248852e -07

<b>d_Bacteria_Myxococcota_Polyangiiia_Polyangiales_B Irii41_Incertae_Sedis</b>	34.4135 644821 086	2.23221 043375 385	0.53435 6398868 743	4.17738 131045 036	2.9488444 893932e- 05	0.0002901 66297756 291
<b>Phaselicystis</b>	11.2735 407383 995	2.45711 765515 328	1.02190 9497243 9	2.40443 763540 719	0.0161973 69643803 7	0.0463320 10841578 1
<b>Aetherobacter</b>	31.0426 791489 592	2.44699 167027 286	0.72616 2489842 354	3.36975 773948 898	0.0007523 42957081 646	0.0040233 99292219 24
<b>Pajaroellobacter</b>	27.1217 095285 609	2.20775 359048 252	0.68303 8490648 301	3.23225 355629 233	0.0012281 80239301 23	0.0058666 47356662 17
<b>Nitrospira</b>	29.8338 446769 982	2.75771 987350 654	0.59087 3591070 706	4.66719 094435 977	3.0534554 2527171e -06	4.5524244 5222327e -05
<b>d_Bacteria_Patescibacteria_Berkelbacteria_Incertae _Sedis_Incertae_Sedis_Incertae_Sedis</b>	4.78480 288131 198	4.03170 435344 201	1.30846 9045040 7	3.08123 785482 185	0.0020614 19048803 52	0.0092201 65200103 02
<b>d_Bacteria_Patescibacteria_Incertae_Sedis_Incertae _Sedis_Incertae_Sedis_Incertae_Sedis</b>	6.71273 889668 581	6.68608 347501 295	1.26168 7674496 45	5.29931 742234 18	1.1623640 3247471e -07	4.8016210 2420531e -06
<b>d_Bacteria_Patescibacteria_Saccharimonadia_Sacc harimonadales_Incertae_Sedis_Incertae_Sedis</b>	16.1761 104254 728	3.75048 528840 327	0.89705 8862751 307	4.18086 866328 973	2.9039756 9380147e -05	0.0002901 66297756 291
<b>d_Bacteria_Patescibacteria_Saccharimonadia_Sacc harimonadales_LWQ8_Incertae_Sedis</b>	14.3858 190010 968	4.21180 340482 9	0.97346 4026103 361	4.32661 432974 391	1.5141874 2235054e -05	0.0001891 14418469 748
<b>d_Bacteria_Patescibacteria_Saccharimonadia_Sacc harimonadales_YM_S32_TM7_50_20_Incertae_Sedis</b>	6.61169 169579 638	5.99592 830888 989	1.16589 1328890 61	5.14278 488939 035	2.7069550 7306665e -07	7.0095889 2604628e -06
<b>d_Bacteria_Planctomycetota_OM190_Incertae_Sedis _Incertae_Sedis_Incertae_Sedis</b>	16.2428 143948 243	2.56997 953545 234	0.73865 4481422 282	3.47927 156754 513	0.0005027 78805457 358	0.0028109 90594147 96
<b>Fimbriiglobus</b>	9.06877 539921 652	2.95175 119426 135	0.96762 5157489 766	3.05051 100771 175	0.0022845 23059273 34	0.0098595 20571600 74
<b>d_Bacteria_Planctomycetota_Planctomycetes_Pirell ulales_Pirellulaceae_Incertae_Sedis</b>	41.1930 268306 794	2.09447 119233 982	0.58490 0074135 903	3.58090 430307 104	0.0003424 07058289 021	0.0020055 27055692 84
<b>Pir4_lineage</b>	35.8978 235813 703	2.03048 694497 898	0.58974 1214707 334	3.44301 346818 135	0.0005752 70664071 368	0.0031801 47940709 13
<b>Pirellula</b>	43.0999 987987 679	2.39587 033412 939	0.61434 0411792 184	3.89990 677504 031	9.6229734 0659178e -05	0.0007173 48926673 206
<b>d_Bacteria_Planctomycetota_vadinHA49_Incertae_S edis_Incertae_Sedis_Incertae_Sedis</b>	3.81602 321658 994	4.65119 073796 488	1.55593 3402553 23	2.98932 507672 401	0.0027959 44890143 32	0.0113686 35421078 6
<b>Caulobacter</b>	4.20646 404772 317	4.58480 511862 011	1.42669 0492303 58	3.21359 477991 427	0.0013108 45265734 13	0.0060843 00667369 76
<b>Dongia</b>	7.01353 704462 949	2.59601 312680 006	0.86105 8758721 443	3.01490 821678 046	0.0025705 70317807 38	0.0108095 77746677 2
<b>Hyphomicrobium</b>	21.9119 803049 954	2.21118 452081 07	0.59030 6294386 048	3.74582 575493 365	0.0001798 01363039 799	0.0011954 36089399 74
<b>Pedomicrobium</b>	34.8009 206385 336	2.45618 511531 085	0.46701 8228356 615	5.25929 174960 448	1.4461129 6990719e -07	4.9095173 9150835e -06

<b>Bauldia</b>	6.77928 650700 866	4.54385 878889 692	1.40175 1778349 17	3.24155 735635 89	0.0011887 85094984 15	0.0057608 87433457 68
<b>d_Bacteria_Pseudomonadota_Alphaproteobacteria_Hyphomicrobiales_Hyphomicrobiales_Incertae_Sedis_Incertae_Sedis</b>	11.8643 305293 252	3.61909 693226 849	0.94604 9539649 64	3.82548 352976 186	0.0001305 15660607 645	0.0009173 38643128 019
<b>d_Bacteria_Pseudomonadota_Alphaproteobacteria_Hyphomicrobiales_Methyloligellaceae_Incertae_Sedis</b>	114.540 690027 576	2.13957 164221 174	0.40626 7735566 237	5.26640 797411 516	1.3911893 4317485e -07	4.9095173 9150835e -06
<b>Pararhizobium</b>	7.29070 292974 902	4.09791 160137 619	1.68389 7254181 36	2.43358 767359 498	0.0149500 14384174	0.0435231 18798897
<b>Pseudorhodoplanes</b>	8.61651 304079 361	3.36605 630660 645	1.11802 2298522 42	3.01072 376736 584	0.0026062 58330436 59	0.0108667 72021820 3
<b>Reyranella</b>	32.6572 320966 481	2.34945 869098 076	0.57618 1032626 914	4.07763 976587 212	4.5495181 8897572e -05	0.0003926 95254206 325
<b>Ellin6067</b>	31.5870 188472 819	4.26703 622174 431	0.78505 1146322 348	5.43536 079366 762	5.4685665 0417107e -08	3.3631684 0006521e -06
<b>MND1</b>	16.9292 330712 847	3.29706 905111 634	0.76479 0341812 305	4.31107 569076 168	1.6246227 790195e- 05	0.0001903 12954113 713
<b>d_Bacteria_Pseudomonadota_Gammaproteobacteria_Burkholderiales_SC-I-84_Incertae_Sedis</b>	100.502 248237 491	2.95688 825313 987	0.44842 1078090 53	6.59399 925117 462	4.2813386 7213239e -11	7.0213954 2229711e -09
<b>d_Bacteria_Pseudomonadota_Gammaproteobacteria_Burkholderiales_TRA3-20_Incertae_Sedis</b>	9.92772 345080 4	2.84182 823942 676	0.90288 8456750 626	3.14748 540440 324	0.0016468 13273997 03	0.0075722 62904734
<b>d_Bacteria_Pseudomonadota_Gammaproteobacteria_CCD24_Incertae_Sedis_Incertae_Sedis</b>	11.7864 667405 086	2.22364 738601 823	0.73011 2101077 276	3.04562 461399 73	0.0023219 75355944 27	0.0099340 16305431 15
<b>d_Bacteria_Pseudomonadota_Gammaproteobacteria_Incertae_Sedis_Incertae_Sedis_Incertae_Sedis</b>	3.98129 325802 247	4.64683 809159 118	1.52795 3020087 63	3.04121 791082 601	0.0023562 32356893 02	0.0099936 75168891 02
<b>Legionella</b>	13.6151 424089 028	2.09269 315349 112	0.62363 8894616 055	3.35561 680254 002	0.0007918 82089904 906	0.0041447 44555672 49
<b>Arenimonas</b>	47.3806 482839 219	3.75074 763332 445	0.61505 7546611 638	6.09820 601988 77	1.0726544 578863e- 09	1.3193649 8320015e -07
<b>Luteimonas</b>	38.3857 760606 175	3.00872 796971 956	0.57276 8962336 256	5.25295 218066 167	1.4968040 8277694e -07	4.9095173 9150835e -06
<b>Pseudoxanthomonas</b>	2.67113 391542 615	4.18092 474081 805	1.66610 7480979 93	2.50939 677574 643	0.0120937 55620313 9	0.0376590 36488572 5
<b>Thermomonas</b>	10.0293 780668 325	4.13865 327544 872	1.71927 3863130 28	2.40721 002290 67	0.0160749 22412367 9	0.0463320 10841578 1
<b>d_Bacteria_Pseudomonadota_Gammaproteobacteria_PLTA13_Incertae_Sedis_Incertae_Sedis</b>	21.8161 648401 705	2.33697 094681 992	0.58908 1125693 049	3.96714 619581 554	7.2738377 2313078e -05	0.0005695 62301118 109
<b>Acinetobacter</b>	40.0389 495876 604	7.55806 589576 27	1.40936 7200154 79	5.36273 718796 108	8.1970227 1901122e -08	4.0329351 7775352e -06
<b>Pseudomonas</b>	16.9592 060140 045	4.21598 408737 584	0.87573 4649758 628	4.81422 550602 27	1.4777186 5906943e -06	2.5070261 3883504e -05

<b>Aquicella</b>	17.6764 859140 82	4.86685 610655 46	1.12492 0614557 97	4.32639 960862 216	1.5156634 9901897e -05	0.0001891 14418469 748
<b>d_Bacteria_Pseudomonadota_Gammaproteobacteri a_Rickettsiellales_Rickettsiellaceae_Incertae_Sedis</b>	11.1503 876136 511	4.46028 592943 593	1.06142 6044550 15	4.20216 363856 631	2.6437590 6523892e -05	0.0002709 85304186 99
<b>d_Bacteria_Pseudomonadota_Gammaproteobacteri a_Steroidobacterales_Steroidobacteraceae_Incertae_</b> <b>Sedis</b>	39.3371 712916 702	2.01750 264143 699	0.48550 4147755 959	4.15547 972300 97	3.2460573 3737389e -05	0.0003013 32115092 067
<b>Steroidobacter</b>	18.5041 940500 251	2.47969 784034 841	0.65902 4831142 405	3.76267 740329 284	0.0001681 03983151 145	0.0011487 10551532 83
<b>Sumerlaea</b>	5.28317 384374 75	2.27381 758699 52	0.88284 9951906 143	2.57554 251669 364	0.0100082 96792448 5	0.0326098 14714468 1
<b>d_Bacteria_Thermodesulfobacteriota_Incertae_Sedis _Incertae_Sedis_Incertae_Sedis_Incertae_Sedis</b>	6.76975 901657 869	2.16592 210130 928	0.90061 3623030 158	2.40494 041609 312	0.0161751 02814289	0.0463320 10841578 1
<b>Oleiharenicola</b>	4.25793 835133 03	5.87306 247599 555	1.56599 7619733 9	3.75036 488049 931	0.0001765 77435789 047	0.0011900 83539838 51
<b>Opitutus</b>	6.96747 026997 173	3.21279 803735 92	0.99153 3734945 732	3.24023 068921 104	0.0011943 30321570 49	0.0057608 87433457 68
<b>ADurb.Bin063-1</b>	14.2484 250461 512	3.18974 202739 11	0.87455 6455134 229	3.64726 829087 498	0.0002650 43138942 956	0.0016300 15304499 18
<b>d_Bacteria_Verrucomicrobiota_Verrucomicrobiia_Pe dosphaerales_Pedosphaeraceae_Incertae_Sedis</b>	46.6070 030674 486	2.44485 828707 65	0.52372 5710971 775	4.66820 367199 475	3.0384461 50432e- 06	4.5524244 5222327e -05
<b>d_Bacteria_Verrucomicrobiota_Verrucomicrobiia_Ve rrucomicrobiales_Verrucomicrobiaceae_Incertae_Sed is</b>	6.93461 256951 174	2.95908 754244 776	0.89265 8201190 345	3.31491 665959 252	0.0009167 04506116 211	0.0046496 76464012 12
<b>Roseimicrobium</b>	11.3747 026956 907	3.72103 736359 496	0.89179 6073788 473	4.17252 045951 209	3.0124853 8996949e -05	0.0002906 16237620 586

### BAC-C12 (0-100mg/kg/)

	baseMe an	log2Fol dChang e	IfcSE	stat	pvalue	padj
<b>Embleya</b>	2.86325 4275190 93	- 4.03619 6408480 95	1.382628 3908954 8	- 2.91921 9969052 45	0.0035090 851237973 6	0.0181166 720344887
<b>d_Bacteria_Armatimonadota_Fimbriimonadia_Fi mbriimonadales_Fimbriimonadaceae_Incertae_Se dis</b>	5.61335 4935687 9	3.20588 3240957 56	1.045122 0821396 6	3.06747 2495073 7	0.0021587 732663888 2	0.0127799 377370218
<b>Fictibacillus</b>	7.60525 5303250 9	4.86505 0718127 28	1.299170 8460739 8	3.74473 5138437 86	0.0001805 841809912 38	0.0017059 441778746 7
<b>Ureibacillus</b>	2.88920 8937313 55	4.91650 0673070 16	1.699225 5161456 2	2.89337 7380668 3	0.0038112 307095565 2	0.0194504 187935988

<b>Solibacillus</b>	13.9526 4449433 19	2.57217 3035508 01	0.778847 5816291 96	3.30253 7102480 98	0.0009581 441146753 5	0.0068615 481760621 8
<b>Sporosarcina</b>	3.26915 9590159 64	4.62973 3242320 63	1.366420 1837647 8	3.38822 0766444 42	0.0007034 761737339 84	0.0053852 313989291 2
<b>Caldicoprobacter</b>	3.53505 6687002 02	2.53916 9301630 48	0.933170 2482134 06	2.72101 3991275 25	0.0065082 006883074 2	0.0297901 144908092
<b>Fonticella</b>	2.90594 9231000 45	3.02966 1536638 52	1.180639 0748768 5	2.56611 9994761 76	0.0102843 243694461	0.0434880 001908008
<b>Clostridium</b>	40.8658 5108287 55	2.09230 8943806 83	0.303642 6928087 67	6.89069 4205259 74	5.5520772 6932553e- 12	4.1085371 7930089e- 10
<b>d_Bacteria_Bacillota_Clostridia_Lachnospirales_Lachnospiraceae_Incertae_Sedis</b>	15.9866 9210646 96	7.26141 5858491 24	1.512234 8463914 4	4.80177 7895687 79	1.5726306 8992148e- 06	3.4912401 3162569e- 05
<b>d_Bacteria_Bacillota_Clostridia_Oscillospirales_Oscillospiraceae_Incertae_Sedis</b>	26.9405 6768014 79	5.69547 9789356 32	1.048112 6495223 6	5.43403 4015286 29	5.5094071 2845812e- 08	2.4461767 6503541e- 06
<b>Ruminiclostridium</b>	8.02736 4798857 15	3.12291 4983691 55	0.867790 0284867 37	3.59869 8857069 52	0.0003198 132587952	0.0027307 132097128 6
<b>Romboutsia</b>	16.1052 1239214 62	2.04422 1429002 38	0.637313 2327208 17	3.20756 1563213 1	0.0013386 540586677 3	0.0091608 269508402 4
<b>d_Bacteria_Bacillota_Limnochordia_Limnochordales_Limnochordaceae_Incertae_Sedis</b>	5.64553 8254163 72	2.61290 7644158 64	0.630894 3399622 3	4.14159 3098323 04	3.4490182 2841695e- 05	0.0004253 789148380 91
<b>Bacteroides</b>	8.84064 4314489 27	23.8468 0166435 39	4.831795 8509684 5	4.93539 0980886 37	7.9990352 6006399e- 07	1.9730953 6414912e- 05
<b>d_Bacteria_Bacteroidota_Bacteroidia_Bacteroidales_Muribaculaceae_Incertae_Sedis</b>	12.6948 3772175 59	24.2675 9205309 08	4.831723 7118814 2	5.02255 3751038 31	5.0988920 8391776e- 07	1.4715759 3252989e- 05
<b>Ferruginibacter</b>	16.0156 0849823 69	2.77433 1698261 28	0.665930 3966523 62	4.16609 8607614 06	3.0985671 7252659e- 05	0.0003930 753784576 59
<b>Flavisolibacter</b>	18.5324 6718262 49	2.39114 8998390 6	0.681748 9479410 93	3.50737 4680389 25	0.0004525 514562926 48	0.0036533 244835261 1
<b>Segetibacter</b>	7.92782 7395052 97	3.99798 5175375 36	1.142236 9728776 2	3.50013 6373018 36	0.0004650 201941206 77	0.0036869 458248139 4
<b>Cytophaga</b>	2.01052 0112320 56	5.06026 9598382 01	1.883254 436118	2.68698 1377201 94	0.0072100 972500852 9	0.0320128 317903787
<b>Sporocytophaga</b>	2.51780 3190454 96	3.61543 6129520 8	1.187512 4963506 1	3.04454 5754787 02	0.0023303 198058300 6	0.0135549 494978645
<b>Pontibacter</b>	2.29800 0241253 66	3.55935 0042603 85	1.062640 2643781 5	3.34953 4326827 68	0.0008094 752475315 73	0.0060916 442356613 3
<b>Flavobacterium</b>	17.4018 5197855 23	2.85982 4332151 96	0.666041 0741647 85	4.29376 5719686 54	1.7566784 3293271e- 05	0.0002689 535255938 36
<b>d_Bacteria_Bacteroidota_Bacteroidia_Sphingobacteriales_AKYH767_Incertae_Sedis</b>	3.12468 0404727 93	3.61353 1923343 76	0.915135 6851292 44	3.94862 9675427 22	7.8599834 6965162e- 05	0.0008309 125382203 15

d_Bacteria_Bdellovibrionota_Oligoflexia_0319-6G20_Incertae_Sedis_Incertae_Sedis	15.5361 9458436 35	3.09810 9911740 67	0.595326 6845425 51	5.20405 0132779 21	1.9499136 6561965e-07	7.2146805 627927e-06
d_Bacteria_Chloroflexota_Anaerolineae_Aggreditilineales_Aggreditilineaceae_Incertae_Sedis	11.5701 6225296 4	2.54112 2899247 5	0.687329 0938186 11	3.69709 7827082 68	0.0002180 783202724 48	0.0019365 354840193 4
d_Bacteria_Chloroflexota_Anaerolineae_Aggreditilineales_Incertae_Sedis_Incertae_Sedis	8.45098 5236912 2	2.55600 0775587 91	0.685071 6666066 45	3.73099 7646200 31	0.0001907 230057929 65	0.0017641 878035849 3
Anaerolinea	3.07422 1935312 35	3.05044 3498906 37	0.959368 0329007 92	3.17963 8464378 36	0.0014745 890122160 2	0.0097719 033048345 4
d_Bacteria_Entotheonellaeota_Entotheonellia_Entotheonellales_Entotheonellaceae_Incertae_Sedis	19.1524 9762274 41	2.36389 8500527 97	0.711148 7393180 06	3.32405 6375034 79	0.0008871 825966788 81	0.0065651 512154237 2
YC-ZSS-LKJ147	7.88091 4631524 52	2.33716 5395567 05	0.792430 5816384 61	2.94936 2947016 29	0.0031842 977244936	0.0171359 591123873
d_Bacteria_Myxococcota_Myxococcia_Myxococcales_Myxococcaceae_Incertae_Sedis	7.14017 1451798 86	4.90390 4587312 29	0.977844 7580024 1	5.01501 3423327 26	5.3029763 3344105e-07	1.4715759 3252989e-05
P3OB-42	1.89924 6050025 13	3.41732 2761806 39	1.235353 0182926 37	2.76627 2240569 37	0.0056701 177297263 4	0.0270702 394838548
d_Bacteria_Myxococcota_Polyangiiia_mle1-27_Incertae_Sedis_Incertae_Sedis	7.40487 8466456 03	2.02818 0902783 66	0.750871 6290796 34	2.70110 2058243 52	0.0069110 127953356 9	0.0309948 452639298
d_Bacteria_Patescibacteria_Incertae_Sedis_Incertae_Sedis_Incertae_Sedis	3.07239 0448813 08	4.50527 0948788 37	1.644768 5670564 2	2.73915 1901991 47	0.0061597 906008048 5	0.0284890 315287224
d_Bacteria_Patescibacteria_SaccharimonadiaSaccharimonadales_Incertae_Sedis_Incertae_Sedis	7.69250 3949404 22	5.53619 8581673 89	1.324593 3853174 5	4.17954 5695335 86	2.9209202 5561287e-05	0.0003929 965434824 59
d_Bacteria_Patescibacteria_SaccharimonadiaSaccharimonadales_LWQ8_Incertae_Sedis	7.68031 0897995 28	5.98276 5409839 61	1.263202 6846026 1	4.73618 8010653 04	2.1777557 2308016e-06	4.3951070 0476177e-05
d_Bacteria_Patescibacteria_SaccharimonadiaSaccharimonadales_YM_S32_TM7_50_20_Incertae_Sedis	3.64596 5687899 52	6.08128 0593800 1	1.598833 0963035 32	3.80357 4374248 48	0.0001426 231469878 48	0.0013880 747641498 4
Aquisphaera	19.6201 5611401 64	- 2.15767 4126545 52	0.690452 6053086 6	- 3.12501 4099383 34	0.0017779 653761451 8	0.0109641 19819562
d_Bacteria_Pseudomonadota_AlphaproteobacteriAzospirillales_Incertae_Sedis_Incertae_Sedis	14.7160 3153859 81	- 2.64250 9986348 88	0.459609 9373282 32	- 5.74946 2254254 35	8.9527736 7128237e-09	4.4167016 7783264e-07
d_Bacteria_Pseudomonadota_AlphaproteobacteriHyphomicrobiales_Methyloligellaceae_Incertae_Sedis	392.460 5443466 31	- 2.10546 7437353 58	0.201423 3063676 8	- 10.4529 4844634 43	1.4203945 1596205e-25	5.1822103 4605761e-23
Ellin6055	9.72019 8060630 06	3.83733 6246419 61	0.829218 6961961 32	4.62765 2830336 06	3.6983329 8045744e-06	6.5682393 7329241e-05
Erythrobacter	3.93813 8596021 16	4.65503 5247629 21	1.346425 6395805 2	3.45732 8136650 37	0.0005455 601047937 96	0.0042496 260794464 1
mle1-7	3.43556 3806370 64	- 3.10006 3777802 82	1.059761 4482376 9	- 2.92524 6793000 44	0.0034418 314575467 2	0.0179785 078488323

<b>Coxiella</b>	2.22090 9855490 32	4.23273 2801089 61	1.524767 2793835 24	2.77598 6118223 1	0.0055034 558195022 1	0.0268457 096030812
<b>Escherichia-Shigella</b>	16.9684 1495675 5	24.8666 9933334 8	4.831681 9830191 7	5.14659 2722936 12	2.6526037 6760789e- 07	8.4125433 7727073e- 06
<b>d_Bacteria_Pseudomonadota_Gammaproteobacteria_Incertae_Sedis_Incertae_Sedis_Incertae_Sedis</b>	3.33212 3825534 02	4.08197 4339297 26	1.252730 7646958 8	3.25846 0999230 14	0.0011201 827241170 1	0.0078946 211033008 3
<b>Legionella</b>	6.82938 8527807 04	3.18511 0279046 3	0.758955 8784378 37	4.19670 0189742 56	2.7083207 3220283e- 05	0.0003879 014209993 73
<b>Acinetobacter</b>	19.8905 6545397 23	8.51596 9626027 26	1.823836 6239709 8	4.66926 1223346 72	3.0228481 1408653e- 06	5.5922690 1106007e- 05
<b>Pseudomonas</b>	14.4447 5128238 94	2.63049 0481768 9	0.821350 8576064 19	3.20263 9234388 42	0.0013617 445467465 2	0.0091608 269508402 4
<b>Aquicella</b>	10.6923 4042349 77	3.36936 4073952 88	0.807622 8395611 67	4.17195 2437332 84	3.0200068 5569357e- 05	0.0003930 753784576 59
<b>d_Bacteria_Pseudomonadota_Gammaproteobacteria_Rickettsiales_Rickettsiaceae_Incertae_Sedis</b>	6.47832 6880463 31	2.57962 1697880 78	0.804832 7410546 78	3.20516 4957007 55	0.0013498 509605805 7	0.0091608 269508402 4
<b>Candidatus_Udaeobacter</b>	590.814 7509205 49	- 2.07954 5305553 53	0.310502 1548201 99	- 6.69736 1912859 26	2.1221559 7562166e- 11	1.3460532 1882288e- 09
<b>Candidatus_Xiphinematabacter</b>	89.6423 7106883 84	- 2.23673 9516944 97	0.339848 7735526 43	- 6.58157 3014264 55	4.6549681 0749205e- 11	2.5835072 9965809e- 09
<b>Luteolibacter</b>	6.17141 5834079 41	2.58986 8879399 99	0.843686 8934884 41	3.06970 3819495 77	0.0021427 114572134 9	0.0127799 377370218
<b>Roseimicrobium</b>	7.78462 6605189 42	2.09372 5912472 74	0.802567 6296647 04	2.60878 4400322 07	0.0090864 471185104 6	0.0391687 623361033

## DDAC-C10 (0-100 mg/kg)

	baseMean	log2FoldChange	IfcSE	stat	pvalue	padj
<b>Candidatus_Solibacter</b>	13.5509 3835301 33	2.00025 4475601 96	0.543087 8680446 09	3.68311 3899789 15	0.0002304 021492388 86	0.0020160 188058402 5
<b>Embleya</b>	4.79881 3592427 42	- 5.54583 5228967 55	1.228906 6618469 4	- 4.51282 0542963 47	6.3971147 6017531e- 06	0.0001164 274886351 91
<b>Chthonomonas</b>	3.24561 3311154 14	2.76910 1305107 63	0.987059 3373109 13	2.80540 5106294 42	0.0050253 376078960 8	0.0265875 419952641
<b>d_Bacteria_Armatimonadota_Fimbriimonadia_Fimbriimonadales_Fimbriimonadaceae_Incertae_Sedis</b>	6.84600 2528945 62	4.24713 5560692 59	1.012483 8866969 1	4.19476 8545451 4	2.7315036 3031647e- 05	0.0003270 616188931 56

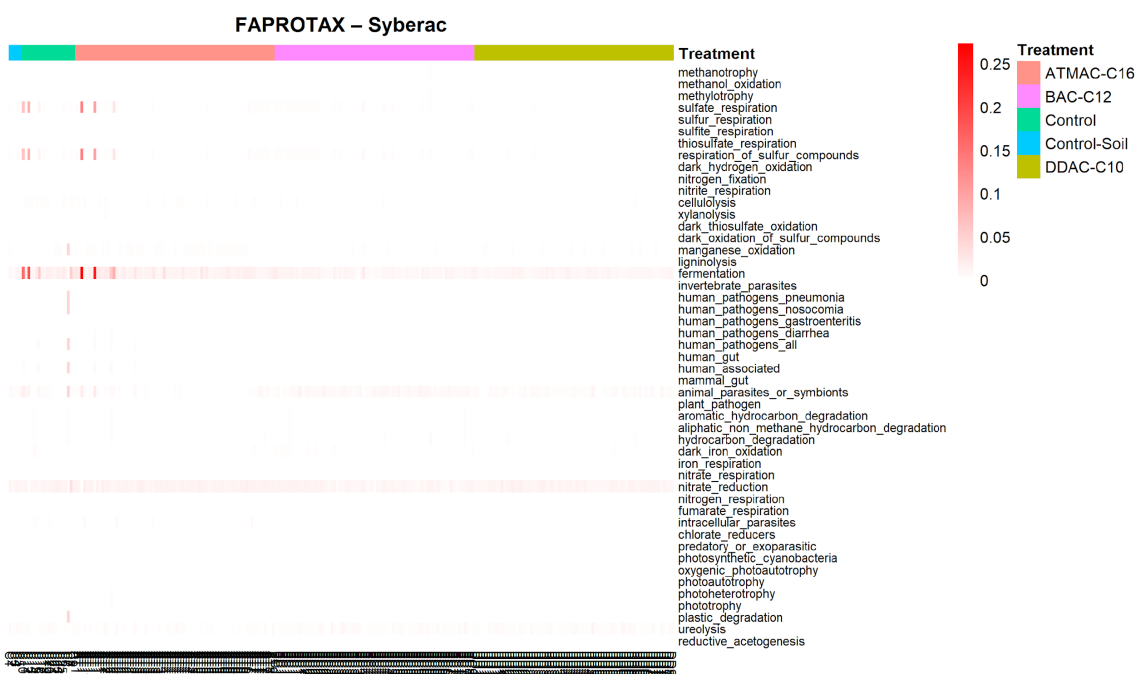
<b>Fictibacillus</b>	11.7295 2254539 56	2.74966 3857426 17	1.037380 7560647 6	2.65058 3058680 25	0.0080352 967382919 5	0.0373067 348563555
<b>Caldicoprobacter</b>	5.17414 8980931 6	2.43204 8220317 2	0.712404 9473439 26	3.41385 6444125 86	0.0006405 031462764 52	0.0046258 560564410 4
<b>d_Bacteria_Bacillota_Clostridia_Clostridia_vadin BB60_group_Incertae_Sedis_Incertae_Sedis</b>	6.99612 9127683 01	3.43144 6103136 63	1.000019 8212199 4	3.43137 8089036 84	0.0006005 229807297 88	0.0045371 031043037 2
<b>Fonticella</b>	3.85219 0051489 49	3.19737 5718477 85	1.155140 8691152 4	2.76795 3073054 05	0.0056409 577363643 1	0.0288386 041578175
<b>d_Bacteria_Bacillota_Clostridia_Lachnospirales_</b> <b>Lachnospiraceae_Incertae_Sedis</b>	20.4361 6609184 69	7.75026 4513022	1.708668 3316926 7	4.53585 0737834 13	5.7371746 3680528e- 06	0.0001087 672691561
<b>d_Bacteria_Bacillota_Clostridia_Oscillospirales_</b> <b>Oscillospiraceae_Incertae_Sedis</b>	35.9872 7534525 92	4.69281 6655308 94	0.983063 5421961 75	4.77366 5642024 66	1.8090262 8215732e- 06	5.1444184 8988488e- 05
<b>Ruminiclostridium</b>	10.4245 8585780 55	3.27586 4934019	0.957213 4396925 6	3.42229 3083422 6	0.0006209 534039586 19	0.0045569 967548576 1
<b>Bacteroides</b>	11.7654 6390494 15	24.5116 4268395 76	4.831800 6982485 8	5.07298 2975651 81	3.9162754 8586411e- 07	1.4849211 2172347e- 05
<b>d_Bacteria_Bacteroidota_Bacteroidia_Bacteroida</b> <b>les_Muribaculaceae_Incertae_Sedis</b>	16.7428 8903851 35	24.9570 8128271 82	4.346541 3360153 2	5.74182 5362599 11	9.3661389 1032965e- 09	7.1026553 4033332e- 07
<b>Aurantisolimonas</b>	7.33592 7692051 02	2.21653 0277904 65	0.820997 3551616 75	2.69980 1971308 61	0.0069380 759978037 1	0.0335832 40202135
<b>Ferruginibacter</b>	27.3867 6684765 72	2.10240 8971277 43	0.496717 3462409 7	4.23260 6304547 1	2.3099866 6963378e- 05	0.0003091 305690245 2
<b>Flaviaestuariibacter</b>	2.55100 1802488 7	5.71206 2910575 51	2.072041 1979140 5	2.75673 2306445 41	0.0058382 125504116 8	0.0288737 685917099
<b>Segetibacter</b>	13.7687 0963277 16	2.31562 3193666 5	0.709174 9672305 22	3.26523 5380077 64	0.0010937 314711711 4	0.0071262 249908518
<b>Flavobacterium</b>	24.1151 3327767 91	2.28180 5823050 54	0.594593 5740262 47	3.83758 9107462 86	0.0001242 481547099 25	0.0012028 278807024 7
<b>d_Bacteria_Bacteroidota_Bacteroidia_Sphingobact</b> <b>eriales_AKYH767_Incertae_Sedis</b>	4.43649 4727560 95	2.25047 3531087 03	0.755437 3436767 79	2.97903 3999211 35	0.0028915 869147801 7	0.0162428 647682096
<b>d_Bacteria_Bacteroidota_Bacteroidia_Sphingobact</b> <b>eriales_env.OPS_17_Incertae_Sedis</b>	1.71485 0439740 22	4.00953 2328638 16	1.570349 1289368 8	2.55327 4462827 64	0.0106715 366951253	0.0466879 730411731
<b>Peredibacter</b>	6.26998 0547983 15	2.76700 9038709 53	0.905992 8631633 43	3.05411 7919923 02	0.0022572 333766534 6	0.0134254 591201189
<b>d_Bacteria_Bdellovibrionota_Bdellovibrionia_Bd</b> <b>ellovibrionales_Pseudobdellovibrionaceae_Incertae</b> <b>_Sedis</b>	2.66989 5982961 47	4.48414 8023905 3	1.367789 6471896 1	3.27839 0089527 91	0.0010440 101200729 5	0.0070899 194721371 9
<b>d_Bacteria_Bdellovibrionota_Oligoflexia_0319-</b> <b>6G20_Incertae_Sedis_Incertae_Sedis</b>	19.4853 8999324 73	3.50272 4361897 12	0.526587 7097653 62	6.65173 9675918 13	2.8964869 0683923e- 11	4.3930051 4203949e- 09
<b>d_Bacteria_Chloroflexota_An aerolineae_Aggre</b> <b>gatilineales_Aggregatilineaceae_Incertae_Sedis</b>	21.0485 6480671 71	2.30446 9495116 29	0.543262 0236760 49	4.24191 1627694 52	2.2162396 2640823e- 05	0.0003055 724333381 04

d_Bacteria_Chloroflexota_Anaerolineae_Aggregatilineales_Incertae_Sedis_Incertae_Sedis	12.3809 3645333 9	2.89824 5217832 66	0.632422 2340749 97	4.58276 9329847 71	4.5885812 6440157e-06	9.4900203 4228507e-05
Anaerolinea	5.51276 3363734 31	2.18516 7885538 35	0.682220 9228567 04	3.20302 0916433 16	0.0013599 410338431 4	0.0084763 447999812 4
d_Bacteria_Cyanobacteriota_Sericytochromatia_Incertae_Sedis_Incertae_Sedis_Incertae_Sedis	4.25606 7444423 73	3.37625 3504246 22	0.920545 9464356 01	3.66766 4299994 19	0.0002447 762626039 91	0.0021013 811223550 2
d_Bacteria_Myxococcota_Myxococcia_Myxococcales_Myxococcaceae_Incertae_Sedis	7.99498 3070434 13	3.68503 2495425 24	0.982193 8989063 76	3.75183 8103991 82	0.0001755 428131525 14	0.0015974 395996878 8
KD3-10	2.49536 0324437 64	3.43166 5848976 61	1.033984 5431513 6	3.31887 5385233 16	0.0009038 075282355 93	0.0062307 943234423 4
d_Bacteria_Patescibacteria_Berkelbacteria_Incertae_Sedis_Incertae_Sedis_Incertae_Sedis	3.69534 8733679 68	5.59304 1714176 26	1.401829 5852549 6	3.98981 5718690 95	6.6124649 3716778e-05	0.0006996 910573049 63
d_Bacteria_Patescibacteria_Incertae_Sedis_Incertae_Sedis_Incertae_Sedis	4.04186 1954641 22	6.61775 7174529 41	1.402017 5647017 4	4.72016 7094295 45	2.3565098 4456843e-06	5.9567332 1821465e-05
d_Bacteria_Patescibacteria_SaccharimonadiaSaccharimonadales_Incertae_Sedis_Incertae_Sedis	11.2075 4174347 12	4.77257 3429312 08	0.840482 7159406 89	5.67837 1891289 28	1.3598281 8876593e-08	8.8388832 2697852e-07
d_Bacteria_Patescibacteria_SaccharimonadiaSaccharimonadales_LWQ8_Incertae_Sedis	10.5902 2180824 55	7.41430 1169580 37	1.148633 0120609 6	6.45489 1241787 58	1.0829664 8225894e-10	1.2318743 7356954e-08
d_Bacteria_Patescibacteria_SaccharimonadiaSaccharimonadales_YM_S32_TM7_50_20_Incertae_Sedis	5.33250 1256735 66	4.96232 7239349 57	1.160085 2469025 1	4.27755 3957865 8	1.8895816 5044946e-05	0.0002774 308076403 39
d_Bacteria_Plantomycetota_vadinHA49_Incertae_Sedis_Incertae_Sedis_Incertae_Sedis	2.89226 6548335 65	2.95381 4540854 37	1.167856 8994790 5	2.52926 0684397 19	0.0114303 094931469	0.0495313 411369698
d_Bacteria_Pseudomonadota_Alphaproteobacteria_Azospirillales_Incertae_Sedis_Incertae_Sedis	11.1687 6812066 98	- 2.42010 0828346 69	0.518488 6536100 38	- 4.66760 6150098 86	3.0472932 2666513e-06	7.2974653 5859281e-05
Ellin6067	30.5360 1040151 35	2.38785 3358880 72	0.555786 5297169 81	4.29634 9823549 46	1.7363350 211171e-05	0.0002730 790773191 02
Coxiella	2.80602 7791094 31	4.33887 7284278 03	1.611030 5227112 7	2.69323 0961866 55	0.0070763 230262756 5	0.0338918 629153202
Escherichia-Shigella	23.1597 8325567 12	25.4528 3166610 02	4.831681 3172529 9	5.26790 3653995 79	1.3799049 2919964e-07	6.2785674 2785835e-06
d_Bacteria_Pseudomonadota_Gammaproteobacteria_Incertae_Sedis_Incertae_Sedis_Incertae_Sedis	4.03600 3799122	5.99154 7270615 24	1.424042 0141142 6	4.20742 3103553 54	2.5829925 4404283e-05	0.0003209 372869876 85
Acinetobacter	25.6625 7191630 84	8.35068 5764544 45	1.487212 4298281 3	5.61499 1911753 64	1.9657143 986766e-08	1.1180000 6424731e-06
Pseudomonas	15.5430 2102350 72	4.11193 5840394 84	0.839105 4380469 61	4.90038 0397921 71	9.5651273 0280764e-07	3.1086663 7341248e-05
Aquicella	13.5766 8563945 41	4.05671 0679363 12	0.700947 0095304 66	5.78747 1269876 07	7.1453903 6131002e-09	6.5023052 2879211e-07
d_Bacteria_Pseudomonadota_Gammaproteobacteria_Rickettsiellales_Rickettsiellaceae_Incertae_Sedis	7.62948 0256773 95	3.67547 1613948 66	0.789396 1127799 49	4.65605 4868328 48	3.2232606 7529272e-06	7.3329180 3629094e-05

<b>Oleiharenicola</b>	1.77047 3614005 78	3.69836 3142319 49	1.428438 5762564	2.58909 4976706 69	0.0096228 549450779 6	0.0429254 803922595
<b>Luteolibacter</b>	7.84241 0931786 57	2.34952 3313682 14	0.775378 6880790 69	3.03016 2357831 72	0.0024442 230724464 9	0.0140774 873159893
<b>Roseimicrobium</b>	11.7429 2565215 05	3.32062 4568096 69	0.630025 4635993 37	5.27061 9617699 18	1.3596398 2753701e- 07	6.2785674 2785835e- 06

- FAPROTAX tables

## Heatmap



## ATMAC-C12

	baseMean	log2FoldChange	IfcSE	stat	pvalue	padj
<b>sulfate_respiration</b>	50.99636576 83444	1.690897091 81679	0.518608627 182497	3.260449215 8241	0.001112358850 60846	0.002406541172 69375
<b>respiration_of_sulfur_compounds</b>	51.42812737 60187	1.655029324 93697	0.508401431 303307	3.255359294 90646	0.001132489963 62059	0.002406541172 69375
<b>cellulolysis</b>	59.11135766 6556	0.659391921 506285	0.228700682 895867	2.883209237 31795	0.003936458708 6566	0.006691979804 71623
<b>xylanolysis</b>	31.11236066 95799	-0.684700284 041423	0.300879315 111413	-2.275664193 75784	0.022866115993 467	0.035338542898 9945

<b>manganese_oxidation</b>	71.05347153 13976	- 0.846410436 979749	0.291975975 753625	- 2.898904386 89369	0.003744690686 35189	0.006691979804 71623
<b>fermentation</b>	511.1669428 42442	1.014419088 1021	0.266741998 613687	3.802997253 42931	0.000142955941 180429	0.000486050200 013457
<b>human_pathogens_all</b>	29.33679172 14767	1.921808901 61881	0.479937957 23746	4.004286122 06629	6.220504010104 38e-05	0.000264371420 429436
<b>human_associated</b>	31.26576114 54627	2.003620565 09336	0.487198796 751279	4.112531842 14294	3.913434728155 16e-05	0.000221761301 262126
<b>animal_parasites_or_sympionts</b>	121.1697475 70313	3.496640964 0981	0.544023881 310233	6.427366673 08933	1.298333831339 02e-10	2.207167513276 34e-09
<b>dark_iron_oxidation</b>	30.82930155 91848	1.612460894 45255	0.494990830 152476	3.257557102 5343	0.001123756463 75867	0.002406541172 69375
<b>intracellular_parasites</b>	30.52289070 38819	2.528544698 42792	0.557818474 326284	4.532916736 9041	5.817475091163 39e-06	4.944853827488 88e-05
	<b>baseMean</b>	<b>log2FoldChange</b>	<b>IfcSE</b>	<b>stat</b>	<b>pvalue</b>	<b>padj</b>
<b>sulfate_respiration</b>	50.99636576 83444	1.690897091 81679	0.518608627 182497	3.260449215 8241	0.001112358850 60846	0.002406541172 69375
<b>respiration_of_sulfur_comounds</b>	51.42812737 60187	1.655029324 93697	0.508401431 303307	3.255359294 90646	0.001132489963 62059	0.002406541172 69375
<b>cellulolysis</b>	59.11135766 6556	0.659391921 506285	0.228700682 895867	2.883209237 31795	0.003936458708 6566	0.006691979804 71623
<b>xylanolysis</b>	31.11236066 95799	- 0.684700284 041423	0.300879315 111413	- 2.275664193 75784	0.022866115993 467	0.035338542898 9945
<b>manganese_oxidation</b>	71.05347153 13976	- 0.846410436 979749	0.291975975 753625	- 2.898904386 89369	0.003744690686 35189	0.006691979804 71623
<b>fermentation</b>	511.1669428 42442	1.014419088 1021	0.266741998 613687	3.802997253 42931	0.000142955941 180429	0.000486050200 013457
<b>human_pathogens_all</b>	29.33679172 14767	1.921808901 61881	0.479937957 23746	4.004286122 06629	6.220504010104 38e-05	0.000264371420 429436
<b>human_associated</b>	31.26576114 54627	2.003620565 09336	0.487198796 751279	4.112531842 14294	3.913434728155 16e-05	0.000221761301 262126
<b>animal_parasites_or_sympionts</b>	121.1697475 70313	3.496640964 0981	0.544023881 310233	6.427366673 08933	1.298333831339 02e-10	2.207167513276 34e-09
<b>dark_iron_oxidation</b>	30.82930155 91848	1.612460894 45255	0.494990830 152476	3.257557102 5343	0.001123756463 75867	0.002406541172 69375
<b>intracellular_parasites</b>	30.52289070 38819	2.528544698 42792	0.557818474 326284	4.532916736 9041	5.817475091163 39e-06	4.944853827488 88e-05

## BAC-C12

	<b>baseMean</b>	<b>log2FoldChange</b>	<b>IfcSE</b>	<b>stat</b>	<b>pvalue</b>	<b>padj</b>
<b>sulfate_respiration</b>	52.54210163 04512	2.299495550 43342	0.457941513 65112	5.021373869 55767	5.13031883390 082e-07	3.84773912542 561e-06
<b>respiration_of_sulfur_comounds</b>	52.74075643 76838	2.3036222656 76489	0.451571722 801961	5.101343907 16745	3.37250103864 5e-07	3.37250103864 5e-06
<b>cellulolysis</b>	30.29207522 29745	1.233295890 89215	0.28684427 225373	4.299528852 00433	1.71161593093 628e-05	0.00010269695 5856177

<b>xylanolysis</b>	8.550074591 94444	1.676098187 5742	0.666801791 60362	2.513637798 63771	0.01194930859 25831	0.02335026200 20438
<b>dark_thiosulfate_oxidation</b>	3.261281679 27876	4.211222526 35896	1.438233540 45885	2.928051952 54689	0.00341093045 748436	0.00852732614 37109
<b>dark_oxidation_of_sulfur_compounds</b>	3.261281679 27876	4.211222526 35896	1.438233540 45885	2.928051952 54689	0.00341093045 748436	0.00852732614 37109
<b>fermentation</b>	289.7545184 08621	2.218273897 84307	0.285540478 018504	7.768684542 50932	7.93054008764 37e-15	2.37916202629 311e-13
<b>human_pathogens_all</b>	14.81122577 08594	1.176275616 30533	0.470693391 254176	2.499027260 9758	0.01245347306 77567	0.02335026200 20438
<b>human_associated</b>	15.10007122 24361	1.253418938 11205	0.474814716 172241	2.639806424 31767	0.00829533938 436965	0.01874206174 50326
<b>aromatic_compound_deg</b> <b>radiation</b>	1572.143286 64271	- 0.244601605 440184	0.104437466 661837	- 2.342086736 28776	0.01917625782 81153	0.03284009926 98597
<b>nitrate_reduction</b>	191.5479470 90748	0.525292501 19613	0.130884896 310395	4.013392805 46468	5.98521893871 663e-05	0.00029926094 6935832
<b>intracellular_parasites</b>	16.27703228 12717	2.210656150 72466	0.414687134 391543	5.330901220 18925	9.77265677182 216e-08	1.46589851577 332e-06
<b>photosynthetic_cyanobacteria</b>	1.600759741 80432	4.231022799 6325	1.437481442 34349	2.943358206 23519	0.00324672513 374398	0.00852732614 37109
<b>oxygenic_photoautotrophy</b>	1.600759741 80432	4.231022799 6325	1.437481442 34349	2.943358206 23519	0.00324672513 374398	0.00852732614 37109
<b>photoautotrophy</b>	1.600759741 80432	4.231022799 6325	1.437481442 34349	2.943358206 23519	0.00324672513 374398	0.00852732614 37109
<b>phototrophy</b>	2.633993883 9818	4.724720856 65041	1.322873542 13329	3.571558963 24849	0.00035486263 29242	0.00152083985 538943
<b>ureolysis</b>	72.15409421 96193	- 0.696430901 290044	0.298649237 644565	- 2.331935975 40301	0.01970405956 19158	0.03284009926 98597
<b>chemoheterotrophy</b>	8969.515565 02438	- 0.105942713 385835	0.040408161 12659	- 2.621814762 96185	0.00874629548 101521	0.01874206174 50326

## DDAC-C10

	<b>baseMean</b>	<b>log2FoldChange</b>	<b>IfcSE</b>	<b>stat</b>	<b>pvalue</b>	<b>padj</b>
<b>sulfate_respiration</b>	51.93878651 34229	3.326973647 25728	0.4526564472 08162	7.349886802 18071	1.983747825505 13e-13	3.77535787832 067e-12
<b>respiration_of_sulfur_compounds</b>	52.24085942 36431	3.318311422 21774	0.4527383752 15635	7.329423799 42337	2.311443598971 84e-13	3.77535787832 067e-12
<b>cellulolysis</b>	43.86459479 21639	0.807002968 204485	0.2284060576 8971	3.533194243 47668	0.000410570694 521411	0.00402359280 630983
<b>fermentation</b>	405.5370807 80465	2.268667196 84342	0.2730199021 60778	8.309530473 37709	9.608148077832 07e-17	4.70799255813 771e-15
<b>human_pathogens_all</b>	22.06786698 22092	0.846255181 554664	0.3203775019 39451	2.641431362 78839	0.008255653305 66447	0.04666304091 09612
<b>human_associated</b>	22.51857398 41103	0.930071038 619084	0.3261670563 44294	2.851517406 58114	0.004351110390 44657	0.03045777273 3126
<b>animal_parasites_or_symbionts</b>	129.5352942 53473	1.068174712 86089	0.3592596346 21547	2.973266712 76647	0.002946482944 54317	0.02406294404 71026

<b>aromatic_compound_degradation</b>	2210.143787 61688	- 0.236295676 333421	0.0898901123 943301	- 2.628717108 47172	0.008570762616 29899	0.04666304091 09612
<b>intracellular_parasites</b>	22.48319078 13505	1.612021850 58549	0.3013713599 82054	5.348955025 72467	8.846351962897 15e-08	1.08367811545 49e-06